Muscle Hypertrophy Is Regulated by Acetylation and Phosphorylation of the Actin Capping Protein CapZ

BY

YING-HSI LIN
B.S., National Taiwan University, 2002
M.S., National Taiwan University, 2004

THESIS

Submitted as partial fulfillment of the requirements
for the degree of Doctor of Philosophy in Physiology and Biophysics
in the Graduate College of the
University of Illinois at Chicago, 2015

Chicago, Illinois

Defense Committee:

Brenda Russell, Advisor
John Kennedy, Chair
R. John Solaro
Carlos Stocco
Allen M. Samarel, Loyola University Medical Center

This thesis is dedicated to my wonderful family, my father Yu-Shan Lin and my mother Su-huei Lin. Since the first day I came to US, they whole-heartedly supported me and always helped me to focus on my course work and research. I also thank other members of my family, my auntie, Professor Sulie Chang in Seton Hall University, my grandpa, Sen Lin, and my deceased granduncle Shan-Chi Lin. The influences from them were vital in determining my fate.

ACKNOWLEDGEMENTS

I am grateful to my thesis committee: Dr. R. John Solaro, Dr. John Kennedy, Dr. Carlos Stocco, and Dr. Allen M. Samarel, for their guidance and support throughout these past five years. I would especially like to thank my mentor and advisor, Dr. Brenda Russell who taught me the how to be a PhD with independent and critical thinking. It was an honor to be her student. I will always be her student, and I will never forget her influence in my road to be a researcher.

I thank current and former members of the Russell lab, including Jieli (Shirley) Li, Mike Mkrtschjan, Elina Sharma, Kathleen M. Broughton, Matthew Curtis and especially Erik R. Swanson. This research would not have been possible without their friendship and support.

I also thank all the members of the UIC Department of Physiology and Biophysics. I would especially like to thank Chad M. Warren from Solaro lab for his expertise and generous help in the proteomics experiments. I appreciate Kathleen Engstrom, Jennifer Guthrie and Lauren Scott for their kind help in administration.

I thank Dr. Samarel for discussion and for the GFP adenovirus, Dr. Timothy A. McKinsey and his lab members for the HDAC inhibitors in the third chapter, as well as suggestions which I appreciate. Miensheng Chu, who was a member of Samarel lab in Loyola University Medical Center, has been a peer mentor for me.

YL

Chapter 1 is a literature review that places my dissertation question in the context of the larger field and highlights the significance of my research. Chapter 2 represents a published manuscript in Journal of Applied Physiology (Lin, 2013) for which I was the primary author and major driver of the research. Jieli Li assisted me in the experiments shown in Figure 9. My research mentor, Dr. Brenda Russell contributed to the writing of the manuscript. Chapter 3 represents unpublished experiments that will ultimately be submitted as a first author manuscript. Chad M. Warren and Jieli Li assisted me in the experiments shown in Figures 13-14 and 18-19 respectively. My research mentor Dr. Brenda Russell will contribute to the writing of this next manuscript as well. Chapter 4 represents my synthesis of the research presented in this thesis and my overarching conclusions. Chapter 5 represents the future directions of this field and this research questions are discussed.

TABLE OF CONTENTS

CHAPTER **PAGE**

TABLE OF CONTENTS (continued)

TABLE OF CONTENTS (continued)

LIST OF TABLES

LIST OF FIGURES

LIST OF FIGURES (continued)

LIST OF ABBREVATIONS

1 or 2DGE	one or two-dimensional gel electrophoresis
ADP	adenosine diphosphate
AMPK	5' AMP-activated protein kinase
ATP	adenosine triphosphate
BSA	bovine serum albumin
caPKCε	constitutively active protein kinase C isoform epsilon
CK2	casein kinase 2
CP	capping protein
cTnI	cardiac troponin I
DAG	diacylglycerol
DCM	dilated cardiomyopathy
dnPKCε	dominant negative protein kinase C isoform epsilon
DRF	Diaphanous-related formin
DTT	dithiothreitol
EDTA	ethylenediaminetetraacetic acid
EGFP	enhanced green fluorescence protein
ELC	essential light chain
ERK	extracellular-signal-regulated kinase
ET-1	endothelin-1
FAK	focal adhesion kinase
FHL1	four and a half LIM domains protein 1
FHOD	FH1/FH2 domain-containing protein
FRAP	fluorescence recovery after photobleaching
G-actin	globular actin

LIST OF ABBREVATIONS (continued)

GFP	green fluorescence protein
H2B	histone H2B
HDAC	histone deacetylase
HF	heart failure
HPLC	high-performance liquid chromatography
h	hour(s)
Hsp70	heat shock protein 70
Hz	hertz
IEF	isoelectric focusing
ILK	integrin-linked kinase
kDa	kilodalton
MAPK	mitogen-activated protein kinases
MARP	muscle ankyrin repeat proteins
MEF	myocyte enhancer factor
MEK1/2	mitogen-activated protein kinase kinase 1/2
min	minute(s)
MLP	muscle Lim protein
MOI	multiplicity of infection
MRF4	muscle Regulatory Factor 4
MS	mass spectrometry
NE	norepinephrine
NRVM	neonatal rat ventricular cardiomyocyte
PBS	phosphate-buffered saline
PE	phenylephrine
PGC-1	peroxisome proliferator-activated receptor gamma coactivator 1-alpha

PIP_2	phosphatidylinositol 4,5-bisphosphate
PKC	protein kinase C
PKD	protein kinase D
PPARα	peroxisome proliferator-activated receptor alpha
PS	pseudosubstrate
PTEN	phosphatase and tensin homolog
PTM	posttranslational modification
PVDF	polyvinylidene difluoride
RACK	receptor for activated C-Kinase
RFP	red fluorescence protein
RLC	regulatory light chain
ROCK	rho-associated protein kinase
ROI	region of interest
SE	standard error
sec	second (s)
ssTnI	slow skeletal troponin I
STAT3	signal transducer and activator of transcription 3
TK	titin kinase

SUMMARY

According to American Heart Association 2015 statistics (Mozaffarian, 2015), in 2011, heart failure (HF) was mentioned for one in nine deaths in the United States. From 2009 to 2012, an approximate 5.7 million Americans (>20 year old) had HF. Projections demonstrates that HF will increase to 46% from 2012 to 2030. This means over 8 million people would have HF. Cardiac hypertrophy is a common response to increased mechanical loading, and is associated with increased risk of heart failure and arrhythmia (Koren, 1991). Heart function in hypertrophy may have good or bad outcomes depending on the different signals that are driving the growth of the muscle. Thus, understanding how heart cells remodel in response to pathological stimuli is of great importance to improve the maladaptive decline. This understanding may eventually lead to new treatment of cardiac myopathy.

This thesis is divided into two main sections to investigate the assembly of the contractile actin thin filament, a major component of the heart cell mass. The focus of this thesis is the actin capping protein, CapZ, which binds to the barbed ends of the actin filaments and regulates their assembly. In the first part, the effects of mechanical cues (cyclic strain) and neurohormonal cues (such as phenylephrine) on CapZ capping and actin filament dynamics are studied. In the second part, the mechanism how CapZ dynamics is regulated is addressed. Biophysical and biochemical assays such as fluorescence recovery after photobleach (FRAP), one and two dimensional gel electrophoresis (1 or 2DGE), mass spectrometry (MS), immunocytochemistry and immunoblotting are used.

SUMMARY (continued)

The time course of the response and recovery after acute activity seen in exercise is not well understood. The goal of the first part of the thesis is to address how proteins of the thin filament (CapZ) are changed by one hour of mechanical stimulation and how these return to baseline over time. Neonatal rat ventricular myocytes (NRVMs) in culture were subjected to cyclic 10% strain at 1 Hz for 1 hour to mimic increased mechanical loading during exercise. CapZ and actin dynamics were analyzed by fluorescence recovery after photobleaching (FRAP) using GFP-CapZβ1, actin-GFP or actin-RFP. After cyclic strain, CapZ dynamics increased above resting controls, and abated 2~3 hours after cessation of the cyclic strain. Similarly, actin dynamics initially increased, and abated 1.5~2 hours after the end of stimulation. Neurohormonal hypertrophic stimulation by phenylephrine or norepinephrine treatments also elevated actin dynamics but required a much longer time of treatment (24~48 hours) to be detectable. The actin capping mechanism was explored by use of expression of CapZβ1 with a C-terminus deletion (CapZβ1ΔC). Increased dynamics of actin seen with CapZβ1ΔC was similar to the response to cyclic strain. Thus, it is possible that mechanical stimulation alters the dynamics for CapZ capping of the actin filament through the CapZβ1 C-terminus, known as the β tentacle, thereby remodeling sarcomeres in cardiac myocytes. This adaptive mechanism for thin filament addition declines a few hours after the end of a bout of exercise.Rapid increases in the dynamics of both actin and the actin capping protein (CapZ) following mechanical flexing suggest post-translational modifications (PTMs) might be the underlying mechanism. Thus, in the second part of this thesis, NRVMs in culture were stimulated to a hypertrophic state

by a neurohormone (10μM phenylephrine, PE, for 24 hours), and PTMs of CapZβ1 were analyzed by 2D gel electrophoresis and mass spectrometry (MS). After PE treatment, 2D spots of CapZβ1 with more negative charges were increased, suggesting that PTMs of CapZβ1 are up-regulated. Increased PTM spots included the acetylation of K199 and phosphorylation of S204, which are both close to the actin-binding region of CapZ. In order to address specific roles of acetylation and phosphorylation, drugs and molecular reagents are used to enhance or diminish particular PTMs. CapZ dynamics and acetylation were increased with class I HDAC inhibitor (5μM trichostatin A / 5 hours) and HDAC1-3 inhibitor (MGCD0103 / 24 hours), and the effect of PE on CapZ dynamics was diminished by HDAC activator (10μM theophylline / 24 hours), suggesting CapZ dynamics were regulated via CapZ acetylation by altered HDAC1-3 activities. The subcellular distribution of HDAC3 was decreased in myofibrillar but increased in the membrane compartment of myocytes, suggesting the diminished HDAC activities in hypertrophic myocytes were due to HDAC translocation. CapZ dynamics and PTMs were increased with constitutively active PKCε (caPKCε) expression, but diminished with dominant negative PKCε (dnPKCε), suggesting that CapZ dynamics can also be regulated by PKCε and CapZ phosphorylation. The inhibitory effects on PTMs and dynamics of CapZ by dominant negative PKCε were counteracted by MGCD0103, suggesting acetylation overrode the increased CapZ dynamics. Together the acetylation of CapZ reduces the capping property and may increase thin filament assembly. Interestingly, PTMs of endogenous CapZβ1 were also elevated in failing human heart

compared to normal human ventricular tissue, suggesting the involvement of PTMs in human heart disease.

This thesis has yielded new information about how CapZ capping responds to mechanical strain and neurohormonal stimulation when myocyte growth occurs. Altogether, results suggest the involvement of two major signaling pathways. These signals are the phosphorylation mediated by PKCε and the acetylation mediated by Class I HDACs. These pathways play important roles in the regulation of CapZ capping and thin filament assembly for the remodeling of the myocytes. Furthermore, this alteration of CapZ capping can occur shortly after mechanical strain and might enable the myocytes to respond quickly to stimulation. The approach is to use failing human heart in addition to cultured NRVMs stimulated for growth. The understanding of these pathways in exercise and chronic disease provides a potential therapeutic target for hypertrophic heart failure.

I. INTRODUCTION

A. Fundamental Aspects of Cardiac Hypertrophy

i. Overview

The heart is a dynamic organ that can change its size and shape in response to different systemic demands. Cardiac remodeling with increased work usually leads to hypertrophy, broadly characterized as an increase in heart mass. Given the fact that ventricular cardiomyocytes constitute up to 70-80% of heart mass (Zak, 1984; Popescu, 2006), one might suspect that the division and proliferation of myocytes account for the increase mass. However, myocytes lose the ability to divide shortly after birth, with very low level of DNA synthesis rate (Soonpaa, 1996; Nakagawa, 1998), indicating the enlargement of heart is primarily due to increased myocyte size, not in number. As for the morphological classification, the classic division is into concentric or eccentric hypertrophy (Grossman, 1975; Katz, 2010). Concentric hypertrophy is the increased heart mass with increased wall-thickness and increased myocyte diameter. In contrast, eccentric hypertrophy is characterized by increased chamber volume with thin walls and elongated cells (Figure 1).

Cardiac hypertrophy can be either beneficial or detrimental. Exercise or pregnancy-induced remodeling is beneficial, usually referred as physiological cardiac hypertrophy. It is characterized by enhanced cardiac function and increasing muscle mass and a proportional change in diameter and length of the cardiomyocytes (Figure 1). However, cardiac hypertrophy can become pathologic due to maladaptation in cardiac diseases. In the human, there is a slow progressive decline in ventricular performance over many years after an initial cardiac event, ultimately leading to loss of cardiac output and

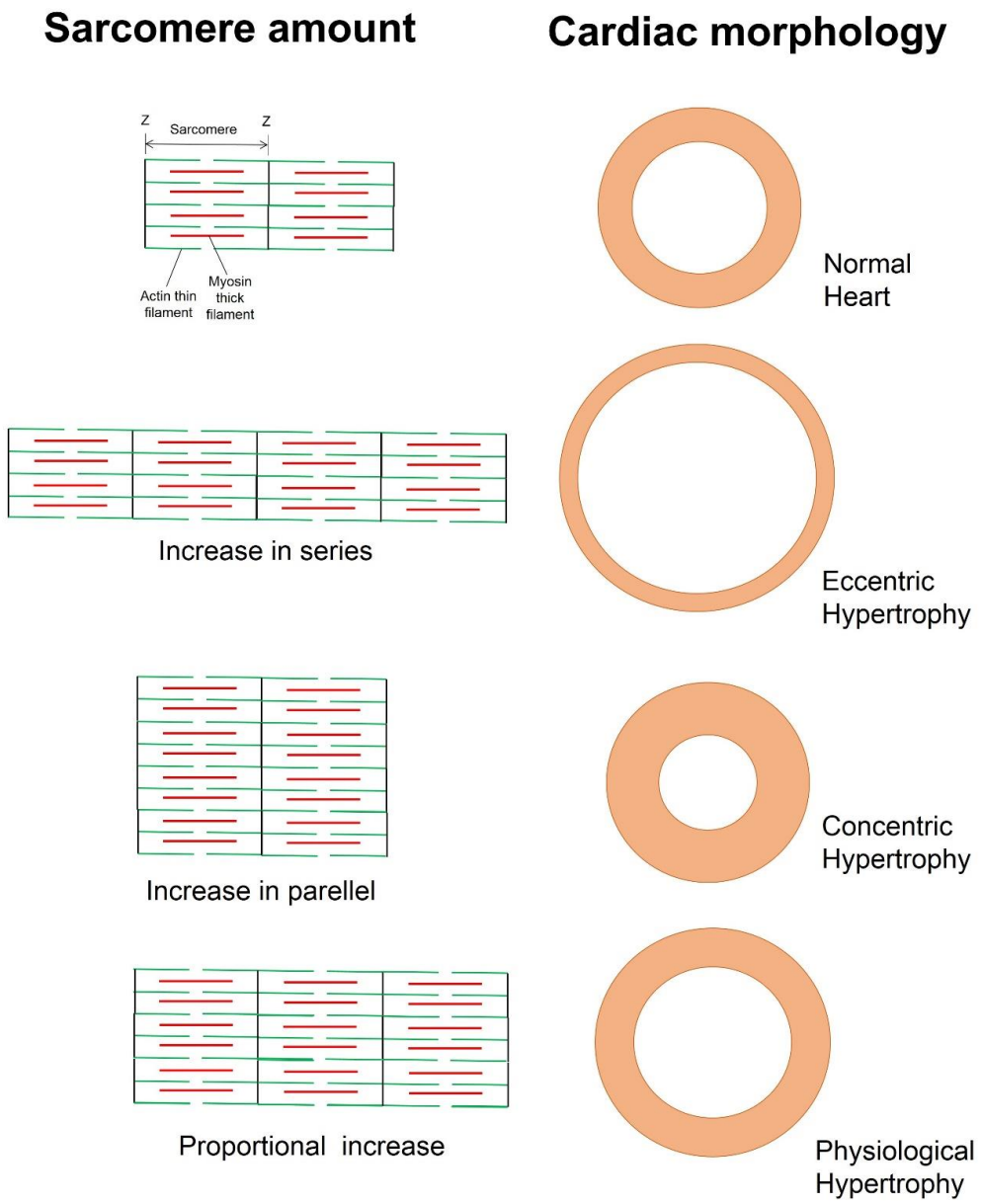

Figure 1. Variation of the sarcomere amount and heart morphology in cardiac hypertrophy. Left: sarcomere arrangement; right: heart morphology to represent left ventricular cross section. During hypertrophy, a myocyte can increase its volume in either width or length. It can be lengthened by the addition of sarcomeres in series, which occurs in eccentric hypertrophy. It can be widened by the addition of sarcomeres side-by-side in parallel, leading to concentric hypertrophy. The addition of sarcomeres can also be proportional, resulting in physiological hypertrophy.

death. Physiological hypertrophy and pathological hypertrophy are different structurally, functionally and metabolically as described in the following sections.

ii. Physiological Hypertrophy

Physiological hypertrophy refers to the proportional postnatal heart growth in response to the increased work load. This growth occurs as a child ages, an adult exercises or a woman is pregnant. In some situations, mechanical loading of the cells leads to the secretion of hormones and neurotransmitters, which also mediate the growth and contraction of myocytes. Thus, it is hard to distinguish the effects of “mechanical stimulation” and “neurohormonal stimulation” on the heart. Physiological hypertrophy is beneficial to heart function with the proportional increase of myocyte width and length.

Different kinds of exercise lead to different heart shapes (Pluim, 2000). In endurance training such as swimming and long distance running, vascular resistance is diminished, producing increased cardiac output with mildly increased pressure. This leads to eccentric hypertrophy with increased chamber volume but no significant changes of wall-thickness / chamber volume ratio. In contrast, in strength training such as weight lifting, compression of blood vessels combining with a pressor response leads to intermittent elevations in blood pressure but only mildly increased cardiac output (MacDougall, 1985). This increases wall-thickness with less chamber enlargement and is more like concentric hypertrophy. The hearts of pregnant women generally share similar physiologic features with the endurance trained athlete because the fetus places additional demands for cardiac output. But with vast differences of hormone (e.g.,

estrogen) and metabolites in pregnancy, the hearts of pregnant women have other distinct features as reviewed (Li, 2012).

In physiological hypertrophy, there are increases in angiogenesis to provide oxygen and nutrients. There are also increases in the fibrillar collagen network for mechanical support to the myocytes. The functions of myocytes in physiological hypertrophy are maintained, but total cardiac output is increased and myofibril mass is greater. Importantly, the enlargement of heart muscle in physiological hypertrophy is a "reversible" adaptation, in which muscle mass can return to the baseline after the cessation of stimulation (Moulopoulos, 1968; Forfar, 1982).

iii. Pathological hypertrophy

Pathological growth of myocytes occurs in response to stress or disease. Pathological hypertrophy can be concentric or eccentric (Grossman, 1975; Katz, 2010). The general understanding is that concentric hypertrophy is produced by chronic pressure overload, such as hypertension caused by increased peripheral resistance or aortic stenosis. In contrast, eccentric hypertrophy occurs with chronic volume overload (e.g., aortic regurgitation). Pathological hypertrophy is accompanied by loss of myocyte function. For example, after an infarct, loss of oxygen to the tissue results in myocyte death from apoptosis or necrosis. The remaining myocytes need to contract harder to compensate for the lost function of the dead cells. Therefore, the increased workload leads to hypertrophy of the surviving myocytes.

A newer classification of cardiac hypertrophy uses the terms hypertrophic (HCM) and dilated cardiomyopathy (DCM), which are based on the different chamber abnormalities of the heart. HCM refers to the widening of the myocytes leading to a thicker ventricular wall of the myocardium. DCM refers to the elongation of the myocyte leading to thinning of the wall and enlargement of the left ventricular chamber volume. Thus, HCM and DCM typify the features of concentric and eccentric hypertrophy, respectively. Besides mechanical stress, genetic mutations of contractile proteins in the sarcomere such as the troponin complex or myosin binding protein-C also leads to HCM or DCM (Knöll, 2012; Lu, 2013). The exact mechanisms leading to HCM or DCM are still not fully understood.

The enlargement of the myocardium in pathological hypertrophy is initially a compensatory response, but sustained pathological hypertrophy progresses slowly to heart failure. In pathological conditions, different neurohormonal factors such as norepinephrine (NE) and endothelin 1 (ET-1) are secreted (Arai, 1995; Rapacciuolo, 2001), stimulating G protein-coupled receptor signaling cascades (Bernardo, 2010). The downstream pathways, including MAPK, PKC, Gp130/STAT3 and HDACs, play a crucial role in gene expression (Frey, 2003). The structural features of pathological hypertrophy are also distinct from physiological hypertrophy. In the case of cardiac hypertrophy after myocardial infarction, because of cell death and loss of myocytes, the space of dead cells is filled by increased fibrotic connective tissue. These scars stiffen the myocardium. This not only impedes the contraction and relaxation of myocytes, but also blocks angiogenesis.

iv. Metabolism in Cardiac hypertrophy

In terms of cardiac metabolism, physiological hypertrophy maintains a similar ratio of fatty acid and glucose oxidation, but with enhanced amount per unit mass of whole heart for the increased demand (Gertz, 1988). The metabolism of pathological hypertrophy is also altered. Instead of using both fatty acid oxidation and glycolysis for the major sources of ATP synthesis as in normal conditions (van der Vusse, 1992), pathological hypertrophy heart mostly relies on glucose metabolism (Allard, 1994; Christe, 1994; Depre, 1998). This is because of the down-regulation of two pivotal regulators of fatty acid oxidation, peroxisome proliferator-activated receptor alpha (PPARα) and peroxisome proliferator-activated receptor gamma co-activator-1 (PGC-1) (Barger, 2000; Sihag, 2009). Carnitine-palmitoyl transferase 1 (CPT1), which facilitates fatty acid transport into the mitochondria, is also down-regulated (Sorokina, 2007). In contrast, hypertrophy also enhance the activity of AMP-activated protein kinase (AMPK), a key regulator for the translocation of glucose transporters to the plasma membrane, leading to increased glucose uptake and glycolysis (Tian, 2001).

B. Sarcomere Structure and Functions

Myocyte growth in cardiac hypertrophy occurs by assembly of sarcomeres into myofibrils. Thus, it is important to have a general understanding of the sarcomere structure. The basic structural unit, the sarcomere, performs the contractile function. The word “sarcomere” is composed of two Greek words *“sarc”* and *“meros”*, meaning “flesh” and “part.” Thus, sarcomere means “the basic unit of meat.” The sarcomere has

highly organized, anisotropic filaments at the ultrastructural level. The early observation of the sarcomere came from seeing striations with light microscopy. There is a regular repeating structure limited by two dark Z-lines, between which are the I-band (for isotropic), A-band (for anisotropic) and H-zone (from the German "heller", brighter) (Eisenberg, 1983). The distance between the two Z-lines, along with the width of I-Band and H-zone, varies throughout the cycle of muscle contraction. Electron microscopy shows that the A-band corresponds to the full length of thick (myosin) filaments, and I-band corresponds to the thin (actin) filaments interdigitating with the thick filaments (Figure 2A). Sir Andrew F. Huxley established the sliding filament theory of muscle contraction and it is now the well-accepted model of contraction (Huxley, 1957) (Figure 2A). Biochemical methods identified the muscle proteins of myosin and actin and subsequently proved that cross bridges of the myosin head could interact with actin using ATP to provide the force for sliding. The contraction of cross-bridge with actin is a calcium-dependent cycle that is consuming ATP (Weber, 1973) (Figure 2B).

i. The Thin and Thick Filament

a. Thin filament

The thin filament has a diameter of 6-10 nanometers and is composed mainly of the actin. The actin filament is formed by the addition of a long series of actin monomers. Thin filaments belong to the cytoskeleton found in all cells. In myofibrils, actin monomers form two helical chains that wind around each other. Each single strand of the actin filament repeats

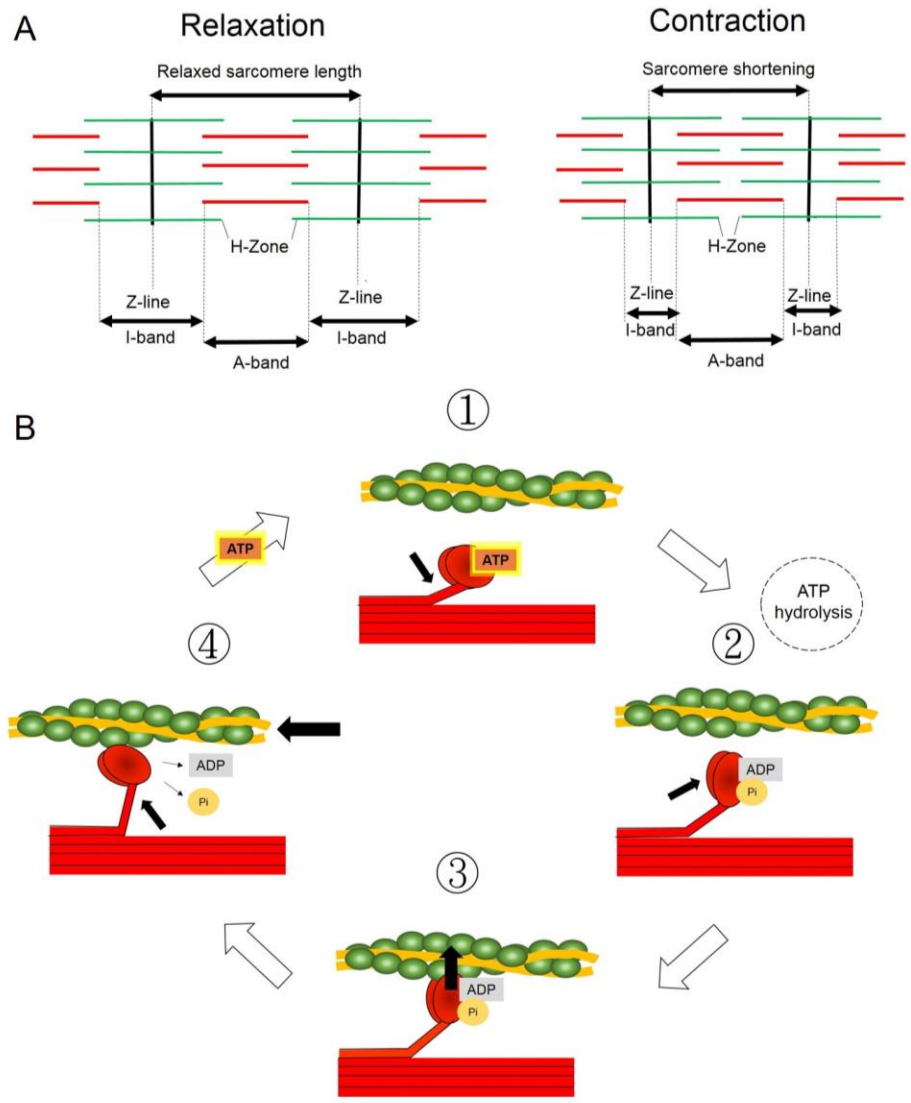

Figure 2. Sliding filament model of muscle contraction and the cross-bridge cycle. (A) During muscle contraction, the thick (myosin) filaments pull the thin filaments toward the center of the sarcomere. When the thin filaments slide over the thick filaments, the I-bands and H-zones become shorter and eventually disappear. During Muscle Relaxation, the thick filaments release the interaction with thin filaments, and slide back to their relaxed positions. I-bands and H-zones are widened again. (B) Cross-bridge cycle. 4 to 1: ATP binds to the myosin head, releasing the cross-bridge; 1 to 2: ATP is hydrolyzed to ADP and P_i, leading to the "cocking" of the myosin head; 2 to 3: Myosin attaches the actin filament; 3 to4: ADP and P_i are released. The myosin head twists and bends, pulling the attached actin myofilament ahead.

approximately every 7 monomers in 35 nm (Figure 3A). Besides the actin filaments, the thin filament also contains some very important regulatory proteins. The first protein is tropomyosin, which is a filamentous protein that folds into the helix structure of the actin filament. Each tropomyosin has a pseudo-repeat in the sequence, allowing its binding to 7 actin monomers. During the resting state, tropomyosin blocks the myosin binding site of actin, preventing the actin-myosin interaction and the formation of a cross-bridge.

The second regulatory protein component is the globular troponin complex (troponin I, troponin T and troponin C), which permits structural changes with tropomyosin in the presence of calcium to expose the myosin binding site for actin. Thus, the muscle contraction occurs only when there is an elevated calcium concentration in the sarcoplasm, unblocking the inhibitory effects of troponin on actin-myosin binding and activating the power stroke. The role of troponin was established by Ebashi in the 1970s (Ebashi, 1974), and the structural basis of the troponin complex has been extensively studied since then. For example, the phosphorylation of troponin I subunit on various sites is widely known for mediating myofibrillar maximum tension and sarcomeric responsiveness to calcium (Solaro, 2010). Recently, findings suggest that troponin I phosphorylation might be also related to thin filament assembly and cardiac metabolic signaling networks (Solaro, 2013).

b. Thick filament

The thick filament has a diameter of about 14-16 nanometers and is composed mainly of myosin molecules. Myosin belongs to the motor protein family, meaning it consumes energy to perform a motor function. The myosin molecule in the thick filament typically

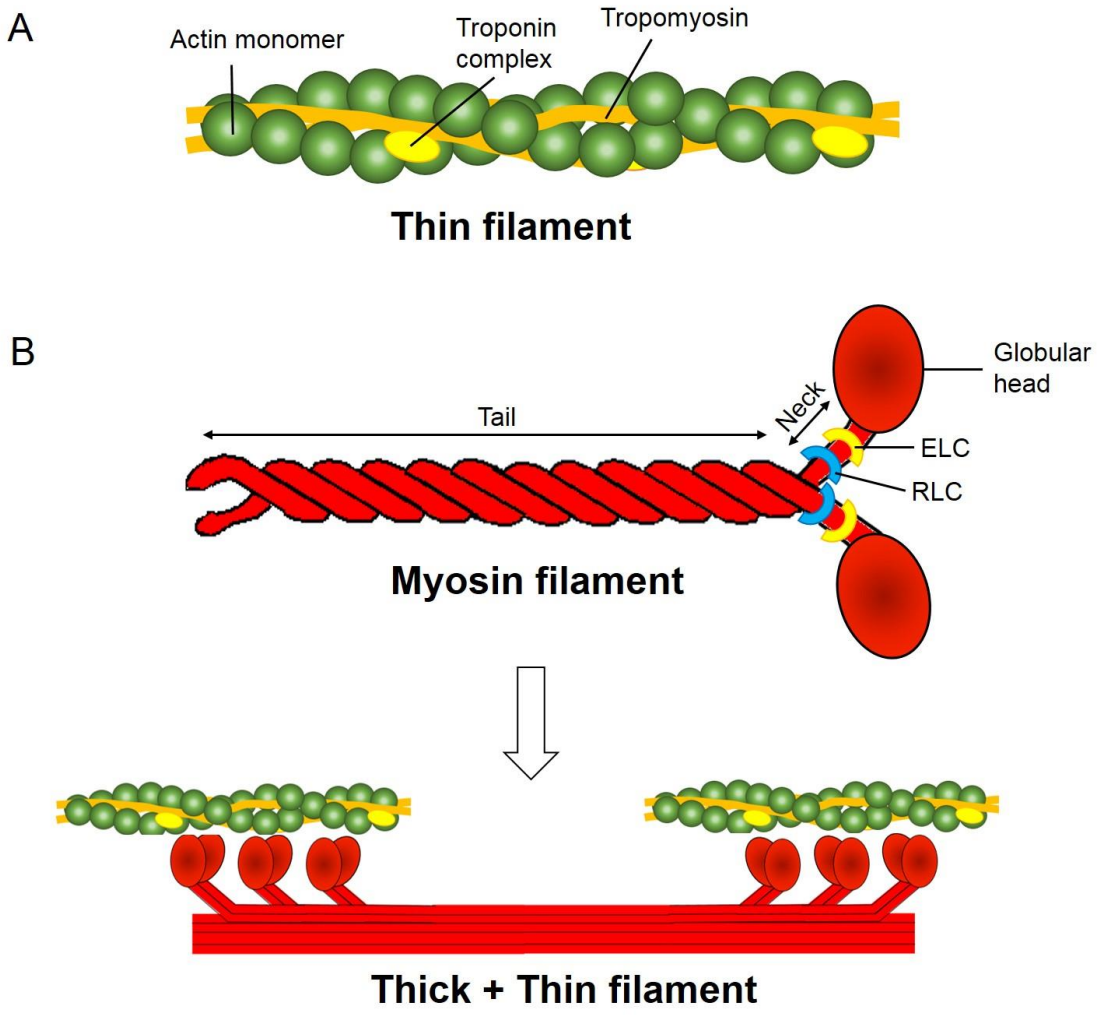

Figure 3. Actin thin filament and myosin thick filament structure. (A) Display of the actin thin filament (green) along with tropomyosin (orange) and troponin (yellow). (2) Top: Single myosin filament contains 2 head chains (red), 2 essential light chains (ELC, yellow) and 2 regulatory light chains (RLC, blue). Bottom: the arrangement of the myosin filament in the thick filament and its interaction with the actin filament.

has three different pairs of subunits: the heavy chain, the essential light chain (ELC) and the regulatory chain (RLC) (Figure 3B). The C-terminal of the heavy chain forms a coiled-coil tail of two myosin molecules. RLC and ELC are located at the “neck” of the myosin molecule, and provide regulatory function and structural stability (Hernandez, 2007; Scruggs, 2009; Kamm, 2011). The N-terminal of the heavy chain forms the two globular heads of a myosin molecule, which is the region that can interact with actin and form the cross-bridges between the thin and thick filaments. This catalyzes the ATPase activity of myosin leading to a conformational change of angle of the globular head that pulls against the actin filament with the consumption of ATP. It is a cyclic response of myosin only present when ATP and actin are available (Figure2B and 3B).

One distinctive feature of the myosin filament in striated muscle is that all myosin molecules are oriented with respect to the Z-disc, with the globular head pointing out towards the Z-disc and the C-terminal coiled-coil region binding to each other at the central region (Figure 3B). When the cross-bridge reacts, the globular heads of the myosin filament pull the adjacent actin filaments in the opposite direction toward the central region, leading to the “contraction” of the myofibril.

Contractility of the myofilaments is modified during hypertrophy with the most straightforward idea being the modulation of myosin motor functions. The switching of myosin heavy chain isoforms (from alpha to beta) and the mutations of myosin essential light chain (ELC) and regulatory light chain (RLC) have been extensively explored (Nakao, 1997; Hernandez, 2007; Scruggs, 2011). Also, alterations of the interaction of the troponin complex to the myosin filament is of great importance. The phosphorylation of the troponin I subunit on multiple sites modifies its calcium sensitivity with direct effect

on the contractile function of the myofibrils (Solaro, 2010). Troponin I also appears to perform a similar isoform switch from cardiac isoform (cTnI) to slow skeletal muscle isoform (ssTnI) under metabolic stresses (Pound, 2011). However, the assembly of myofilaments during cardiac hypertrophy is a very poorly understood field. Since the process of myofibrillogenesis has been hypothesized to start with a stress fiber-like actin filament structure as templates for the assembly of myofibrils (Sanger, 2006; Ono, 2010), our lab mainly focuses on the assembly of sarcomeric actin filaments.

ii. Z-disc

The Z-disc, also called Z-line or Z-band, defines the lateral boundaries of the sarcomere from the German word Zwischen (between). The name “Z-disc” comes from its disc like shape determined by electron microscopy. There had been a long debate about the structure of the Z-disc, which was originally thought to be a transverse membrane structure across the fiber (the “Krause membrane”; Huxley, 1955). It was not until the invention of the electron microscope that more structural information of the Z-disc was revealed. In 1962, Knappeis & Carlsen did the first significant structural analysis that showed that the Z-disc was actually where the thin filaments extend out in opposite directions (Knappeis, 1962). In 1990, two structural states of the Z-disc were obtained at rest and in contraction (Goldstein, 1990).

The Z-disc is a very complex structure where the barbed ends of the actin filaments of the adjacent sarcomere come in and are cross-linked by α-actinin (Suzuki, 1976). Besides α-actinin, many different proteins have also been found in the Z-disc (Pyle,

2004). Since the Z-disc is associated with so many proteins, it may mediate myocyte function in the several ways.

a. Structural support

The Z-disc is associated with titin (Gregorio, 1998), desmin (Clark, 2002) and nebulin (Pappas, 1998). Titin is a giant muscle protein, spanning half the length of the sarcomere from the Z-disc to the M-band (center of the thick filament). Titin provides the mechanical basis for the elastic recoil of the myofibrils on relaxation. Nebulin is known for its function of maintaining actin filament length (Witt, 2006). Desmin is an intermediate filament found in many cells. Desmin surrounds a myofibril at the periphery of the Z-disc and provides a lateral linkage for the alignment of one myofibril to the next one (Clark, 2002). Thus, the connection of the Z-disc with these proteins is crucial for the mechanical stability of muscle.

b. Mechanotransduction

As mentioned above, cardiac function is modified in response to altered mechanical loading. The Z-disc plays an important role in the mechanosensing of a myocyte to mechanical stimulation. One well-studied mechanosensing protein in the Z-disc is titin. The region of titin in the Z-disc is a “nodal point” for mechanosensing. Telethonin (also known as “Tcap”) is a 19 kDa protein found in the Z-disc that binds the N-terminal portion of titin (Zou, 2006). Recently, it is found that maladaptation to biomechanical stress in the heart is associated with telethonin deficiencies in mouse and human hearts (Knöll, 2011), suggesting it might play a pivotal role in the mechanosensing complex with titin and other Z-disc proteins.

The muscle LIM protein (MLP) is also found in the Z-disc and is a mechanosensing molecule. MLP is a nucleocytoplasmic shuttling protein that also binds α-actinin in the Z-disc (Henderson, 2003). When MLP is translocated to the nucleus, it binds myoD, myogenin, and MRF4 to initiate transcription of contractile proteins (Kong, 1997). Our lab has found that mechanical strain or neurohormonal hypertrophy induced nuclear translocation of MLP, suggesting that shuttling of MLP plays a crucial role in myocyte remodeling and hypertrophy (Boateng, 2007 and 2009). Furthermore, MLP also binds to telethonin (Knöll, 2010), making it possible that MLP and telethonin are part of a mechanosensing complex on the N-terminal end of titin in the Z-disc.

c. Actin assembly

The regulation of actin assembly in cells is complex and includes many actin binding proteins (Alberts, 2008). Actin assembly into the thin filament starts at the barbed ends located in the Z-disc, which is regulated by formin, and the capping protein, CapZ.

The formin protein family stimulate actin assembly directly at the barbed end both *in vivo* and *in vitro* (Pruyne, 2002). Formins usually dimerize to be functional with two FH2 domains forming a donut-like structure that wraps around the actin filament and controls its processive elongation. FH1/FH2 domain-containing proteins, FHOD1 and FHOD3, are sometimes classified as Diaphanous-related formins (DRFs). FHOD1 was first discovered in the spleen (Westendorf, 2001) and later FHOD3 was found in the heart, kidney and brain (Katoh, 2004). Two isoforms of FHOD3 exist, and the heart contains only the larger one (Kanaya 2005, Ehler 2010). This cardiac specific FHOD3 is localized

to the Z-disc and is required for myofilament maintenance in cardiomyocytes (Taniguchi, 2009; Iskratsch, 2010). FHOD3 can be activated by the Rho-kinase pathway, suggesting myofibrillogenesis during myocyte growth is initiated through the activation of FHOD3 (Iskratsch, 2013).

In contrast to formin, CapZ slows actin polymerization down. Like many molecules in living cells, there is a rate of exchange of old protein off an organelle and new one on to it. This on / off rate can be measured to determine the dynamics of the exchange. Our lab has reported that CapZ exchange rate is elevated with neurohormonal hypertrophy (Hartman, 2009). This thesis studies the regulation of CapZ dynamics under mechanical stimuli. The structural basis of CapZ, and its interaction with the actin filament are introduced in depth in the following section.

C. CapZ Structure and Function

The actin capping protein (CP) was first discovered in the 1960s by Maruyama and colleagues, but was initially named β-actinin (Maruyama, 1965). They reported that increasing the concentration of CP decreased the lengthening of F-actin polymers *in vitro*. In 1980, CP was first purified to homogeneity, and found to be composed of two major subunits close to 30kDa in size that pair to cap the barbed end of actin filaments (Isenberg, 1980). The dimeric CP binds to the barbed ends of the actin filaments, stabilizing them, and slowing down polymerization and depolymerization (Cooper, 1985; Caldwell,1989). In 1986, CP in muscle cells was discovered, and was named as “CapZ” because of its localization to the Z-disc (Casella; 1986).

i. CapZ Subunits and Isoforms

CapZ is a mushroom-like heterodimeric protein composed of α and β subunits (Figure 4A). The α1 and α2 isoforms are found throughout many tissues though their expression varies widely, and the α3 isoform is specific to the testis. In cardiac tissue, the ratio of α1 to α2 is approximately 1.2 to 1 (Hart, 1997). The β1 and β2 isoforms are also found in various tissues, with β3 isoform specific to the testis. Because each β isoform is generated through alternative splicing, they contain great sequence similarity. The β1 and β2 isoforms share exactly the same sequence except for the C-terminus (β1 is 31 amino acids, β2 is 26 amino acids). β3 is identical to β2 with the addition of 29 amino acids at the N-terminal (Hug, 1992; Schafer, 1994; von Bulow, 1997) (Fig 4B). The β1 and β2 isoforms have distinct tissue specificity and subcellular locations (Schafer, 1994). The β1 isoform is highly expressed in muscle tissue with a ratio of β1 to β2 approximately 2:1, whereas the β2 isoform is predominately expressed in non-muscle tissue (Schafer, 1994; Hart, 1997, Hart, 1999). Furthermore, the β1 isoform localizes to the Z-disc in striated muscle, whereas the β2 isoform localizes to the intercalated discs and plasma membrane (Schafer, 1994). Overexpression of the β1 isoform in cardiac tissue leads to disruptions in the intercalated discs, and overexpression of the β2 isoform leads to deformation of myofibril architecture (Hart, 1999).

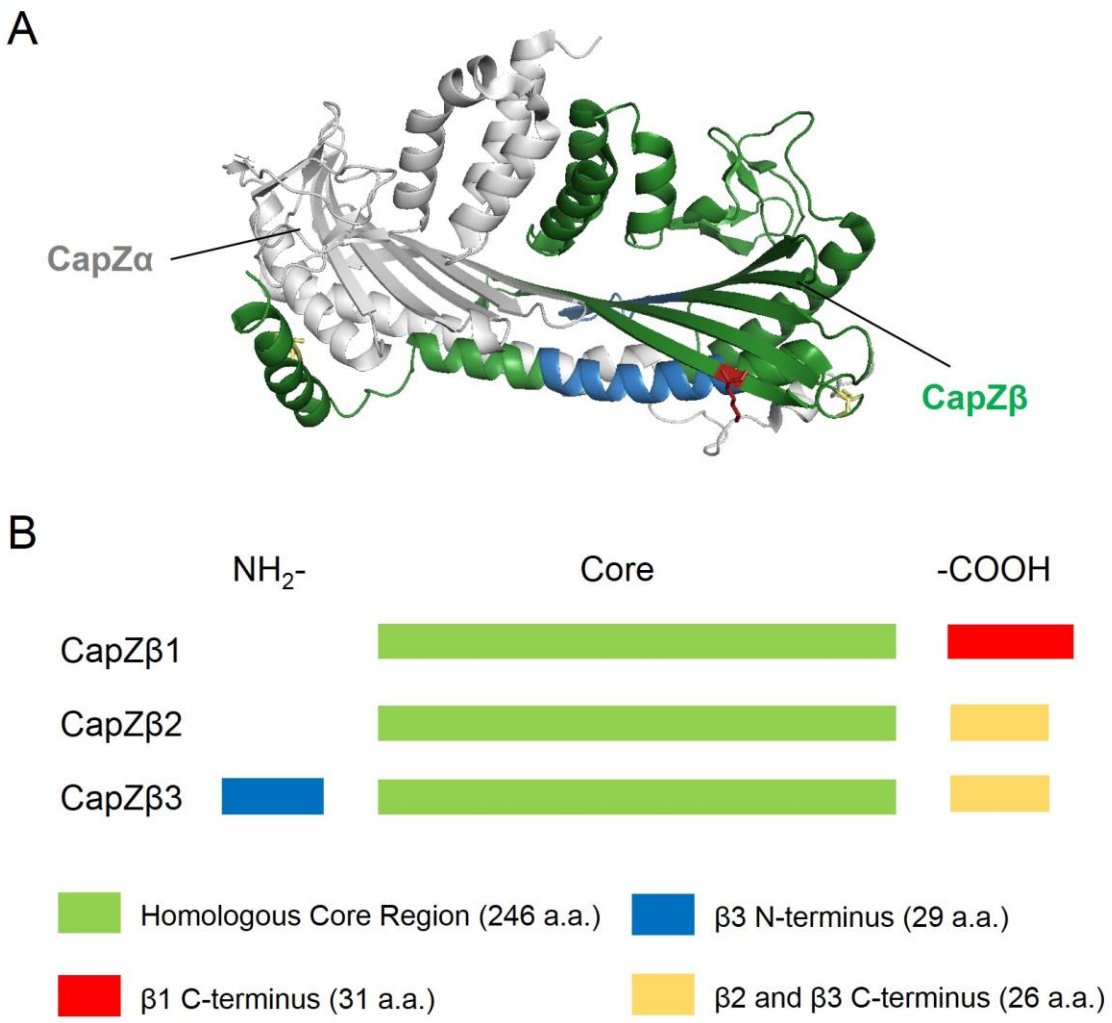

Figure 4. CapZ structure and sequence conservation. (A) Crystal structure of CapZα/β heterodimer. CapZα: grey; CapZβ: green. (B) CapZβ isoform sequence comparison. There are a 246 amino acids conserved core region of all isoforms, a unique 31 amino acids C-terminal extension of the β1 isoform, a common 26 amino acids C-terminal extension of β2 and β3 isoforms and a unique 29 amino acids N-terminal extension of the β3 isoform.

ii. CapZ Structure and Actin Capping

In 2003, Yamashita et al. proposed that the CapZ α/β is a mushroom-like heterodimeric protein (Figure 4). The two subunits have a similar secondary structure, leading to the pseudo-two-fold axis of rotational symmetry (Yamashita, 2003). The C-terminus of both α and β subunits have amphiphilic α-helices (helix 6) which bind to the hydrophobic cleft of actin. The hydrophilic sides of the C-terminus have isoform specific charge distributions and may be involved in isoform tissue specific recognition (Yamashita, 2003). Thus, the two C-termini of CapZ are hypothesized to govern both actin binding and specific protein targeting. Furthermore, when CapZ binds to F-actin by only its β-tentacle, the molecule is able to 'wobble' because of the flexible structure. Therefore, this may expose additional binding sites for other regulatory molecules (Kim, 2007). Data suggest that CapZ is intrinsically flexible allowing it to interact with the barbed-end of actin in both a high and low affinity state (Taketa, 2010), while the two C-termini are necessary for high-affinity actin binding (Wear, 2003; Kim, 2010). Modifications and mutations affecting the C-terminal binding region vastly reduce the actin capping ability (Kim, 2010).

In 2006, based on affinity and x-ray crystallography studies, Narita et al. proposed a "two-step" model: (i) the basic residues on the α tentacle and surrounding region (on helix 5) interact electrostatically with the barbed end of actin (ii) a conformational change of CapZ to a high-affinity form occurs, and (iii) supportive binding of the β tentacle strengthens the association (Kim, 2010). Thus, actin filaments might randomly dissociate from the α subunit C-terminal and only be connected to CapZ by the β subunit C-terminus. The flexibility of β tentacle would permit the body of CapZ to wobble,

allowing additional actin monomers to incorporate. Throughout these processes, CapZ might be regulated by the interaction with other proteins, phospholipids and post-translational modification. Together, these molecular changes may alter the CapZ capping properties, eventually affecting actin polymerization rates.

D. Mechanotransduction of the Myocytes

Muscles have a very complex mechanotransduction system since they can not only receive the mechanical signals from the environment but also generate internal loading by the contraction of the myofibrils. The study of the mechanotransduction system of the heart is decades old and is known to depend on wall stress of the myocardium related to the hypertrophic growth of the heart (Grossman, 1975). The field of mechanics notes that forces are transmitted throughout an entire structure. Thus, whether forces are delivered externally or generated internally, all parts of the muscle fibers are mechanically connected. Based on the location where the mechanosensing occurs, the mechanosensors can be either at the cell membrane or intracellular.

Cells are exposed during their lifetime to a variety of physical forces. These forces come from interaction with other cells, to extracellular matrices, to external mechanical stimuli or even from the forces generated internally by the cross-bridges. Alterations in these forces, either during development or changes in activity, result in modifications in cell biochemistry and adaptation in structure and function. The term mechanotransduction broadly refers to the mechanism by which cells convert mechanical stimulation into biochemical cellular signals. One primary mechanosensing structure of the cells is a

“focal adhesion”, which is a large macromolecular assembly on the membrane of cells. Connection between focal adhesions and the extracellular matrix generally involves integrins. Integrin is a transmembrane heterodimer (α and β subunit) with much variety based on the different combinations of α and β isoforms in different cell types (Humphries, 2000). Integrins sense the chemical composition and mechanical status of the extracellular matrix, and convert signals into intracellular chemical pathways, thereby affecting cell function in response to the environment.

i. Mechanotransduction at the Costamere

External forces encountered by cells include membrane stretch, altered adhesion and increase in pressure. In response to the stimuli, a mechanotransduction system is necessary. The most important extracellular mechanosensor of the myocyte is the costamere, which is a rib-like band of the focal adhesion complex that encircles the myocyte on membrane at the Z-line (Pardo, 1984; Samarel, 2005). The costamere is comprised of focal adhesions, which are a mechanotransduction apparatus in all cell types. Similar to the focal adhesions in other cell types, muscle cells have their specific integrin receptors, with integrins α1β1, α5β1, and α7β1 being the most highly expressed (Israeli-Rosenberg, 2014). Integrins “sense” the mechanical force from the environment, activating two major focal adhesion protein complexes: the dystrophin-glycoprotein complex and the integrin-vinculin-talin complex (Peter, 2011). The activated protein complex then aids the recruitment and activation of downstream signaling kinases such as focal adhesion kinase (FAK), Src, Rho-associated protein kinase (ROCK), mitogen-

activated protein kinases (MAPKs) and integrin-linked kinase (ILK). Together, this costamere complex provides the cell response to the mechanical stimulation.

ii. Intracellular Mechanotransduction

Since myofibrils provide the structural support as well as the contractile force of the myocyte, a mechanosensor might also be located inside the muscle fiber. The role of the Z-disc in mechanotransduction was introduced in the previous section. Another mechanosensor mentioned above in the sarcomeres is titin. Titin is a giant sarcomeric protein with very high elasticity and connects to many structural proteins in the sarcomere. When the cell is mechanically strained, all proteins including titin are pulled. The extension and deformation of the elastic titin might make several protein binding sites more accessible. For example, mechanical stretch increases the binding of muscle ankyrin repeat proteins (MARP) to the titin mechanosensor complexes (N2A) in the I-band (Miller, 2003). The extension of titin may make the N2A domain more accessible for MARP. Thus, MARP is activated by its interaction with titin, and can affect transcription and regulate myofibrillar assembly, cardiogenesis and myogenesis (Kojic, 2011). N2B is another titin mechanosensor complex in the I-band. With mechanical stimulation, N2B binds with LIM protein 1 (FHL1), which can activate the RAF, MEK1/2 and ERK pathways and induce hypertrophy (Sheikh, 2008). Proteins in the M-line can also be activated by mechanical strain (Lange, 2005). Titin kinase (TK) is in the M-line region of the C-terminus of the titin. Activated TK has a significant function of coordinating the muscle-specific ubiquitination pathways and myofibrillar protein turnover (Bogomolovas, 2014).

E. Protein kinase C

The mechanisms of signaling pathways are to transfer information from a detector to a downstream target. Protein phosphorylation or dephosphorylation of a protein within the cell is a major end point of signaling. Kinase refers to the enzyme which performs the phosphorylation of an amino acid, namely serine, threonine or tyrosine. The protein kinase C (PKC), a serine / threonine kinase, was one of the earliest kinases to be discovered (Takai, 1977). The PKC family has a variety of isoforms and numerous downstream substrates. Also, Diacylglycerol (DAG) and phorbol ester are the products of many cellular reactions and activate PKC, making this signal a wide-ranging and powerful one (Newton, 1995). Therefore, PKC is important in the regulation of many cellular processes including survival, proliferation, differentiation, apoptosis and migration. Later, the phosphatases remove the phosphate allowing the signaling to begin again (Scruggs, 2011).

i. Protein Kinase C Structure and Isoforms

To date, three families and ten isoforms of PKCs have been identified, expressed by nine genes (Tarafdar, 2014). The three families are: (1) The ‘classical’ PKCs (cPKC: α, βI, βII, and γ), activated by calcium, DAG and phosphatidylserine; (2) the ‘novel’ PKCs (nPKCs: δ, ε, η, φ, and μ), activated by DAG and phosphatidylserine; (3) the ‘atypical’ PKCs (aPKCs: ζ and λ) that require only phosphatidylserine for activation.

PKCs contain the following conserved domains, as shown in Figure 5.

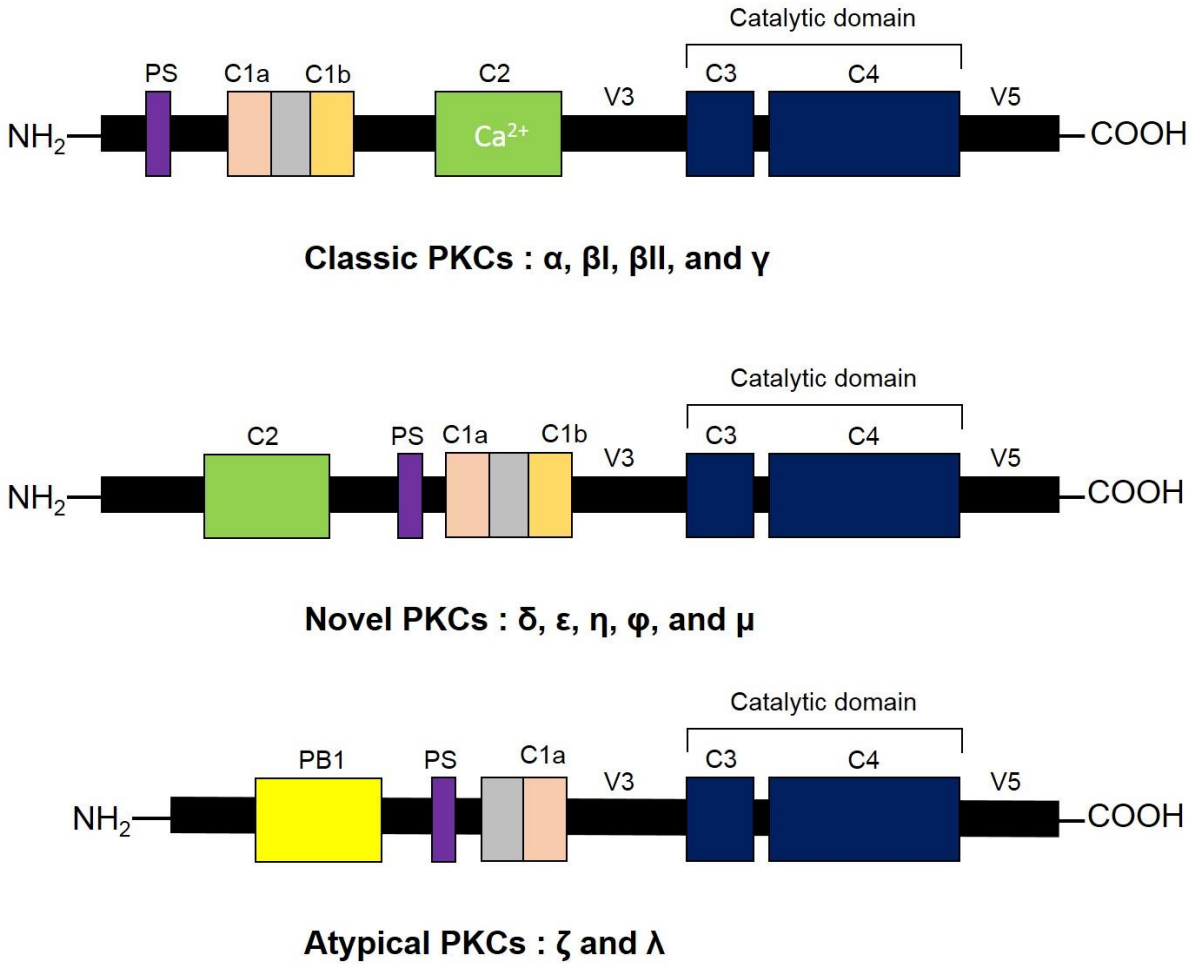

Figure 5. Domain structure of the different subgroups of the PKC family. PS: N-terminal pseudosubstrate domain; C1: DAG / phorbol ester binding domain; C2: calcium / phospholipids binding domain; PB1: aPKCs specific domain for the formation of aPKCs-containing complex; V3: the hinge region; C3 & C4: catalytic kinase domain; V5: a phosphorylatable region involved in the activation of some isoforms.

(1) N-terminal PS domain (pseudosubstrate domain): a regulatory domain that interacts with the kinase domain and blocks kinase activity in the unactivated molecule (House, 1987).

(2) C1 domain (DAG / phorbol ester binding domain): a cystine-rich domain that provides the ability to bind diacylglycerol / phorbol esters, with the C1b segment being critical for this function. C1 domain has a tandem repeat: C1a and C1b, which both presents in cPKCs and nPKCs. aPKCs do not have C1b, so that their C1 domain is not accessible to DAG or to phorbol esters.

(3) C2 domain (calcium / phospholipids binding domain): the domain with aspartate-rich residues that confers the ability to bind calcium. nPKCs do not have the calcium binding site, so that they only need phospholipids for activation. aPKCs do not have C2, so that they do not need both (calcium and phospholipids) for activation.

(4) PB1 domain: only aPKCs contains PB1, helping the formation of aPKCs-containing complex that might be related to target specificity (Moscat, 2009).

(5) V3 (hinge region): a hinge region, allowing the auto-inhibition of the PS domain to interact with the kinase domain. V3 is susceptible to proteolytic cleavage that releases the auto-inhibition, which can be used to generate some constitutively active isoforms (Steinberg, 2008).

(6) C3 & C4 domain (catalytic kinase domain): an extremely conserved domain among all PKCs, so it cannot be used to identify specific isoforms.

(7) V5 region: a phosphorylatable region, which is involved in the activation of some isoforms. There is very high variation among all isoforms at the extreme end of the C-terminal. Therefore, the C-terminus is often used for specific antibody production.

PKCs require a series of phosphorylations to become fully mature and to transduce their signaling function (Newton, 2003). The phosphorylation regions are on the "activation loop" in the kinase domain, in the "turn" and in the "hydrophobic" motif in the V5 region (Keranen, 1995). PKCs that are not phosphorylated at all three locations will not be ready for activation by the second messengers- diacyl-glycerol (DAG) and phosphatidylserine (PS) (Zeng, 2012). The exception are the aPKCs, which do not require the phosphorylation on the hydrophobic motif. The formation of DAG on the plasma membrane is classically described as the IP3/DAG pathway: phospholipase C (PLC) hydrolyzes phosphatidylinositol-4,5-biphosphate (PIP_2) into inositol 1,4,5-triphosphate (IP3) and DAG through activation of Gqα receptors, with IP3 being released into cytosol while DAG remains on the membrane. For cPKC, calcium binds the C2 domain, targeting it to the plasma membrane. There is the C1 domain which binds PS and DAG with receptors for activated PKC (RACKs) (Ron, 1995). RACKs have high specificity for their substrate PKCs, contributing to the localization and activation of PKCs (Mellor, 1998).

ii. Regulatory Functions of PKCε in the Heart

PKCε was first discovered among the novel PKC isotypes by cDNA cloning. PKCε can target to a specific cellular compartment, depending on second messengers and the

activated adapter proteins in response to extracellular signals (Dorn, 2002). In the heart, the relative proportions of PKC isozymes have been controversial since different results were reported in different species. PKCε was initially described as the major PKC isozyme in the rat heart (Bogoyevitch, 1993). Later, many other PKCs (PKCα, PKCδ, and PKCζ) were also found (Mackay, 2001). General consensus now is that two novel PKC isozymes, PKCε and PKCδ, along with the classic PKCα, are the predominantly expressed PKCs in human and rodent hearts (Duquesnes, 2011). PKCε enhances cardiac contractility and remodeling (Deng, 1997; Pi, 2000), and has a cardio-protective function in pre-conditioned heart (Chen, 2001). Also, transgenic overexpression of PKCε leads to concentric cardiac hypertrophy (Takeishi, 2000). When activated, PKCε translocates to the Z-disc (Disatnik, 1994; Dorn, 1999; Robia, 2001). A dominant-negative mutant of PKCε prevents the assembly of the optimal resting length of the sarcomere after sustained mechanical strain, suggesting that it has a regulatory role (Mansour, 2004). Interestingly, in transgenic models of CapZ downregulation, PKC dependent regulation of myofilament function is abolished, and activated PKCε and PKCβ binding to the myofilament is diminished (Pyle, 2002). Furthermore, alteration of CapZ dynamics was measured by fluorescence recovery after photobleaching (FRAP) in neurohormonally stimulated myocytes and shown to alter hypertrophy through PKCε and PIP_2 dependent pathways (Hartman, 2009).

F. Histone Deacetylases

Transcription in eukaryotes is strongly influenced by chromatin and the tight helical winding of DNA. A histone complex is necessary for this winding, which effectively blocks gene expression. Post-translational modifications, such as reversible acetylation of the lysine residues of histone, have long been linked to transcriptional activation because of the role of histones in DNA winding. The histone deacetylases (HDACs), the enzymes that remove acetyl groups from the acetylated lysine residues of histone, were first discovered by Taunton et al. in 1996. Histone acetylation alters chromatin structure and gene expression. Therefore, HDACs were generally regarded as transcriptional repressors and acting only on histones. In 2000, Luo et al. first found that HDAC1 can also work on a non-histone protein, p53 (Luo, 2000). Later, some HDACs, such as Class IIb HDAC6 and SIRT2 (a Class III HDAC), were found to be predominantly in the cytosol and deacetylate the cytoskeletal protein α-tubulin (Hubbert, 2002; North, 2003). More functions for HDAC activities in the cytosol continue to be reported. Thus, in hindsight, the term “histone” deacetylase is not correct, and is ought to be renamed “lysine deacetylase (KDAC)” (Choudhary, 2009).

i. Classes, Isoforms and Functional Differences of HDACs

To date, eighteen mammalian HDACs have been identified. They are encoded by distinct genes and grouped into four classes based on their homology to yeast HDACs, subcellular localization and catalytic activities (Thiagalingam, 2003) (Figure 6):

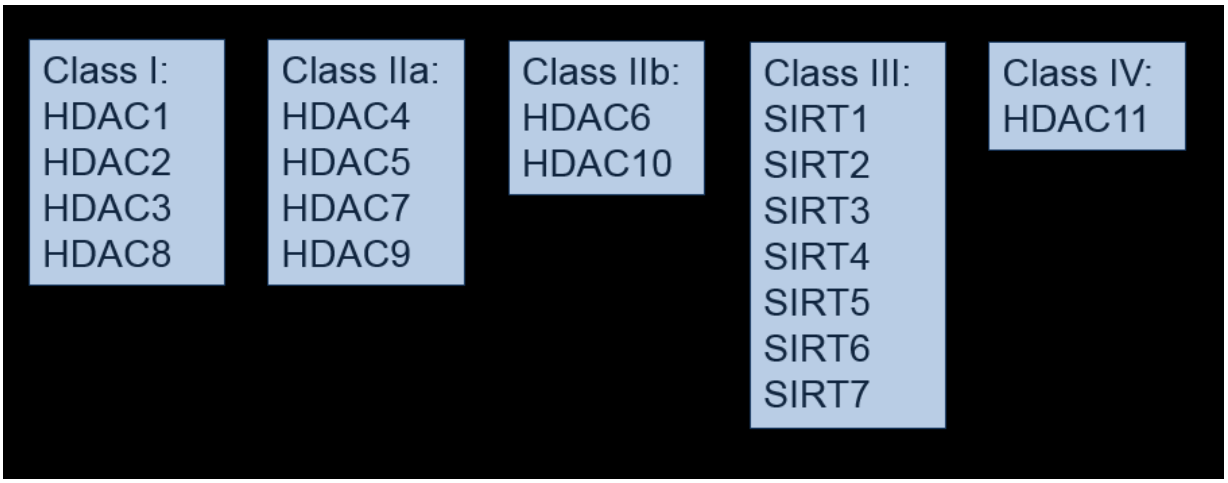

Figure 6. Histone deacetylase (HDAC) classes. HDACs are categorized into four classes. Class II HDACs have two sub-classes, IIa and IIb. Class I, II, and IV HDACs are zinc-dependent enzymes. Class III HDACs are NAD^+-dependent.

(1) The Class I HDACs (1, 2, 3 and 8), homologs to the RPD3 in yeast. They are mostly in the nucleus and have ubiquitous expression in different human cell lines and tissues

(2) The Class IIa HDACs (4, 5, 7 and 9), homologs to the Hda1 in yeast. They are able to shuttle between the nucleus and the cytoplasm. A nuclear localization signal (NLS) containing arginine / lysine-rich motif can be found in the N-terminal domain of all four Class IIa HDACs.

(3) The class IIb HDACs (6 and 10) are found in the cytoplasm. They are the only HDACs that contains two catalytic domains. For example, HDAC6 has an α-tubulin deacetylase domain targeting the α-tubulin (Hubbert, 2006).

(4) The Class III HDACs (SIRT1, 2, 3, 4, 5, 6 and 7) are homologs to the Sir2 of yeast. They are distinct from other HDACs because they need NAD+ for their activities in response to changes in the cellular redox status.

(5) The Class IV HDAC11, the only member. It shares sequence of the catalytic core regions (zinc-dependent) with class I and II HDACs, but does not have enough similarity to be either of them (Gao, 2002).

The zinc-dependent catalytic activities of Class I and II HDAC are now used in the production of HDAC inhibitors, which usually have zinc-chelating functions (Marks, 2010).

ii. The Role of HDACs in the Cardiac Hypertrophy

Recent studies reported that manipulating the activities of HDACs in the heart by transgenic gene deletion and overexpression can mediate the generation of cardiac hypertrophy:

a. Class I HDACs mediate hypertrophic pathway:

A cardiac-specific knockout of either HDAC1 or HDAC2 does not affect the phenotype of the hypertrophic heart, while the HDAC1 / HDAC 2 double knockout can lead to dilated cardiomyopathy and heart failure. The need for either HDAC1 or HDAC2 expression suggests redundant functions, but may play a crucial role in myocardial growth, morphogenesis, and contractility (Montgomery, 2007). Furthermore, cardiac-specific HDAC2 overexpression leads to serious hypertrophy (Trivedi, 2008). Taken together, Class I HDACs appear to induce the enlargement of the heart through myofibril growth by activation of the expression of the hypertrophy-related genes.

b. Class IIa and Class III HDACs are cardio-protective:

The myocyte enhancer factor 2 (MEF) is a transcription factor that is activated in myocytes by hypertrophic stimulation. Class IIa HDACs bind the myocyte enhancer factor 2, inactivating the downstream hypertrophic responses (Lu, 2000; McKinsey, 2002). Furthermore, gene deletion of Class IIa HDACs results in hypertrophy, while overexpression of them suppresses the MEF2-induced hypertrophy response (Chang, 2005; Backs, 2006). Similarly, overexpression of Class III HDAC SIRT1 counteracts the oxidative-stress induced apoptosis, while overexpression causes apoptosis (Alcendor, 2007). Taken together, Class II and Class III HDACs prevent myocytes from hypertrophy and increase their viability.

iii. Therapeutic Potential for HDAC Inhibitors in the Heart

Pathological hypertrophy is generally regarded irreversible in cardiac disease, meaning the downward progress of the hypertrophic heart to maladaptation is almost inevitable (Frey, 2003). Epigenetic regulation of hypertrophy-related genes to stop maladaptation by HDAC inhibitors has been a new target in the treatment of heart disease. In recent years, preliminary trials of HDAC inhibitors in cardiac hypertrophied have made remarkable achievements: Pan Class I&II HDAC inhibitors, such as Trichostatin A and Valproic acid, were shown to have beneficial effects on the hypertrophy heart injured by transverse aortic constriction (TAC) (Antos, 2003; Cook 2003). However, pan HDAC inhibitors also blunt the function of Class II HDACs, which are cardiac-protective. Thus, the trial of more Class I specific drugs, such as MGCD0103 for HDACs1-3, or of BA-60 for HDACs 1-2, needs to be tested further in the hope of achieving a better therapy.

G. Hypothesis and Specific Aims

Cardiac hypertrophy is widely regarded as a general outcome of cell remodeling after volume or pressure overload, which eventually leads to heart failure. Many subcellular components in cardiomyocytes are affected by hypertrophic stimulation for which the contractile filaments are crucial. Thus, the regulation of actin filament assembly by the actin capping protein (CapZ) needs to be better understood. Furthermore, additional research is needed regarding the post-translational modification (PTM) of the actin thin filament capping protein, CapZ, which might lead to the increased thin filament assembly in hypertrophic hearts. PKCε belong to novel PKCs, and can translocate to the Z-disc when myocytes are stimulated by hypertrophic agonists. Also, Histone

deacetylases (HDACs) are a family of enzymes that can mediate the generation of cardiac hypertrophy. The approach is to use failing human heart in addition to cultured NRVMs stimulated for growth. The roles of HDAC3 and PKCε activities in the mediation of CapZ PTMs and actin capping are explored in living myocytes.

Hypothesis 1. Increased CapZ dynamics reduce the capping property and result in an increase of actin dynamics, eventually leading to actin filament assembly during hypertrophy

Specific Aim 1.1. What is the time course of increase of CapZ dynamics in NRVM after the initial hypertrophic stimulation?

NRVMs are treated for one hour of 10%, 1Hz cyclic strain. The time course of the increase and recovery of CapZ dynamics is monitored by FRAP of GFP-tagged CapZ in NRVM after strain.

Specific Aim 1.2. Does initiation of hypertrophic stimulation increase actin dynamics in NRVM?

The time course of the alterations of actin dynamics is observed by FRAP of actin-GFP in NRVM. The time course of the alteration of CapZ and actin dynamics is compared to see how actin dynamics is related to CapZ dynamics

Specific Aim 1.3. Does CapZ dynamics directly affect actin dynamics?

Adenoviral infection of NRVM with CapZβ1ΔC mutant forces the increase of CapZ dynamics in NRVM to simulate the initiation of the hypertrophic stimulation. Actin dynamics is measured by FRAP in these infected cells.

Hypothesis 2. Actin assembly and myocyte growth is regulated via CapZ phosphorylation mediated by PKCε and by acetylation mediated by HDACs. The coordination of these two PTMs blunts CapZ capping, leading to thin filament assembly.

Specific Aim 2.1. To identify the PTMs of CapZ in failing heart tissue or hypertrophic NRVMs.

2D gel electrophoresis and mass spectrometry are used to identify the sites and types of post-translation modifications. The goal of this aim is to test whether acetylation and phosphorylation are crucial in the regulation of protein functions.

Specific Aim 2.2. To test whether PKCε-mediated CapZ phosphorylation alters CapZ and actin dynamics with myocyte growth after mechanical stimulation.

Adenovirus expressing constitutively active PKCε and dominant negative PKCε are used to test how PKCε activities affect CapZ and actin dynamics by FRAP. Also, 2D western blots are performed in NRVMs to test whether CapZ phosphorylation is directly mediated by PKCε.

Specific Aim 2.3. To test whether HDACs-mediated CapZ acetylation alters CapZ and actin dynamics with myocyte growth after mechanical stimulation.

Specific HDAC inhibitors are used to test how HDAC activities affect CapZ and actin dynamics by FRAP. Also, 2D western blot are performed to observe the variation of CapZ acetylation.

Specific Aim 2.4. How are acetylation and phosphorylation signals coordinated by CapZ?

The approach is to control acetylation and/or phosphorylation of CapZ as in Specific Aim 2.2 and 2.3, confirme by 2D DIGE and measure the effects on cell size, actin and CapZ dynamics.

II. CAPZ AND ACTIN CAPPING DYNAMICS INCREASE IN MYOCYTES AFTER A BOUT OF EXERCISE AND ABATE IN HOURS AFTER STIMULATION ENDS

A. Introduction

The heart muscle remodels to the demands of exercise by regulation of the size and shape of the myocytes. To study mechanisms of cytoskeletal dynamics, myocytes can be cyclically strained to mimic exercise (Terracio, 1988). Also, hypertrophy resulting from chronic demands can be mimicked by neurohormones such as norepinephrine (Fischer, 1965). Hypertrophy requires addition of new sarcomeres controlled by the Z-disc-associated proteins for addition of actin molecules to thin filaments. Most research studies several days of cyclic strain or chronic neurohormonal treatment in neonatal myocytes, but less attention is given to the normal, briefer pattern of activity seen in physiological cyclic strain as in athletes. Here, a one hour period of activity is applied to mimic the normal duration of activity and changes are evaluated over several hours after the stimulation ends.

Sarcomeres are assembled with hypertrophy, which requires the incorporation of the actin and myosin into the contractile filaments. The actin cytoskeleton in mature muscle cells is a very stable structural component. Nonetheless, mature sarcomeric actin filaments in muscle cells incorporate G-actin within minutes, indicating their dynamic nature (Glacy, 1983; McKenna, 1985). In recent studies, the dynamics of non-sarcomeric β-actin increased in adult cardiac myocytes under neurohormonal

stimulation (Balasubramanian, 2010), but stimulation of α-sarcomeric actin has not been explored.

Pressure or volume overloading, such as aortic stenosis or increased peripheral resistance, initiates cardiac remodeling. When loads are encountered, cardiac myocytes integrate extracellular, intercellular, and intracellular forces into intracellular signals through the mechanotransduction pathways (Samarel, 2005; McCain, 2011). However, the destination for the signaling cascades and how filament assembly and sarcomere remodeling occur are less well understood. CapZ capping is dynamic, as assessed by fluorescence recovery after photobleaching (FRAP) of GFP-CapZβ1 (Hartman, 2009). That study also found the dynamics of CapZ were elevated by neurohormonal stimulation such as phenylephrine (PE) and endothelin-1 (ET1) through a PKC- and a PIP_2-dependent pathway. Also, although calcium signaling plays an important role in mechanical activation of a myocyte, CapZ is not modified by intracellular calcium (Kilimann, 1982).

The goal of these experiments using neonatal rat ventricular myocyte (NRVM) in culture is to find how CapZ regulates sarcomeric actin filament remodeling with cyclic strain and how this returns to baseline after stimulation ends. The hypothesis is that 1 hour of mechanical stimulation is sufficient to regulate actin dynamics by CapZ in NRVM, which returns to the control level over time. First, the dynamics of CapZ in NRVM are analyzed after 1 hour of cyclic mechanical strain, and the time course is tracked for the next 3

hours. Second, the dependence of actin dynamics on CapZ is measured. Finally, a CapZ β tentacle mutant determines its role in both CapZ and actin dynamics.

B. Materials and methods

i. Cell culture

Primary heart cultures were obtained from neonatal rats according to Institutional Animal Care and Use Committee and National Institutes of Health guidelines for the care and use of laboratory animals. Hearts were removed and cells were isolated from 1- to 2-day-old neonatal Sprague-Dawley rats with collagenase (Worthington), as previously described (Boateng, 2003). The cells were re-suspended, filtered through a metal sieve to remove large material, and plated at high density (1,000 cells / mm2) in PC-1 medium (Biowhittaker / Cambrex) on fibronectin coated (25 µg / ml) FlexCell silicone membranes (200,000 cells/cm2). Cells were left undisturbed for 24 hours in a 5% CO_2 incubator. Unattached cells were removed by aspiration, and PC-1 media was replenished. Cells were left in incubator for another 24 hours before the experiment.

ii. Cyclic mechanical strain

Seventy-two hours after cell isolation, with or without viral infection, cyclic mechanical strain was generated with a Flexcell Strain Unit (model FX-4000, Flexcell International, Hillsborough, NC). NRVMs were strained at 10% elongation biaxially at 1 Hz sinusoidally for 1 hour in PC-1 medium. Strain magnitude, time, and waveform were

user-assigned to the system that controls vacuum pressure to deliver calibrated strain values to available elastic substrates housed in the incubator.

iii. Neurohormonal hypertrophic stimulation

Control cells were either stimulated or left unstimulated before photobleaching. The neurohormonal treatment times chosen were sufficient to induce hypertrophy (Hartman, 2009; Simpson, 1983). Phenylephrine (10 μM, Sigma-Aldrich) treatment was for 4 or 24 hours before FRAP analysis. Norepinephrine (20 μM, Sigma-Aldrich) treatment was for 24 or 48 hours before FRAP.

iv. Adenovirus

Forty-eight hours after cell isolation, recombinant adenoviruses used are GFP-CapZβ1 and GFP-CapZβ1 with the C-terminal deletion (GFP-CapZβ1ΔC). NRVMs were infected with CapZβ1 (MOI 20) or CapZβ1ΔC (MOI 20) for 60 min at 37°C diluted in PC-1 medium. Viral medium was then replaced with virus-free PC-1 medium for 24 hours.

v. Actin-GFP and actin-RFP expression

Forty-eight hours after cell isolation, actin-GFP and actin-RFP expression were induced by CellLight Reagents BacMam 2.0 actin-GFP or actin-RFP (Invitrogen). Two days after NRVM isolation, appropriate volume of CellLight Reagent (30 μl / 1,000,000 cells) was

used as modified from the manufacturer's instructions. Infected NRVMs are returned to the culture incubator for at least 16 hours.

vi. Immunostaining and confocal microscopy

NRVMs were washed with PBS, fixed with 4% paraformaldehyde (Sigma Aldrich) for 10 min, placed in cold 70% ethanol, and stored at −20°C until immunostaining. Cells were rehydrated in PBS (Sigma Aldrich) for 10 min. After rehydration, cells were incubated on a shaker table in 1% BSA in PBS for 1 hour at 25°C. Primary α-actinin (AbCam) antibody was diluted (1:250) in 1% BSA in PBS. The antibody was allowed to incubate on a shaker table at 4°C overnight. Cells were then rinsed in PBS at 25°C and blocked in 1% BSA in PBS for 1 hour at 25°C. Secondary antibody (Molecular Probes) was diluted at a ratio of 1:500 in 1% BSA in PBS and incubated for 1 hour at 25°C. Cells were washed in PBS. Anti-fade reagent with DAPI (Molecular Probes) was added, and cover slips were mounted on glass slides.

vii. Analysis of fluorescence recovery after photobleaching

FRAP analysis was referred to previous publications (Li, 1999; Sprague, 2004). For FRAP of GFP-CapZβ1, up to ten beating and well-striated cells (as evidenced by GFP-CapZβ1) were randomly selected for each FRAP. The intensity of the region of interest (I_{frap}) was observed both before (t_0) and immediately after (t_1) bleaching at full power, and intermittently every 2 min with lower excitation power (1~3%) and 800~1000 msec duration until the end of the 15 min. Further details are given in Table I. Images were

analyzed using Zeiss Imaging Browser. Plotted intensity values are given as a percentage of the difference between I_{frap} (t_0) and I_{frap} (t_1). Binding of CapZ to the actin filament has two binding states (30), so FRAP curves of CapZ were fit using non-linear regression in OriginPro (OriginLab, Northampton, MA):

$$I_{frap}(t) = 1 - C_1 e^{-Koff1\, t} - C_2 e^{-Koff2\, t} \quad (1)$$

The average kinetic constant (K_{frap}) for dynamics was calculated using the following formula:

$$K_{frap} = C_1 K_{off1} + C_2 K_{off2} \quad (2)$$

For FRAP of actin-GFP and actin-RFP, the intensity of the region of interest (I_{frap}) was observed both before (t_0) and immediately after (t_1) bleaching at full power, and intermittently every 10 sec (actin-GFP) or 20 sec (actin-RFP) with lower excitation power (1~3%) and 800~1000 msec duration until the end of the 8 min, referred to the recovery time of actin-GFP (28). Further details are given in Table II. Since actin binding activity has one-binding state (Pollard,1981), the equation for curve fitting using non-linear regression in OriginPro was:

$$I_{frap}(t) = 1 - C_1 e^{-Koff1\, t} \quad (3)$$

The average kinetic constant (K_{frap}) was calculated using the following formula:

$$K_{frap} = C_1 K_{off1} \quad (4)$$

viii. Data analysis

Data were presented as means ± SE. For FRAP assays, the sample number was defined as individual cells, of which one to five cells were analyzed per culture in at

least three separate cultures analyzed per experimental condition. Statistical significance was determined for FRAP curves by Student's t-test. Significance was taken at $P < 0.01$ or $P < 0.05$ as indicated.

C. Results

i. Effects of cyclic mechanical strain on sarcomeric CapZ dynamics.

A To test the potential of mechanical stimulation to induce thin-filament remodeling, the dynamics of the CapZ was measured by FRAP in NRVMs with or without 1 hour of 1-Hz, 10% cyclic strain (Fig. 7, A and B). Within 1 hour after cyclic strain, the FRAP profile was altered significantly (Fig. 7C). The kinetic constant (K_{frap}) gained from the results of curve fitting (Eq. 2) was significantly increased by ~80% within 1 hour after cyclic strain (Figure 7D and Table I) compared with nonstrained cells. The increased CapZβ1 dynamics abated after cessation of cyclic strain and returned to the control level by 2 hours after the end of strain (Figure 7D).

ii. Effects of cyclic mechanical strain on sarcomeric actin dynamics

Because of the role of CapZ in the regulation of actin filament assembly, the dynamics of the sarcomeric actin may also be altered. NRVMs infected with actin-GFP fusion protein showed the striated pattern, permitting dynamics of sarcomeric actin to be tested by FRAP (Figure 8, A and B). The profile of recovery of actin-GFP fluorescence is changed at the end of 1 hour of cyclic strain (Figure 8C). The kinetic constant (K_{frap}) of actin-GFP gained from the results of curve-fitting (Eq. 4) is significantly increased by

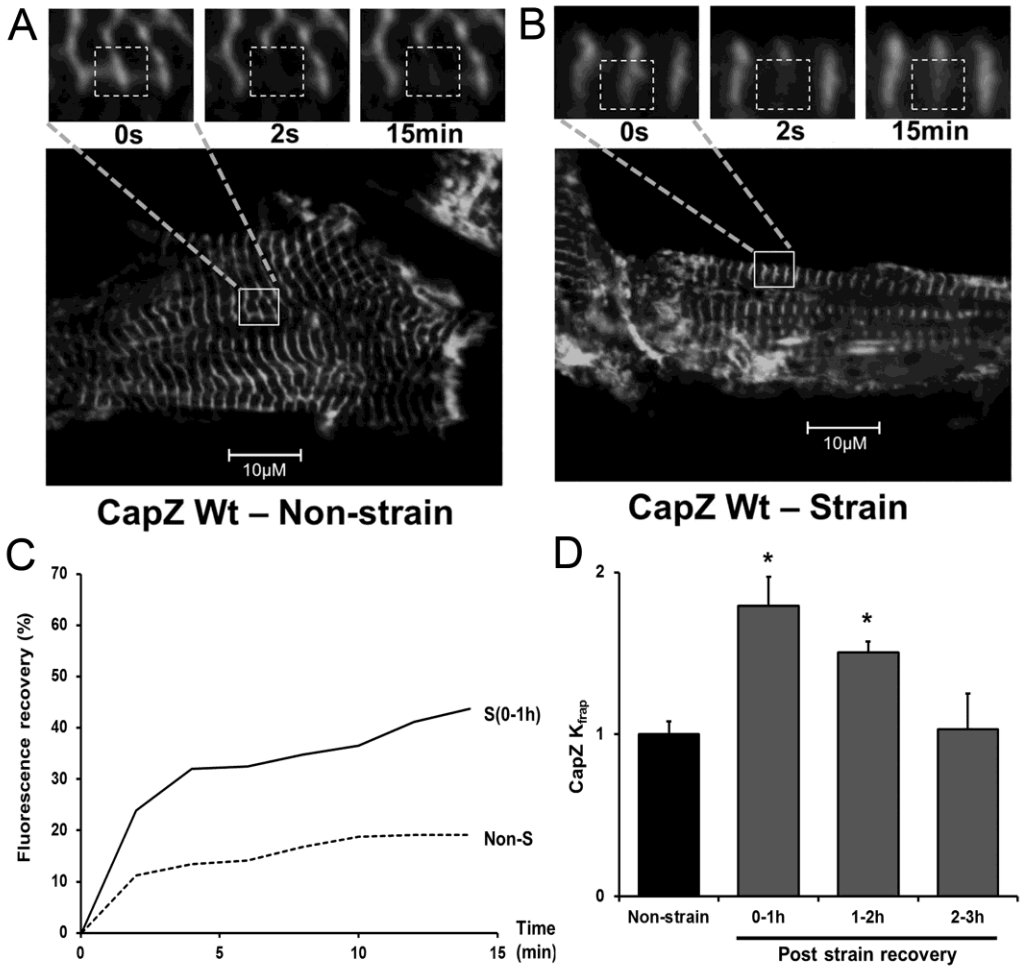

Figure 7. Time course of CapZβ1 dynamics after cyclic mechanical strain. Neonatal rat ventricular myocytes (NRVMs) infected by GFP-CapZβ1 were either unstrained or subjected to 1-Hz cyclic 10% strain for 1 hour. A and B: confocal images of GFP-CapZβ1 with FRAP shown before bleach (0 s), after bleach (2 s), and 15 min later in cells in the following conditions: A, unstrained with resting spontaneous beating or B, 1 hour after cyclic strain has ended. Region of interest (ROI) shown as dashed white boxes (3.75 μm × 3.75 μm). Inset: higher magnification images of area delineated by the solid white boxes in the lower magnification image. C: fluorescence recovery after photobleaching (FRAP) of GFP-CapZβ1 as a percentage of prebleach intensity with unstrained control (dashed line, Non-S) and within 1 hour after cyclic strain ended [solid line, S (0–1 h)]. D: K_{frap} values for CapZβ1 normalized to unstrained cells; 0 to ~1 hour (n = 5), 1 to ~2 hours (n = 4), and 2 to ~3 hours (n = 4). Values are means ± SE. *Significant difference ($P < 0.01$).

Table I. Comparison of parameters for CapZβ1 with cyclic strain or CapZ mutant

Curve fitting data: $I_{frap}(t) = 1 - C_1 e^{-Koff1\ t} - C_2 e^{-Koff2\ t}$

$K_{frap} = C_1 K_{off1} + C_2 K_{off2}$

	C_1 ($x10^{-1}$)	K_{off1} ($x10^{-2}$) (sec^{-1})	C_1 x K_{off1} ($x10^{-3}$) (sec^{-1})	C_2 ($x10^{-1}$)	K_{off2} ($x10^{-4}$)	C_2 x K_{off2} x(10^3)(sec^{-5})	K_{frap} ($x10^{-3}$) (sec^{-1})	n
Non-S	1.98 ± 0.37	1.44 ± 0.39	2.67 ± 0.20	8.07 ± 0.66	1.08 ± 0.99	8.10± 4.68	2.76 ± 0.37	4
S(0-1h)	3.03 ± 0.59	1.77 ± 0.31	4.84 ± 0.43*	7.04 ± 0.61	1.52 ± 1.50	11.93 ± 5.89	4.96 ± 0.42*	5
S(1-2h)	2.61 ± 0.21	1.60 ± 0.20	4.11 ± 0.21*	7.43 ± 0.23	0.54 ± 0.66	4.14 ± 2.84	4.15 ± 0.19*	4
S(2-3h)	2.25 ± 0.37	1.40 ± 0.45	2.82 ± 0.60	7.78 ± 0.39	0.30± 0.30	2.30 ± 2.10	2.84 ± 0.62	4
CapZΔC	2.66 ± 0.45	2.14 ± 0.44	5.28 ± 0.77*	7.44 ± 0.39	1.39 ± 0.38	10.65 ± 3.93	5.39 ± 0.79*	4

Ifrap, fluorescence intensity; t, time (sec); C1, equilibrium coefficient for 1st binding state; Koff1, kinetic constant for 1st binding state; C2, equilibrium coefficient for 2nd binding state; Koff2, kinetic constant for 2nd binding state; Non-S, Non-strain; S(0-1h), 0-1 hr after strain; CapZΔC, CapZβ1 with C-terminal deletion. Mean ± SEM. P values were obtained by Student's t-test. *P<0.01 vs. Non-S.

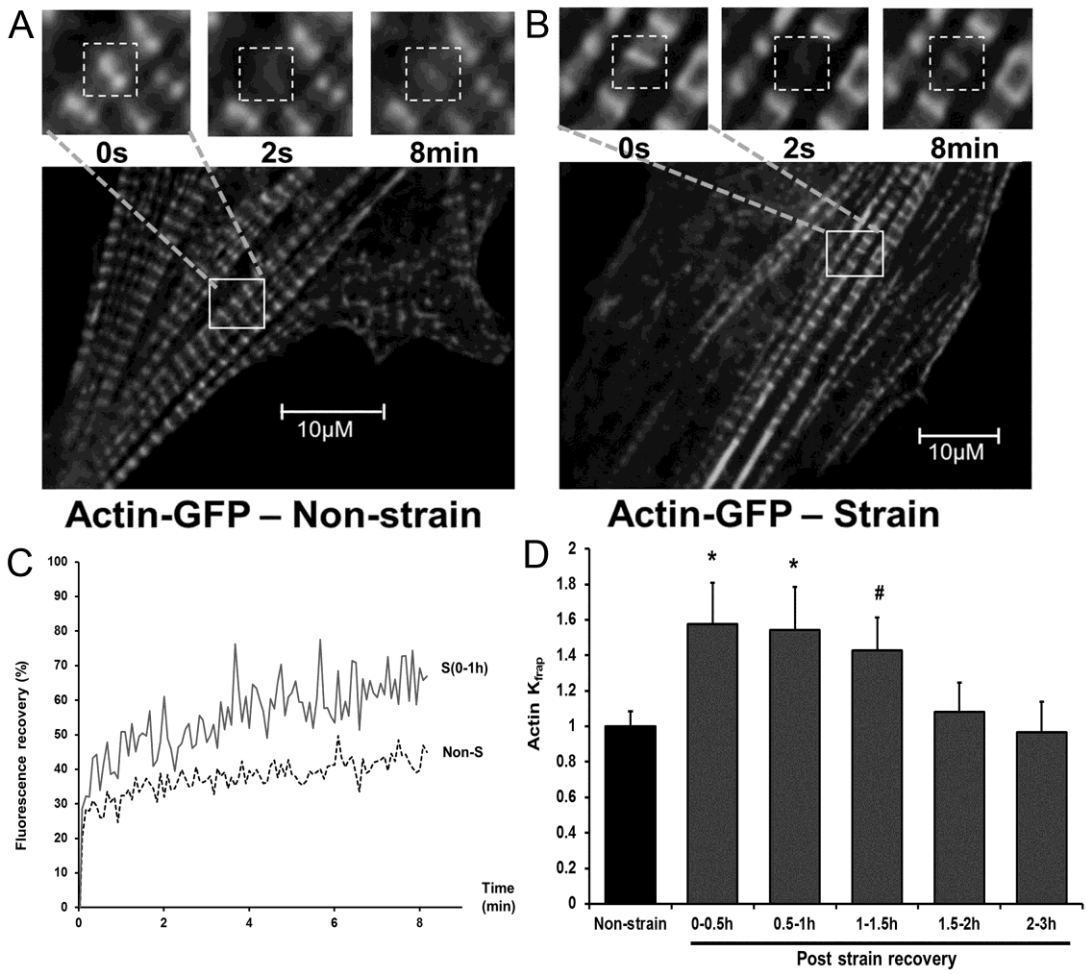

Figure 8 Time course for actin dynamics after cyclic mechanical strain. NRVMs infected by actin-GFP were either unstrained or subjected to 1-Hz cyclic 10% strain for 1 hour. A and B: confocal images of actin-GFP with FRAP shown before bleach (0 s), after bleach (2 s), and 8 min later in cells in the following conditions: A, unstrained with resting spontaneous beating B, 1 hour after cyclic strain has ended. Regions of interest (ROIs) are shown as dashed white boxes (3.75 × 3.75 μm). Inset: higher magnification images of area delineated by the solid white boxes in the lower-magnification image. C: FRAP of actin-GFP as a percentage of prebleach intensity with unstrained control (dashed line, Non-S) and within 1 hour after cyclic strain ended [solid line, S (0–1h)]. D: K_{frap} values for actin-GFP normalized to unstrained cells; 0 to ~0.5 hour (n = 6), 0.5 to ~1 hour (n = 5), 1 to ~1.5 hour (n = 4), 1.5 to ~2 hours (n = 8), and 2 to ~3 hours (n = 7) after strain were compared. Values are means ± SE. Significant difference: *P < 0.01; #P < 0.05.

Table II - Comparison of parameters for actin-GFP with or without cyclic strain

	Curve fitting data: $I_{frap}(t) = 1 - C_1 e^{-Koff1\ t}$ $K_{frap} = C_1 K_{off1}$			
	C_1 (x10^{-1})	**K_{off1} (x10^{-4}) (sec^{-1})**	**K_{frap} (x10^{-4}) (sec^{-1})**	**n**
Non-S	7.36 ± 0.20	6.36 ± 0.56	4.67 ± 0.39	13
S(0-0.5h)	6.70 ± 0.37	11.0 ± 1.66*	7.36 ± 1.09*	6
S(0.5-1h)	7.84 ± 0.37	9.19 ± 1.45$^{\#}$	7.20 ± 1.12*	5
S(1-1.5h)	7.51 ± 0.49	8.90 ± 0.12$^{\#}$	6.67 ± 0.86*	4
S(1.5-2h)	7.05 ± 0.43	7.19 ± 1.13	5.04 ± 0.77	8
S(2-3h)	7.14 ± 0.14	6.29 ± 1.13	4.51 ± 0.81	7

I_{frap}, fluorescence intensity; t, time (sec); C_1, equilibrium coefficient for 1st binding state; K_{off1}, kinetic constant for 1st binding state; Non-S, Non-strain; S(0-0.5h), 0-0.5 hour after strain; S(0.5-1h), 0.5-1 hour after strain; S(1-1.5h), 1-1.5 hour after strain; S(1.5-2h), 1.5-2 hours after strain; S(2-3h), 2-3 hours after strain. Mean ± SEM. P values were obtained by Student's t-test. *P<0.01 vs. Non-S; 0.01< $^{\#}$P <0.05 vs. Non-S.

~50% within 1 hour after cyclic strain (Figure 8D and Table II). The elevated sarcomeric actin dynamics returned to the control level 1.5 to ~2 hours after the cessation of cyclic strain (Figure 8D).

iii. Effects of neurohormonal hypertrophic stimulation on sarcomeric actin dynamics

To test whether the sarcomeric actin dynamics are also elevated by neurohormonal stimulation as shown for CapZ (Hartman, 2009), NRVMs were treated with PE (10 μM) or norepinephrine (NE; 20 μM), and FRAP of actin-GFP was measured (Figure 9). FRAP results demonstrated that actin dynamics increased by ~65% 24 hours after PE treatment and by ~90% 48 hours after NE treatment. The treatment time of 24 or 48 hours for neurohormonal stimulation was much longer than the 1 hour of cyclic strain.

iv. Localization and dynamics of mutant GFP-CapZβ1 fusion proteins in vitro

Since both CapZ and sarcomeric actin dynamics have similar time courses in response to cyclic strain and the previous studies are all from *in vitro* experiments, a possible interaction between CapZ and the actin filaments was addressed. It is known that the CapZβ1 mutant with its tentacle (C-terminus) deleted (CapZβ1ΔC) is critical in CapZ-actin interaction (Barron-Casella, 1995). In our study, the GFP-CapZβ1ΔC showed a Z-disc localization (Figure 10, A and B), but the recovery profile of GFP-CapZβ1ΔC in NRVMs showed a significant difference from wild-type GFP-CapZβ1 (Figure 10C).

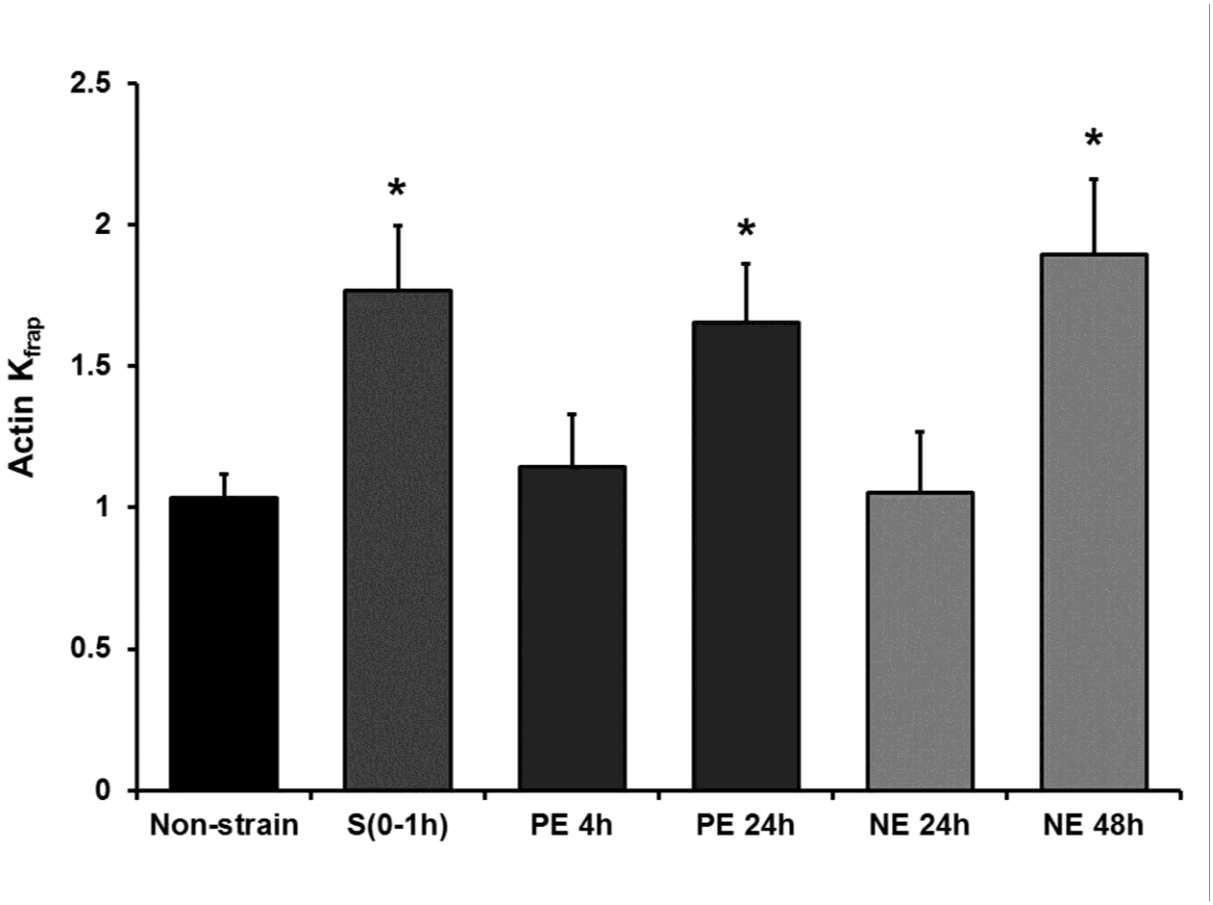

Figure 9 Actin dynamics after neurohormonal stimulation. K_{frap} values for actin-GFP FRAP in cells 4h (n = 5) or 24h (n = 4) after phenylephrine (PE) treatment and 24h (n = 6) or 48h (n = 4) after norepinephrine (NE) treatment, normalized to unstrained cells (Non-strain) or 0–1h after strain. S (0–1h), 0–1 hour after strain. Values are means ± SE. *Significant difference ($P < 0.01$).

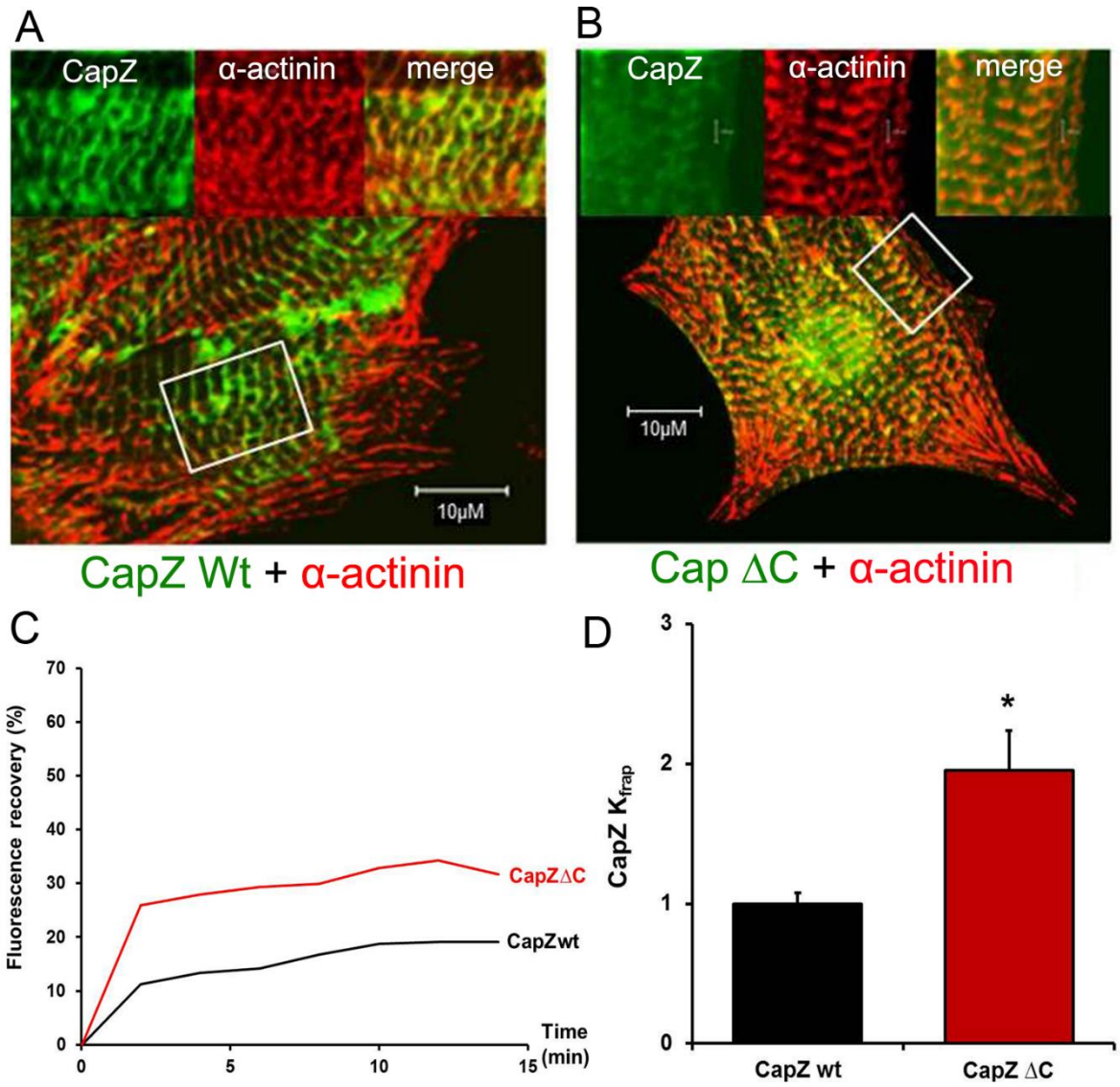

Figure 10 NRVMs expressing GFP-CapZβ1ΔC have higher CapZ dynamics than wild-type GFP-CapZβ1. A and B: GFP and α-actinin antibodies show colocalization of both the wild-type and the mutant GFP-CapZβ1 to the Z-disc. Boxed areas in whole cell are enlarged in insets. C: FRAP of wild-type GFP-CapZβ1 (black line, CapZwt) or C-terminal deletion CapZ (red line, CapZΔC) as a percentage of prebleach intensity. D: K_{frap} values normalized to unstrained cells have higher dynamics for GFP-CapZβ1ΔC (red bar, n = 4) compared with wild-type GFP-CapZβ1 (black bar, n = 4). Values are means ± SE. *Significant difference ($P < 0.01$).

Results of curve-fitting by the two binding-state model (Equation 2) demonstrated that CapZβ1ΔC had elevated K_{frap} by ~95%, confirming the importance of the β1 tentacle for CapZβ1 binding (Figure 10D).

v. Effects of CapZβ1 C-terminal tentacle on sarcomeric actin dynamics

Alterations of the interaction between CapZ and actin filaments affect the rate of actin assembly in a polymerization assay (Kim, 2004). To test whether changes of CapZ binding by the CapZβ1 C-terminus affect sarcomeric actin dynamics directly, NRVMs were infected with either wild-type GFP-CapZβ1 or GFP-CapZβ1ΔC, followed by expression of actin-RFP. The cells expressing actin-RFP, GFP-CapZβ1 + actin-RFP, or GFP-CapZβ1ΔC + actin-RFP (Figure 11, A and B) were subjected to FRAP of actin-RFP. The recovery profile of actin-RFP in NRVMs showed no major difference between actin-RFP alone and GFP-CapZβ1 + actin-RFP, but a significant difference in GFP-CapZβ1ΔC + actin-RFP was seen (Figure 11C). Results of curve-fitting demonstrated that expression of GFP-CapZβ1ΔC significantly elevated dynamics of actin by ~70% compared with cells expressing wild-type GFP-CapZβ1 (Figure 11D and Table III), suggesting that the β tentacle directly regulates actin dynamics.

D. Discussion

In this chapter, three novel findings are reported. First, in the NRVM primary culture system, the dynamics of CapZ, one of the major regulators of actin-filament assembly,

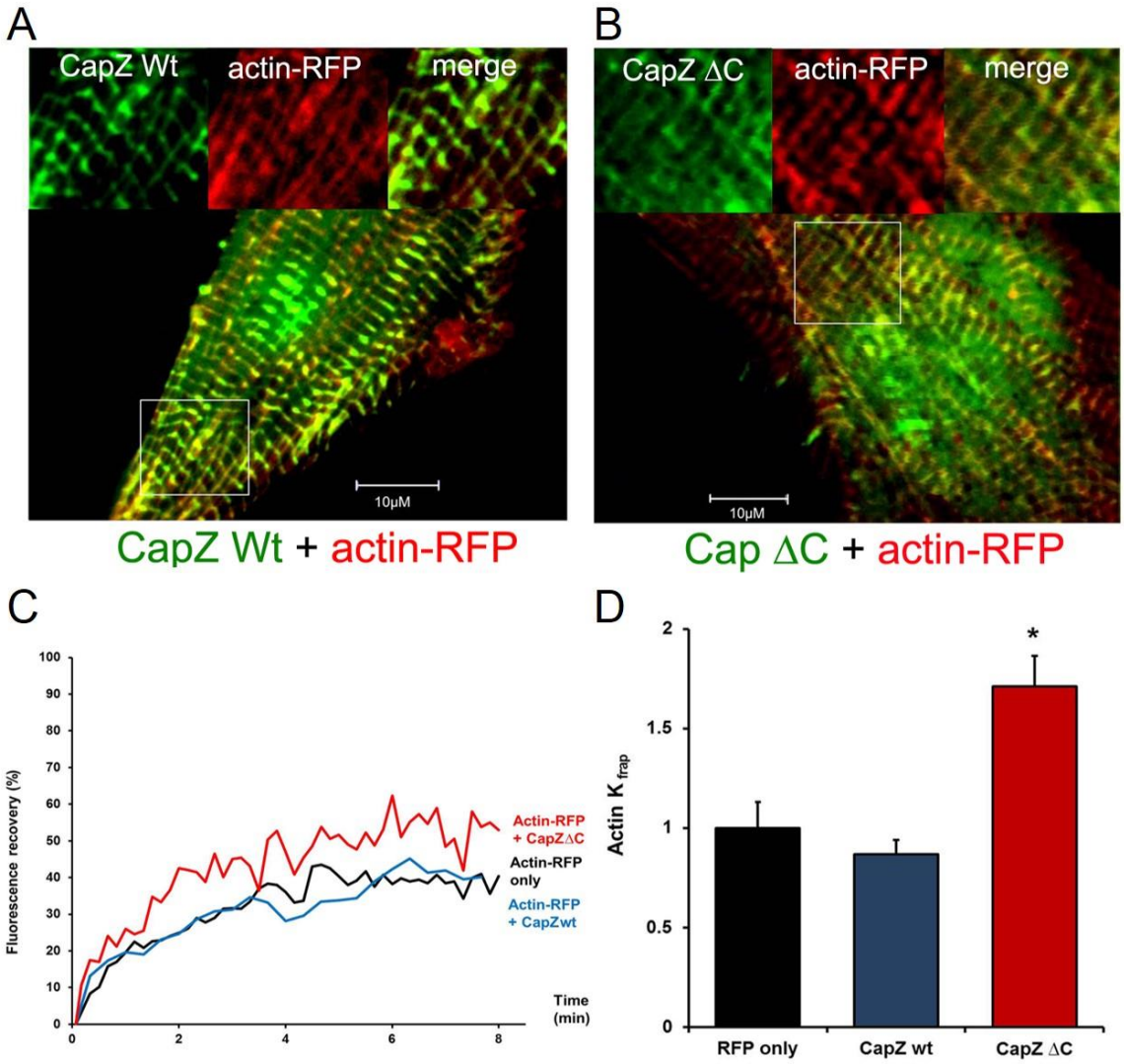

Figure 11 NRVMs expressing GFP-CapZβ1ΔC have higher actin dynamics than wild-type GFP-CapZβ1. A and B: confocal images show localization of CapZ and its mutant at the Z-disc, and actin-RFP localization adjacent to Z-disc in the I-band. C: actin-RFP FRAP alone as a percentage of prebleach intensity in cells (black line, actin-RFP), or actin-RFP also expressing either GFP-CapZβ1 (blue line, actin-RFP + CapZwt), or expressing the C-terminal deletion CapZ (red line, actin-RFP + CapZΔC). D: K_{frap} values normalized to the cells expressing actin-RFP alone (n = 4) show a higher recovery rate of actin-RFP in the cells expressing GFP-CapZβ1ΔC (red bar, n = 5) than the cells expressing wild-type GFP-CapZβ1 (blue bar, n = 5). Values are means ± SE. *Significant difference ($P < 0.01$).

Table III - Comparison of best-fitting parameters for actin-RFP with wild type or mutated CapZ

	Curve fitting data: $I_{frap}(t) = 1 - C_1 e^{-Koff1\ t}$ $K_{frap} = C_1 K_{off1}$			
	C_1 (x10^{-1})	**K_{off1} (x10^{-4}) (sec^{-1})**	**K_{frap} (x10^{-4}) (sec^{-1})**	**n**
Actin-RFP only	8.24 ± 0.20	10.5 ±1.62	8.64 ± 1.42	4
CapZ wt + actin-RFP	8.81 ± 0.25	8.96 ± 0.55	7.93 ± 0.63	5
CapZΔC + actin-RFP	8.40 ± 0.32	18.7 ± 2.11*	15.6 ± 1.39*	5

I_{frap}, fluorescence intensity; t, time (sec); C_1, equilibrium coefficient for 1st binding state; K_{off1}, kinetic constant for 1st binding state. Mean ± SEM. P values were obtained by Student's t-test. *P<0.01 vs. CapZ wt + actin-RFP.

was found to be elevated by mechanical strain at the end of a brief period of stimulation but to abate over the next 2 hours. Second, the dynamics of sarcomeric actin in NRVMs share a similar time course to CapZ for both the increase and abatement. Third, the β1-tentacle C-terminus of CapZβ1 may play an important role in filament assembly since sarcomeric actin dynamics are significantly enhanced when the tentacle is deleted. Thus it seems possible that muscle hypertrophy stimulated by mechanical forces 1) begins to remodel the actin filament within an hour, 2) abates over 2 hours after cessation of stimulation, and 3) involves the tentacle of the β1 subunit of CapZ.

i. Time course of the response of NRVM to mechanical stimulation

Mechanotransduction rapidly reacts to stimulation through signaling and posttranslational modifications, such as phosphorylation of existing proteins, thereby initiating sarcomeric remodeling. Phosphorylation of focal adhesion kinase (FAK) peaks within 1 hour after mechanical strain (Senyo, 2007; Torsoni, 2003) and returns to baseline levels 1–2 hours after stimulation ends (2). The increased dynamics of both actin and CapZ after a brief period of cyclic strain are in the same time frame as for FAK. Thus the time course of CapZ and actin dynamics 2 hours after stimulation ends suggests a reversal mechanism, such as dephosphorylation might occur. For example, protein phosphatase 1 (PP1), a well-known phosphatase in NRVM, dephosphorylates PKC α in an hour (Belin, 2007) and possibly participates in the increase and abatement of CapZ dynamics. Also, the tensin homolog (PTEN) is a phosphatase that rapidly regulates the synthesis of phosphoinositide (PI), which itself is an important regulator of CapZ capping (Schafer, 1996). Its role of dephosphorylating FAK in muscle cells

(Aikawa, 2002; Gupta, 2009; Seqqat, 2012) may suggest that it is a potential candidate for regulation of the active time course in response to mechanical stimulation.

ii. Comparison of the effects of mechanical strain and neurohormonal hypertrophic stimulation

Both mechanical strain and neurohormonal stimulation result in the increase of CapZ and sarcomeric actin dynamics, suggesting that both alter actin filament assembly during hypertrophy. PE and NE elicit hypertrophy and cardiac remodeling via small G proteins and share many signaling pathways with mechanical stimulation, such as Ras, Rac, Rho, and the downstream activation of MAPKs (Li, 1999). Noticeably, although only 1 hour of cyclic mechanical strain alters actin capping and actin dynamics, it takes days for neurohormonal stimulation to produce similar changes (1 day for PE, 2 days for NE). Furthermore, our lab reported that the rapid response of actin dynamics to mechanical strain is triggered by an increased PIP_2 level and its binding to CapZ (Li, 2013).

iii. Role of the β1 tentacle of CapZ in regulation of capping properties in NRVM

A model is proposed for the mechanism by which the interaction between CapZ and actin regulates actin assembly after a brief period of mechanical stimulation (Figure 12). This model is based on results in NRVM of CapZ and actin dynamics after cyclic strain or with the CapZβ1 terminal deletion mutant. Under normal conditions when adaptation

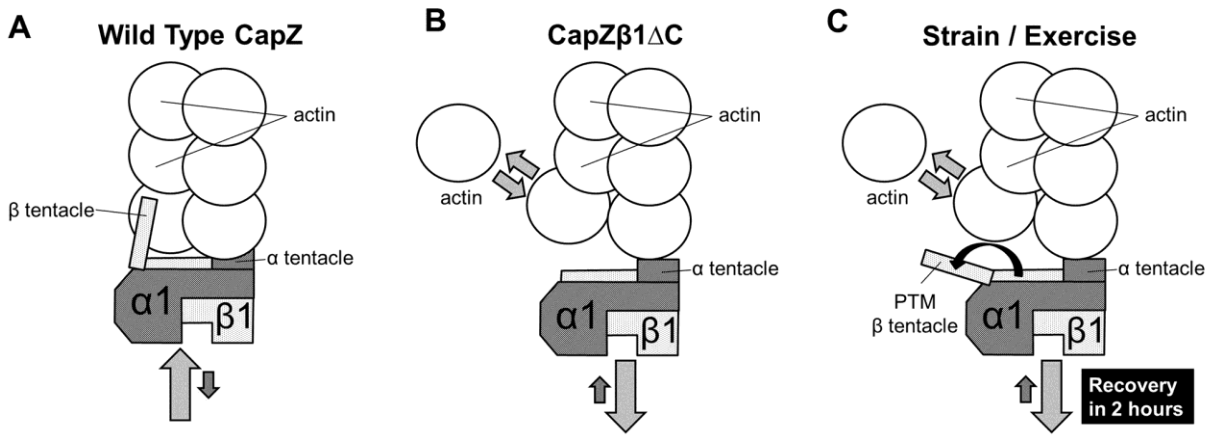

Figure 12 Model of interactions between CapZ and sarcomeric actin. A: in unstrained conditions when NRVMs beat spontaneously but are not growing, the CapZ tightly caps the barbed end of the actin filament [on rate (light gray arrow) > off rate (dark gray arrow)]. B: the deletion of β tentacle significantly increases CapZ dynamics [off rate (light gray arrow) > on rate (dark gray arrow)], which weakens the binding of CapZ to the actin filament. The dynamics of the actin monomer on and off the actin filament is elevated (arrows with two directions). C: mechanical stimulation also significantly increases CapZ dynamics [off rate (light gray arrow) > on rate (dark gray arrow)], possibly because of structural change of the β tentacle (black arrow) through posttranslational modification. The β tentacle of CapZ is released from its actin-binding state, which leads to an elevated actin off rate (arrows with two directions).

is not occurring, the two tentacles of CapZ tightly cap the barbed end of the actin filament, resulting in a low actin mobility and a low actin off rate (Figure 12A). The deletion of the β tentacle significantly weakens the actin capping and increases CapZ dynamics, thus elevating the off rate of actin (Figure 12B). After brief mechanical stimulation, the capping of CapZ is also decreased, and the off rate of actin is elevated (Figure 12C). This is possibly due to posttranslational modifications of the β tentacle of CapZ that alter the actin off rate. The model suggests a relationship between CapZ capping and actin dynamics, but the experiments do not prove actin assembly directly in cultured cells. However, this is a likely mechanism, since biochemical methods in vitro show actin assembly when the capping is altered (Wear, 2003; Kim, 2010). The binding of CapZ to the actin filament, however, is not controlled only by the CapZβ tentacle. The CapZα tentacle is the target of CapZ inhibitors (Takeda, 2010), but the regulatory role of the α tentacle in mechanical strain-induced sarcomeric actin remodeling has not yet been investigated. Undoubtedly, other partnering proteins, posttranslational modifications, and ions, such as calcium, are also involved in control of actin filament assembly in response to different functional demands of the heart.

E. Conclusion

In conclusion, the interaction of CapZ and actin in the thin filament is altered after strain in NRVM in culture. A model is proposed to explain the possible role of the β tentacle of CapZ in NRVM after mechanical stimulation. One hour of cyclic strain is sufficient to increase the dynamics of sarcomeric actin through CapZβ1, and this process returns to

baseline in only a few hours after cessation of the stimulation. Thus remodeling of actin thin filaments in cardiac myocytes lasts for only a few hours after a bout of exercise and may involve the C-terminus (β tentacle) of CapZβ1. It is possible that cycles of activity and rest may be important for a healthy muscle, whereas the sustained stimulation may be a factor in the maladaptation that occurs in chronic cardiac disease.

III. ACTIN ASSEMBLY IS REGULATED THROUGH PHOSPHORYLATION AND ACETYLATION OF THE ACTIN CAPPING PROTEIN CAPZ IN CARDIOMOCYTES

A. Introduction

Hypertrophic stimulation can lead to both long term modification in gene expression and short term modification in the proteome (Hunter, 1999). In chapter II, the increased CapZ and actin dynamics of myocytes occur very quickly (within 0-1 hour) in response to mechanical strain, suggesting the possible involvement of PTMs which are nearly instantaneous but may affect protein functions. The effects of PTMs on the binding affinity of actin regulatory proteins have been reported. For example, the phosphorylation of the C-terminal of the cardiac specific formin (FHOD3) releases its auto-inhibiting property and increases actin polymerization (Iskratsch, 2013). However, the effect of PTMs on CapZ capping has not been studied in depth and is the subject of this chapter of the thesis.

PTM by phosphorylation is known to be critical in mechanotransduction signaling pathways. An example is the protein kinase C (PKC) isoform ε, which modulates both cardiac contractility and remodeling. When activated, PKCε translocates to the Z-disc (Disatnik, 1994; Dorn, 1999; Robia, 2001). A dominant-negative mutant of PKCε prevents the assembly of the optimal resting length of the sarcomere after sustained mechanical strain, suggesting its regulatory role (Mansour, 2004). Interestingly, in transgenic models of CapZ downregulation, PKC dependent regulation of myofilament function is abolished, and the binding of activated PKCε to the myofilament is

diminished (Pyle, 2002), suggesting the involvement of CapZ in PKCε signaling. Furthermore, increased CapZ dynamics in neurohormonally stimulated myocytes were shown to be association hypertrophy through PKCε and PIP_2 dependent pathways (Hartman, 2009).

Modification by acetylation is another major posttranslational event, which is regulated by enzymes that acetylate or deacetylate. Histone deacetylase (HDAC) removes the acetyl group from an ε-N-acetyl lysine residue on histones (López-Rodas, 1993) to alter the accessibility to DNA in the nucleus. However, there is a large family of HDACs whose activities occur both inside and outside the nucleus. For example, HDAC3 has an extra segment close to the C-terminus and can shuttle in and out of the nucleus (Yang, 2002; Gao 2006). In myocytes, the HDAC nuclear export is stimulated by protein kinase D (PKD) and is involved in the hypertrophic processes (Monovich, 2010). Additionally, in cardiomyocytes, HDAC3 is localized to both the M band and the Z-disc, and acetylation alters contractility (Samant, 2011). HDAC6 is also abundant on myofibrils, and the knockout of HDAC6 elevates the maximum force of myofibrils (Demos-Davies, 2014). Furthermore, HDACs can deacetylate α-tubulin, another cytoskeletal protein (Catley, 2006; Hubbert, 2002). Thus, it is possible that CapZ is also regulated by one or more HDACs since CapZβ can be acetylated in multiple spots (Lundby, 2012).

The goal of this chapter is to investigate how the increase of CapZ dynamics is regulated during sarcomeric actin filament remodeling. The hypothesis is that CapZ is

post-translationally modified through an HDAC and PKCε-mediated pathway, thereby regulating actin filament assembly. First, PTMs of CapZ in NRVMs are observed and identified. Second, variations of PKCε and HDACs by activators or inhibitors are applied to test whether phosphorylation or acetylation leads to increased CapZ and actin dynamics in neonatal rat ventricular myocytes (NRVMs). The coordination of phosphorylation and acetylation on CapZ capping is approached by manipulating both pathways simultaneously. Also, the PTMs of CapZ are observed in normal and failing human heart to explore their clinical relevance. Further understanding about the roles of PKCε and HDACs in heart failure is required to lay the foundation for the discovery of innovative treatment targets.

B. Materials and methods

i. Hypertrophic stimulation

Hypertrophic stimulation:

(1) Neurohormonal stimulation of NRVM: For cell culture methods see Chapter II. Control cells were either stimulated or left unstimulated prior to experiments. The neurohormonal treatment times chosen were sufficient to induce hypertrophy (Simpson, 1983; Hartman 2009). Phenylephrine (10 μM, Sigma-Aldrich) treatment was for 24 hours prior to experiment analysis.

(2) Mechanical strain of NRVM: Seventy-two hours after cell isolation, with or without viral infection, cyclic mechanical strain was generated with a Flexcell Strain Unit (model

FX-4000, Flexcell International, Hillsborough, NC). NRVMs were strained at 10% elongation biaxially at 1 Hz sinusoidally for 1 hour in PC-1 medium. Strain magnitude, time, and waveform were user-assigned to the system that controls vacuum pressure to deliver calibrated strain values to available elastic substrates housed in the incubator.

(3) Cell size measurement: NRVMs were washed with PBS, fixed with 4% paraformaldehyde (Sigma-Aldrich) for 10 min, placed in cold 70% ethanol, and stored at −20°C until immunostaining. Primary anti-α-actinin antibody (Catalog No. ab9465, mouse IgG; Abcam, Cambridge, MA), was diluted (1:200) in 1% BSA in PBS (with 0.1% Triton X-100) and allowed to incubate on a shaker table at 4°C overnight. Cells were then rinsed in PBS at 25^{o}C and blocked in 1% BSA in PBS for 1 hour at 25^{o}C. Secondary antibody (Molecular Probes) was diluted at a ratio of 1:500 in 1% BSA in PBS and incubated for 1 hour at 25^{o}C. Cells were washed in PBS. Anti-fade reagent with DAPI (Molecular Probes) was added and cover slips were mounted on glass slides. For cell size measurement, the cells were plated in PC-1 media for 48 hour before treatment, NRVM boundaries were visualized by α-actinin antibody staining. Surface area was measured by Image J.

ii. Left ventricular tissue from DCM and normal human hearts

Samples of left ventricular (LV) tissue were obtained from Loyola University Medical Center's (LUMC's) Cardiovascular Institute Tissue Repository with IRB approval from both LUMC for procurement and from UIC (IRB approval #: 2012-0061). All samples were de-identified before shipment to UIC. The detailed protocol and informed consent

documents were reviewed by LUMC's Institutional Review Board prior to tissue acquisition. Following informed consent, human LV tissue was obtained from patients undergoing heart transplantation for dilated cardiomyopathy (DCM). Tissue samples were quickly frozen in liquid nitrogen in the operating room and stored at -80^{o}C. For normal human heart, following informed consent from organ donor family members, donor hearts judged unsuitable for cardiac transplantation were stored in cardioplegic solution on ice and delivered within 4 hours of cardiac extirpation by the Gift of Hope Organ and Tissue Donor Network. Tissue samples were then quickly frozen in liquid nitrogen, and stored at -80^{o}C.

iii. HDAC inhibition

HDAC inhibitors were used at the indicated final concentrations and treating time: trichostatin A (TSA) (5 μM, 5 hours; Sigma), MGCD0103 (500nM, 24 hours; Selleck) and tubastatin A (1 μM, 24 hours; Selleck). BA-60 (1 μM, 24 hours) was synthesized in-house and graciously provided by Dr. Timothy A. McKinsey in University of Colorado at Denver.

iv. Adenoviral constructs and infection

Recombinant adenoviruses for GFP-CapZβ1, constitutively active PKCε (caPKCε) and dominant negative PKCε (dnPKC-ε) were kindly provided by Dr. Allen Samarel (Loyola University Chicago Stritch School of Medicine, Maywood, IL) as previously described (Hartman, 2009). Two days after NRVM isolation, NRVMs were infected with CapZβ1 (MOI 20), caPKCε (MOI 100), or dnPKCε (MOI 250) for 60 min at 37°C diluted in PC-1

medium. The viral medium was then replaced with virus-free medium, and cells were left undisturbed for 24 hours.

v. Actin-GFP expression

Actin-GFP expression was induced by CellLight® Reagents *BacMam 2.0* actin-GFP (Invitrogen). Two days after NRVM isolation, an appropriate volume of CellLight® Reagent (30μL per 1,000,000 cells) was used as modified from the manufacturer's instructions. Infected NRVMs were then returned to the culture incubator for at least 16 hours.

vi. Subcellular fractionation

For subcellular fractionation of myocytes, the Calbiochem ProteoExtract Subcellular Proteome Extraction Kit was used (Catalog No. 539790; EMD Millipore, Billerica, MA), following a previously described detergent-based protocol (Boateng, 2007). Cellular proteins were sequentially extracted into four compartments: cytosolic, membrane / organelles, nuclei, and cytoskeleton. Digitonin-EDTA was used to remove the cytosol. Triton-EDTA was used to remove the membrane-organelle fraction. Tween / deoxycholate / benzonase was used to remove the nuclei. Finally, SDS was used to remove the cytoskeleton. Cells were briefly washed three times in PBS between each extraction fraction to prevent cross-contamination. After each fraction, cells were observed by light microscopy to ensure that they were still attached to the dish. Cell integrity was maintained throughout the fractionation process. The accuracy of the fractionation method was verified with antibodies to well-documented subcellular

distribution markers [heat shock protein (Hsp)70 for cytostol, β1-integrin for membrane, H2B for nucleus and tropomyosin for myofibrils].

vii. Immunoblotting

Protein extracts from whole cell lysates or different subcellular fractions were resolved by SDS/PAGE, transferred to polyvinyl difluoride (PVDF) membrane and probed with antibodies for CapZβ (Santa Cruz; sc-27551); 4370), HDAC2 (Cell Signaling Technology; 4631), HDAC3 (Cell Signaling Technology; 4668), Hsp70 (Santa Cruz Biotechnology Technology; sc-24), β-integrin (EMD Millipore; MAB1900), H2B (Abcam; ab18977), and tropomyosin (provided by Dr. R. John Solaro at the University of Illinois at Chicago).

viii. Two-dimensional gel electrophoresis (2DGE)

Cells were placed on ice and lysed using ice cold MF buffer (75mM KCl, 10mM Imidazole, 2mM MgCl2, 2mM EDTA, 1mM NaN3) containing protease and phosphatase inhibitors (Sigma, St. Louis, MO). The pellet was then resolubilized in urea-thiourea-chaps (UTC) buffer (8M Urea, 2M Thiourea, 4% Chaps). The total protein concentration was measured using the RC DC^{TM} protein assay (Bio-Rad) with crystalline bovine serum albumin as standard. For the first dimension electrophoresis, each protein sample (~1000 µg) was mixed with 200µl of IEF buffer (GE Healthcare) containing IPG buffer (ampholytes, GE Healthcare). The program for the IEF cell was set up as an active rehydration at 50V for 10-16 hours, 250 V rapid 15min, 10000V linear 3 hours, 10000 rapid. After completion of the first dimension electrophoresis, the strip was

incubated with 2ml of IEF EQ buffer (6M urea, 5%SDS (w/v), 30% glycerol (v/v)) with 1% (w/v) DTT), and placed on a shaker at 50rpm for 15min. After 15min, the strip gel was taken out and incubated in IEF EQ buffer with 2.5% (w/v) iodoacetamide, and then placed on shaker for another 15min (50rpm). The second dimension electrophoresis was run under constant 30 mA for 2~3 hours. After the second dimension electrophoresis was complete, the protein was transferred to PVDF membrane under the CAPS transfer buffer and run according to conventional protein transfer procedures.

ix. Mass Spectrometry

The CapZβ1 migrating spots on Coomassie blue-stained two-dimensional gel were cut out and the gel pieces were placed in distilled water for processing by the Proteomics Core Facility (UIC). The gel spots were first destained to remove Coomassie blue, followed by reduction with DTT to remove disulfide linkage throughout the protein and then alkylation to confer stability to the peptides resulting from protease digestion. The protein was subjected to an in-gel digestion with trypsin and the peptides were extracted from the gel matrix. Electrospray Ionization Fourier Transform Ion Cyclotron Resonance Mass Spectrometry (ESI-FTICR, Applied Biosystems, Inc.) was employed to acquire site-specific information regarding the PTMs of each of the CapZβ1 sites. MS/MS results were analyzed by Mascot MS/MS ion search database (fixed modifications: carbamidomethyl; variable modifications: acetyl (K), acetyl (protein N-terminal), oxidation (M), phosphorylation (ST), phosphorylation (Y); mass value: monoisotopic; protein mass: unrestricted; peptide mass tolerance: ± 10 ppm; fragment mass tolerance: ± 0.6 Da; max missed cleavages: 1) and Scaffold program (Proteome Software).

x. Data analysis

Sample sizes were at least 4 immunoblots, 4 FRAP or 4 MS analyses per group. Spot density of 2D western blot was analyzed by ImageLab software. Values of spot density were analyzed using a paired Student's T Test to make comparison between control and designated treatment. $P<0.05$ was considered significance.

C. Results

i. Post-translational modifications of CapZ are increased in hypertrophic NRVM

Due to the rapid response of CapZ dynamics to hypertrophic stimulation (Lin, 2013), I hypothesized that PTMs of CapZ affect the capping of CapZ to the actin filament. To address this hypothesis, myofibrillar proteins extracted from NRVM with or without PE treatments were separated by two dimensional gel electrophoresis (2DGE). Phenylephrine (PE) treatment resulted in CapZβ1 2D spots shifting toward a lower isoelectric point (spots 2-4, Figure 13A and B). This left shift meant there were more negative charges on the protein, which indicated the presence of PTMs. Interestingly, the 2D blot pattern of CapZβ1 in NRVMs was similar to endogenous CapZβ in human heart tissue. Increased PTMs of CapZ were also observed in hypertrophic heart from dilated

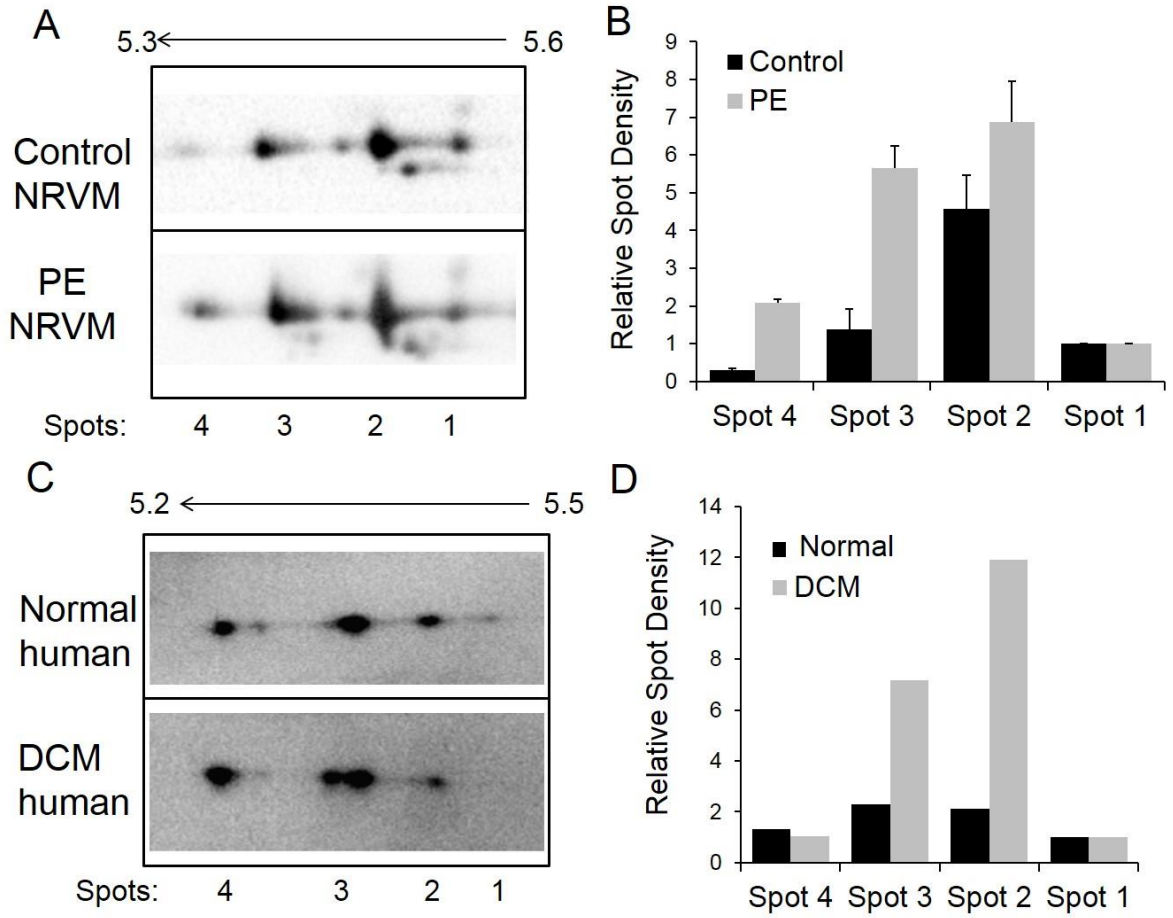

Figure 13. PTMs of CapZβ1 are elevated in hypertrophic NRVM and failing human heart. (A) NRVM Immunoblot of 2D gels with isoelectric point 4.7- 5.9 range using a CapZβ antibody for CapZβ1. PE= 10 μM phenylephrine / 24 hours. (B) Densiometric quantification of major spots shows increased levels of CapZβ1 with more negative charges (spot 2, 3 and 4) after stimulation by PE (n=3). (C) Immunoblot of 2D gels for endogenous CapZβ1 in human heart tissue from normal and dilated cardiomyopathy (DCM). (D) Densiometric quantification of major spots shows increased levels of endogenous CapZβ1 with more negative charges in DCM human heart tissue (n=1).

cardiomyopathy patients (Figure 13C and D), suggesting that the alterations of CapZ PTMs were relevant to human heart disease.

ii. Identification of PTM sites and locations on CapZ

While 2DGE is a useful technique for observing the existence of posttranslational modifications on proteins, it does not identify where these sites are located. Therefore, mass spectrometry was used to identify the sites conclusively and types of post-translation modifications. Four major spots of CapZβ1 on 2D gel stained by Coomassie Blue (Figure 14A) were cut out and each gel piece was placed in distilled water for processing by ESI-FTICR. The results analyzed by Mascot MS/MS ion search database and Scaffold program demonstrated that acetylation of lysine (K199) of CapZβ1 was found at spot 2 (Figure 14B and C), consistent to our finding in the immunoblots of CapZβ1, in which spots 2-4 were recognized by the acetyl-lysine antibody (Figure 14D). MS also showed phosphorylation of serine (S204) residue of CapZβ1 at spot 3 (Figure 14B). PyMOL Molecular Graphics System demonstrated that K199 and S204 were very close to the helix 5 of CapZβ and the C-terminal of CapZα (Figure 15).

iii. Effects of caPKCε and dnPKCε on CapZ and sarcomeric actin dynamics

Adenoviral infection by caPKCε or dnPKCε was tested for the role of PKCε in CapZ activities. FRAP analysis of CapZ showed that the K_{frap} was increased with caPKCε, whereas the increased K_{frap} of CapZ stimulated by PE were counteracted by dnPKCε

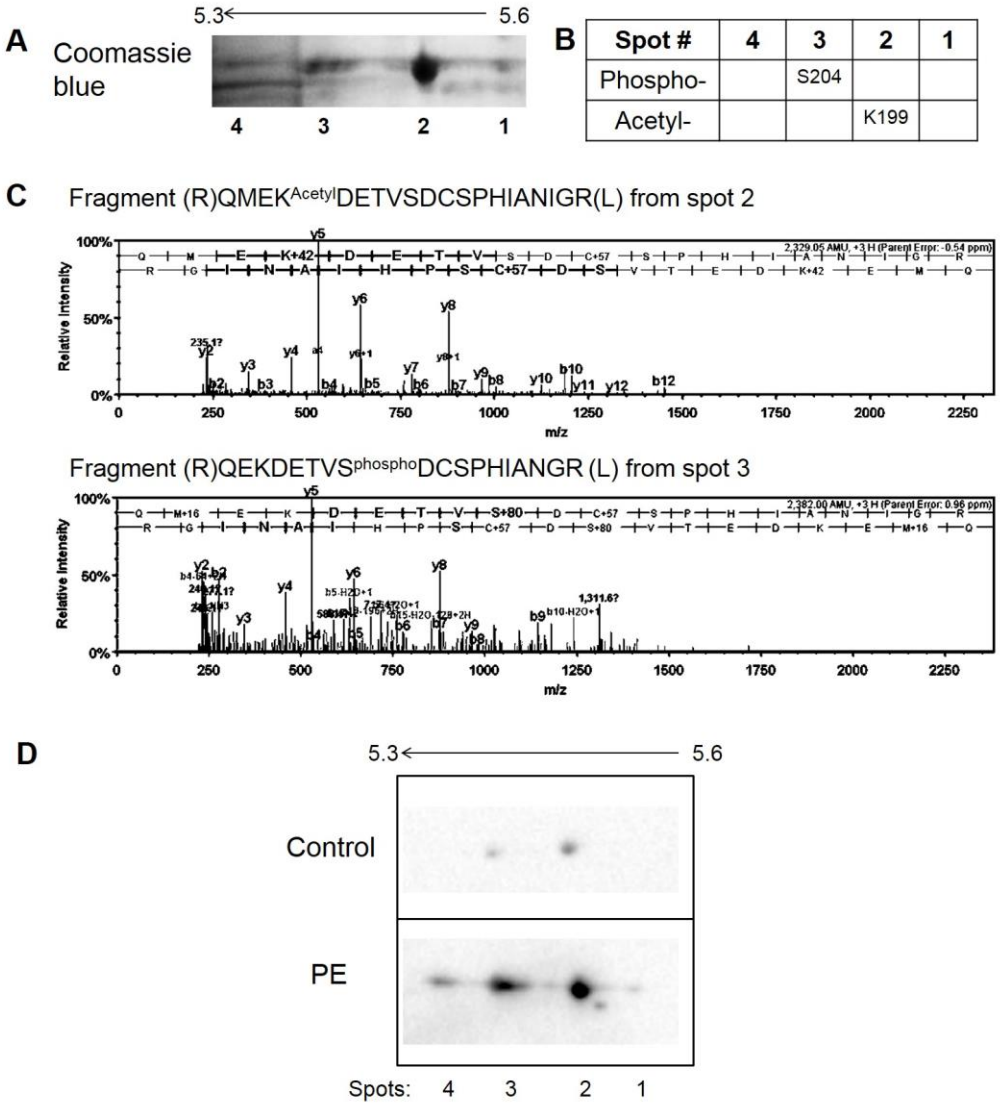

Figure 14. CapZβ1 is both phosphorylated and acetylated in hypertrophic NRVM.

Figure 14 legend:

(A) After 2DGE, 4 major CapZβ1 spots on 2D gel electrophoresis (Coomassie blue stained). (B) ESI-FTICR acquired site-specific information for CapZβ1. Spot 2 has acetylation at Lysine199 (K199); spot 3 has phosphorylation at Serine204 (S204). (C) Annotation of representative mass spectra of trypsin digested protein samples (spots 2 and 3). The degree symbol designates b or y ions with water and/or ammonia loss. (D) Immunoblot of 2D gels with isoelectric point 5.3- 5.6 range for CapZβ1 with acetyl-lysine antibody. PE treatment= 10 μM phenylephrine / 24 hours. n=1.

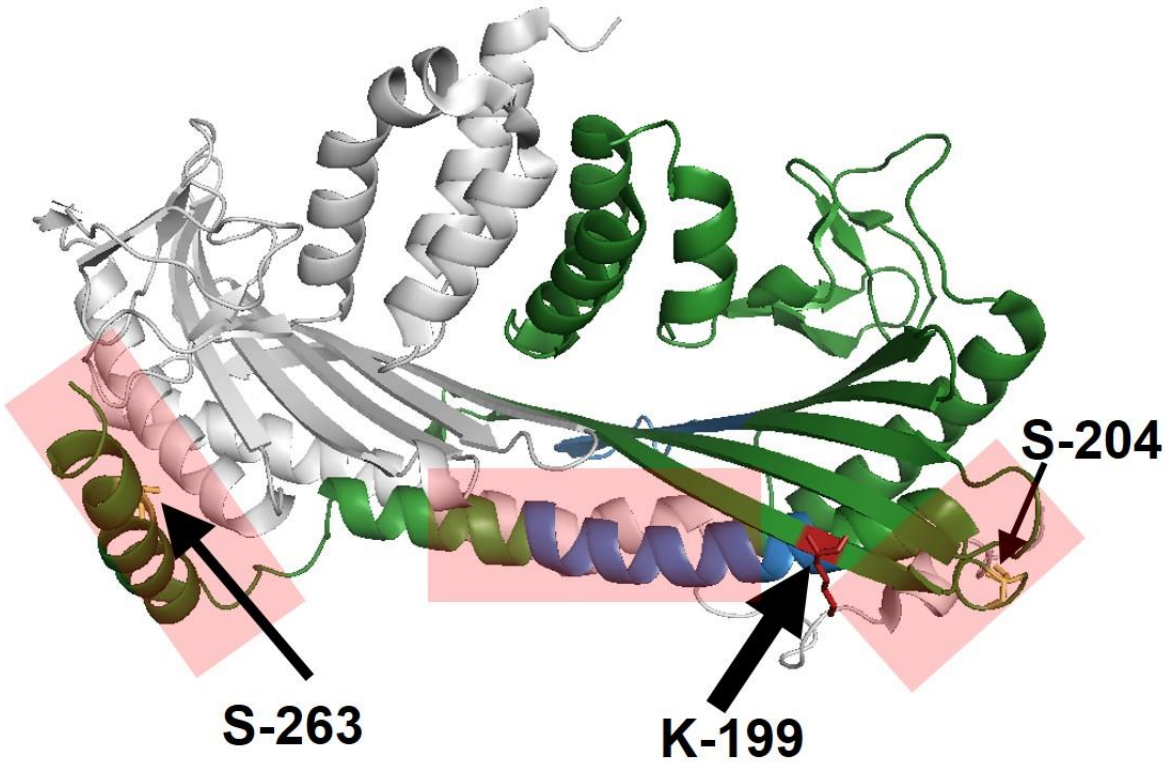

Figure 15. Display of phosphorylation and acetylation sites in a three-dimensional structure of CapZ. The actin binding region defined by Kim and Cooper (2010) indicated by pink shadow. The position of S204 and S263 phosphorylation (small arrow) and K199 acetylation (large arrow). All of these residues are adjacent to the actin-binding surface of CapZ

(Figure 16A). Consistently, 2D western blotting for CapZ showed that the PTMs (both spot 2 and spot 3) of CapZ were diminished by dnPKCε, suggesting the regulatory role of PKCε in the PTMs of CapZ dynamics (Figure 16B and 16C).

iv. Effects of HDAC inhibitors and activators on CapZ and sarcomeric actin dynamics

I hypothesized that HDACs mediate the acetylation of CapZ in hypertrophic myocytes. Thus, the effects of different HDAC isoforms on myocyte growth and CapZ status were tested by specific inhibitors. NRVM size was increased by MGCD0103, the HDAC1-3 inhibitor, but not by tubastatin A, the HDAC6 inhibitor (Figure 17A and B), suggesting that activities of HDAC1-3 were relevant to myofilament assembly. To test whether HDACs affect CapZ capping and actin assembly, dynamics of the CapZ were measured by FRAP. The kinetic constant (K_{frap}) of CapZ was doubled by MGCD0103 and tricostatin A, the pan HDAC Class I and II inhibitor (Figure 17C). In contrast, elevated CapZ dynamics stimulated by PE were counteracted by theophylline, which was shown to activate Class I HDAC activities (Ito, 2002). Furthermore, spot 2 of CapZβ1 on 2D western blot was increased by MGCD0103, suggesting that HDAC1-3 directly mediated CapZ acetylation (Figure 17D). The dynamics of the sarcomeric actin were also tested. The kinetic constant (K_{frap}) of actin was significantly increased by MGCD0103, confirming the importance of the HDAC1-3 for CapZ capping and actin assembly (Figure 17E).

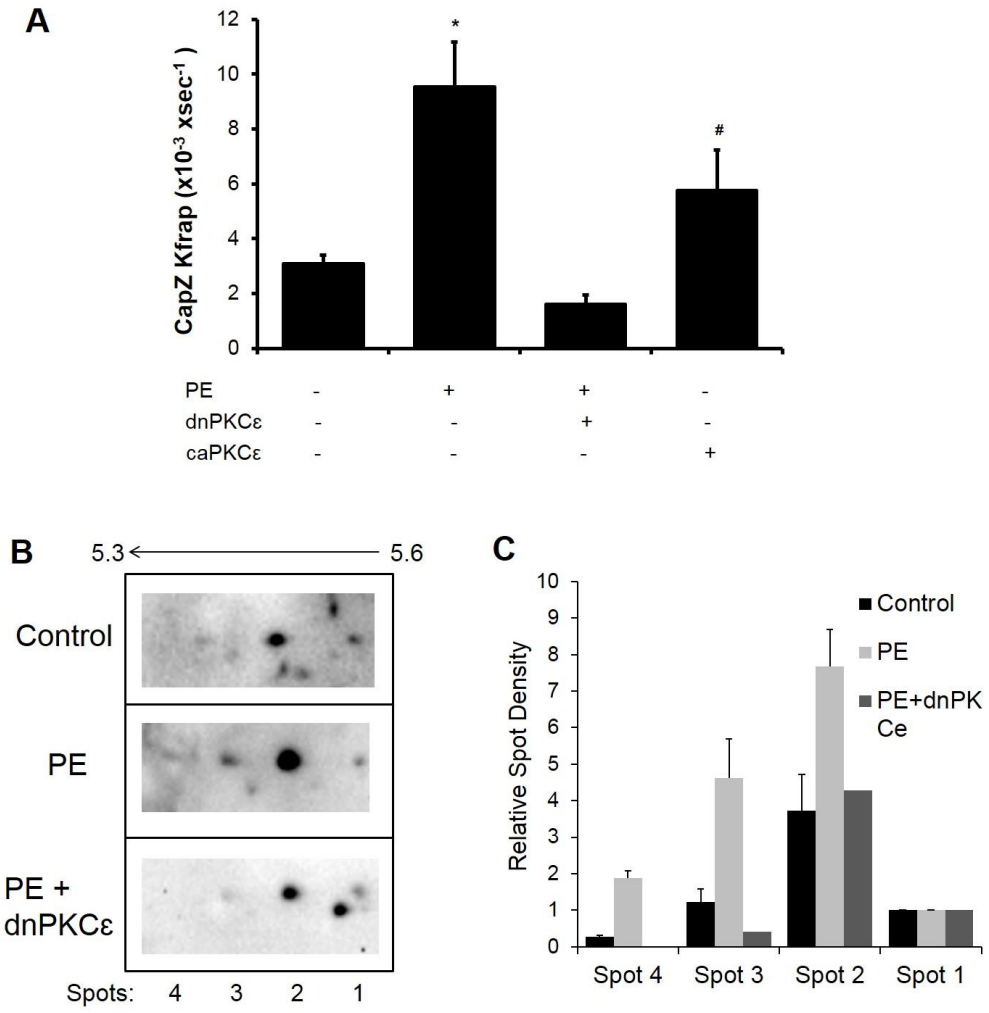

Figure 16. Increased CapZ dynamics and PTMs in NRVMs after phenylephrine treatment is regulated by PKCε. NRVMs were treated with caPKCε, or dnPKCε, and also with or without phenylephrine treatment (PE, 10μM / 24h). (A) K_{frap} values for GFP-CapZβ1 in cells is significantly increased by phenylephrine (n=8), but the effect of PE is blunted by dnPKCε (PE+ dnPKCε, n=3). K_{frap} values for GFP-CapZβ1 in cells with caPKCε is significantly increased even without PE (caPKCε, n=9). (B) NRVM Immunoblot of 2D gels with isoelectric point 4.7- 5.9 range for CapZβ1 with CapZβ antibody. (C) Increased spots 2 and 3 of CapZβ1 in PE-treated cells are both withdrawn in the presence of dnPKCε (n=1). Values are means ± SE. Significant difference: *P < 0.01.

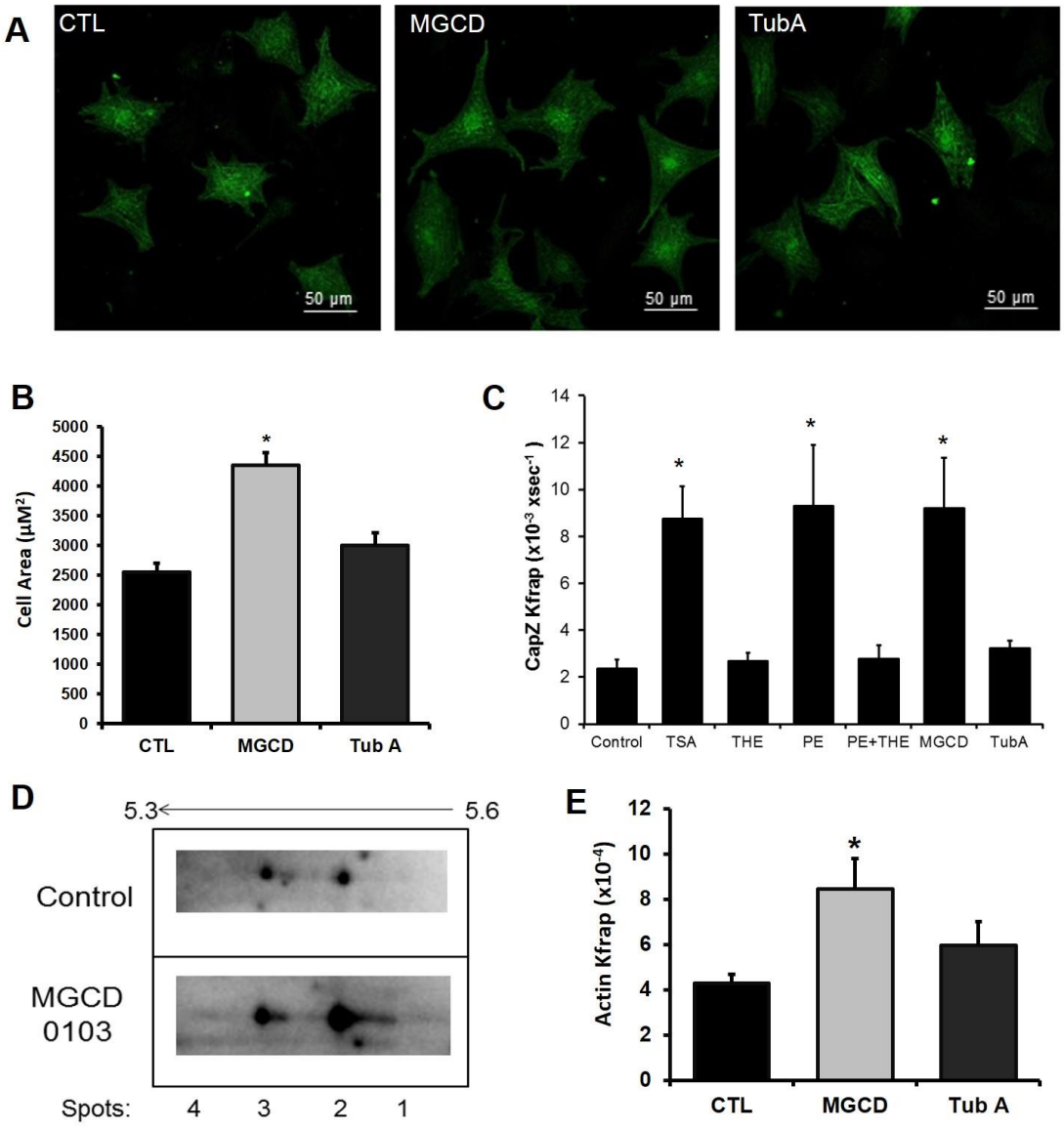

Figure 17. CapZ capping and NRVM size are both mediated by Class I HDACs.

Figure 17 legend:
(A) NRVMs with or without HDAC inhibitors were stained with α-actinin antibody (green). (B) Cell area showing size of MGCD0103-treated cells is significantly larger than untreated cells, compared to tubastatin A. CTL= control; MGCD= MGCD0103 (5μM / 24h); Tub: Tubastatin A (10μM / 24h). n>20 for each group. (C) K_{frap} values for GFP-CapZβ1 FRAP in cells untreated (n=9) or treated with trichostatin A (TSA, 10μM / 5h, n=5), theophylline (TSA, 10μM / 24h, n=5), phenylephrine (PE, 10μM / 24h, n=5), phenylephrine + theophylline (PE+THE, n=8), MGCD0103 (5μM / 24h, n=11) and Tubastatin A(10μM / 24h, n=4). CapZ K_{frap} is significantly elevated by TSA, MGCD and PE, while the effect of PE is withdrawn by THE. (D) Immunoblot of 2D gels with isoelectric point 4.7- 5.9 range for CapZβ1. MGCD= 10 μM MGCD0103 / 24 hours. Spot 2 of CapZβ1 is clearly increased with MGCD0103 treatment. (E) K_{frap} values for actin-GFP FRAP in cells untreated (n=15) or treated with MGCD0103 (5μM / 24h, n=5) and tubastatin A (10μM / 24h, n=4). Actin K_{frap} is significantly elevated by MGCD0103, but not by tubastatin A. Values are means ± SE. n=number of cells Significant difference: *P < 0.01.

v. HDAC3 translocates out of the sarcomere in hypertrophy

It appeared that during cardiac hypertrophy, HDAC activities were diminished, increasing the acetylation of myofilament proteins in response to the increased loading. I hypothesized that the translocation of HDAC3 out of sarcomere might alter PTMs and affect hypertrophy given the ability of HDACs (HDAC3, 4 and 5) to shuttle between the cytosol and the nucleus (Yang, 2002, Sucharov, 2008; Monovich, 2010), combined with HDAC1-3 regulation of both CapZ and actin dynamics (Figure 17). HDAC3 was localized in the Z-disc and had direct interaction with CapZβ1 (Figure 18A and B). With PE treatment, the amount of HDAC3 was decreased in myofibrillar but increased in membrane fractions (Figure 19A and B). Interestingly, HDAC3 translocation with PE treatment was diminished by dnPKCε expression, indicating a regulatory role for PKCε in HDAC3 localization during hypertrophy.

vi. Acetylation alone is sufficient to regulate CapZ dynamics

Since deacetylation and phosphorylation regulated the dynamics of CapZ, we investigated the interaction between HDAC and PKC. The approach was to control acetylation and/or phosphorylation of CapZ, and measure the effects on CapZ dynamics. Theophylline was applied to elevate the deacetylation of HDACs in NRVMs with caPKCε expression. CapZ FRAP results showed that K_{frap} of CapZ with caPKCε expression had no significant increase in the presence of theophylline, compared to caPKCε alone (Figure 20). Furthermore, treatment of MGCD0103 on NRVMs in addition to PE and dnPKCε increased CapZ dynamics (Figure 20). Taken together, acetylation alone in the absence of phosphorylating kinases appeared to be sufficient to increase

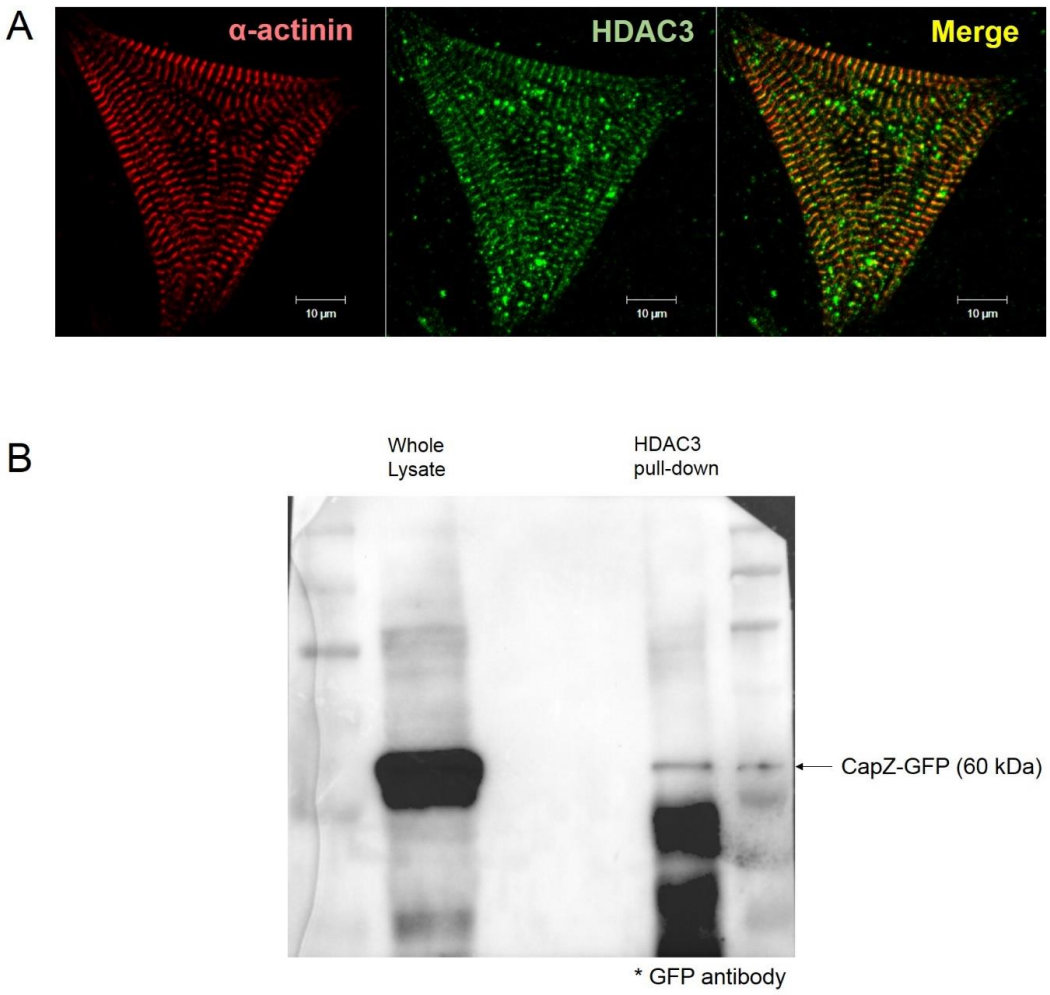

Figure 18. HDAC3 is localized in Z-disc and interacts with CapZ. (A) NRVMs were permeabilized with digitonin-EDTA to remove the cytosol. Triton-EDTA was used to remove the membrane-organelle fraction. The remaining cytoskeletal fraction was stained for HDAC3 (green) and α-actinin (red). Staining result shows that HDAC3 is colocalized with α-actinin in the Z-disc. Bar = 10 μm. (B) HDAC3 protein in cell lysate was immuno-precipitated by HDAC3 antibody. The bound CapZβ1 is detected with anti-GFP antibody by Western blot analysis. *Data in collaboration with Jieli Li, M.D., Ph.D.*

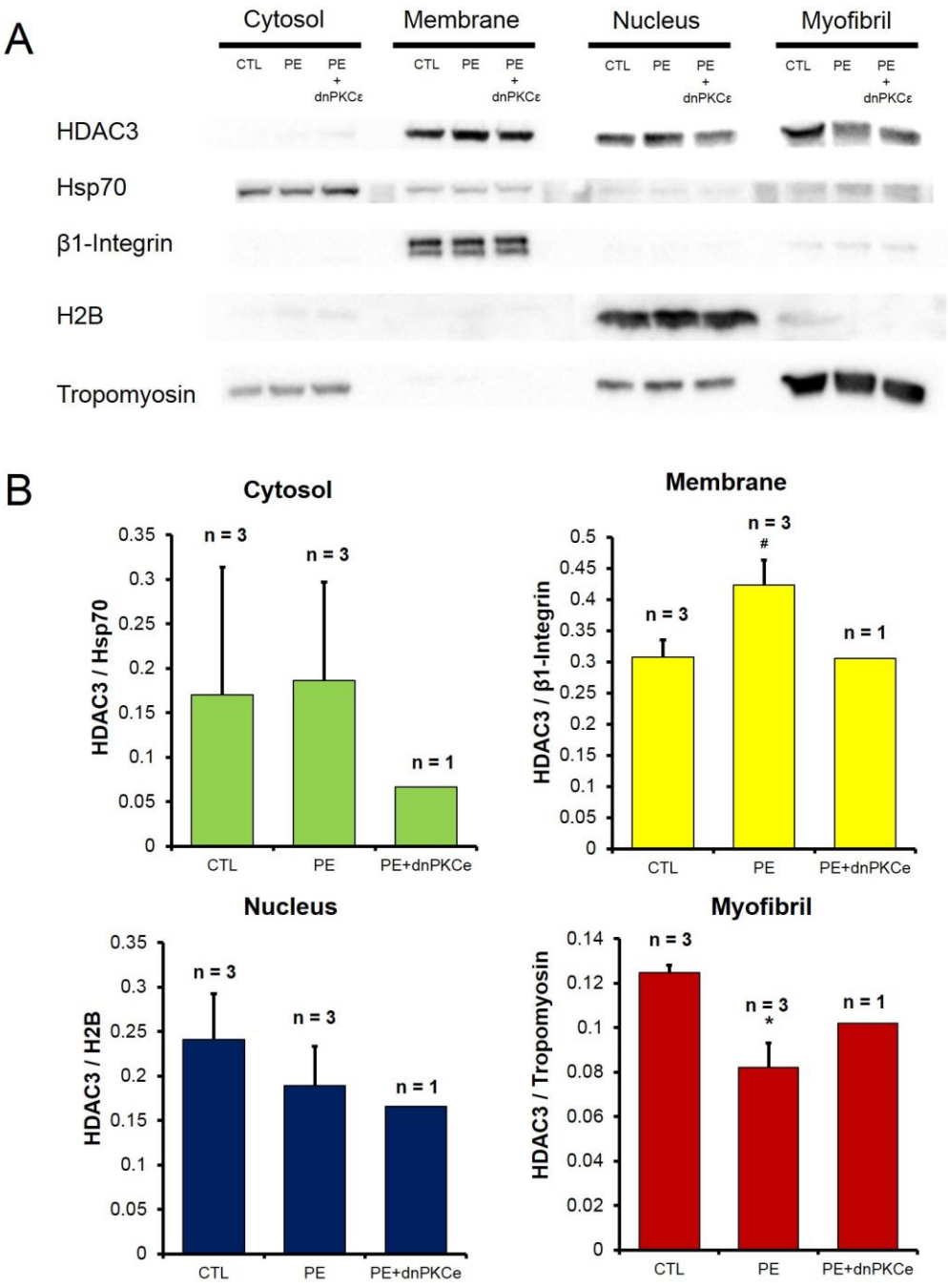

Figure 19. Translocation of HDAC3 out of the sarcomere by phenylephrine treatment.

Figure 19 legend:
Subcellular distribution of HDAC3 in untreated, PE (phenylephrine, 10μM / 24h) and PE+dnPKCε treated NRVMs. (A) and (B): Western blot and analysis for subcellular fractionation: cytosolic, membrane, myofibrillar and nuclear fractions. Internal controls are hsp70 for cytosolic, β1-integrin for membrane, tropomyosin for myofibrillar and histon 2B (H2B) for nuclear fraction. Distribution of HDAC3 in myofibrillar fraction is decreased by phenylephrine, and membrane fraction is increased. Values are means ± SE. Significant difference: *P < 0.01; #P < 0.07.

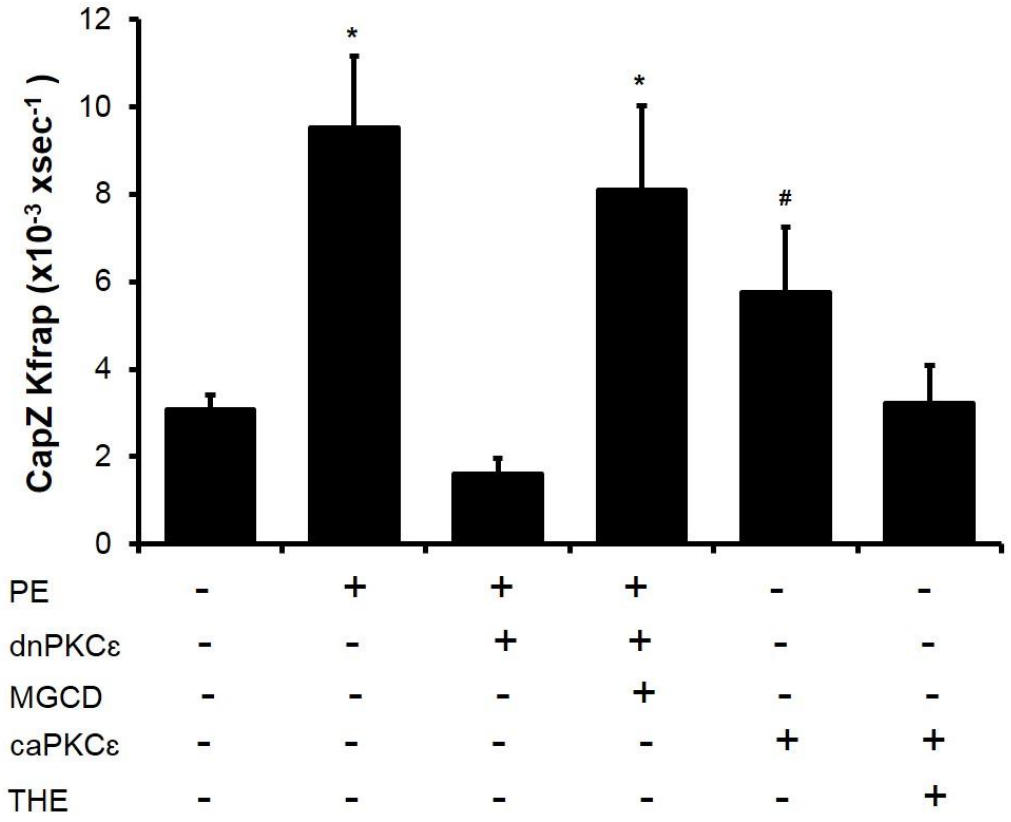

Figure 20. Coordination of phosphorylation and acetylation on CapZ dynamics. NRVM treatments were done in combination as shown before. Mean values for K_{frap} are shown as histogram. (1) Treatment of MGCD0103 in addition to PE + dnPKCε significantly increases K_{frap} (n=7). (2) Treatment of THE in addition to caPKCε does not result in elevated K_{frap} values (n=9). Values are means ± SE. Significant difference: *P < 0.01; #P < 0.05.

CapZ dynamics.

D. Discussion

This chapter reports several novel findings. First, in the NRVM primary culture system, posttranslational modifications of both acetylation and phosphorylation of CapZ were elevated by hypertrophic stimulation. Moreover, the locations of these PTMs with respect to the actin binding interface were crucial for CapZ capping to the actin filament. The acetylation of CapZ (K199) was mediated by Class I HDACs, leading to increased CapZ dynamics, actin dynamics, and myocyte growth. The activities of HDACs were diminished during hypertrophy possibly because of their translocation from the myofilament to the nucleus. CapZ phosphorylation (S204) mediated by PKCε also occurred in hypertrophic myocytes. However, acetylation alone was sufficient to increase CapZ dynamics and induce cell hypertrophy.

i. The PTMs of CapZ in NRVMs with sarcomeric growth

In recent years, various PTM sites on CapZ have been identified (phosphosite.org database); however, the functional effects of those PTMs have not been specifically addressed. Ser-9 of CapZα has been shown to be phosphorylated by CK2 (Canton, 2005), which inhibited the CapZ capping property. The C-terminus, along with part of the helix 5 of CapZα and β are the major actin binding sites of CapZ to the actin filaments (Kim, 2010). The acetylation of K199 and phosphorylation of S204 observed by us are very close to the actin binding surface (Figure 15). K199 is at the end of β strand 9 of CapZβ. Acetylation of K199 increases hydrophobicity so that the K199 might not be able to maintain its original location on the outer surface of CapZ. S204 is at the

loop between helix 5 and helix 6 of CapZβ, where it is adjacent to the CapZα C-terminal. Phosphorylation could increase the hydrophilic property, which might twist the S204 site out to protein surface and alter the angle and position of the CapZα C-terminal. These two sites have not been reported in previous proteomic screenings possibly because studies were done on unstimulated myocytes, so that the low level of acetylation and phosphorylation were not detectable. Undoubtedly the PTMs on CapZα could also regulate the capping property of CapZ, and further investigation is necessary.

ii. The regulation of PKCε in cardiac hypertrophy

Although many studies have reported translocation of activated PKCε to the Z-disc, the identities of the binding partners of PKCε at the Z-disc remain unclear. Some have suggested Cypher-1, enigma homologue protein, PDZ domain containing proteins that also bind α-actinin, several RACKs and F-actin (Mochly-Rosen, 1995; Prekeris, 1996; Zhou, 1999; Nakagawa, 2000). The PKCε complex pulled-down by a PKCε monoclonal antibody showed binding to α-actinin and desmin, components of the Z-disc (Ping, 2001). PE-induced myofilament-PKCε association was found to be diminished in the transgenic mouse heart with reduced CapZ expression, suggesting that CapZ might be a binding target for PKCε (Pyle, 2002). In this current study, we show that PKCε mediates the phosphorylation and dynamics of CapZ in hypertrophic myocytes. Thus, the translocation of PKCε to the Z-disc by hypertrophic stimulation might lead to the phosphorylation of CapZ. Furthermore, PKCε also mediated the acetylation of CapZ (Figure 16), suggesting the existence of a phosphorylation-acetylation cascade.

iii. HDACs in the regulation of CapZ in hypertrophic NRVMs

The role of HDACs in the regulation of hypertrophic signaling has been extensively studied. Both general and more specific HDAC inhibitors have been shown to have significant therapeutic potential (Kong, 2006; Cho, 2010; Iyer, 2010). Most studies for HDACs in cardiology focused on the long-term transcriptional regulation because of their function of mediating the accessibility of chromatin in the nucleus. However, reports now show that HDAC activities also occur in the cytosol in various types of cells. Here, I demonstrate that HDAC3 is located in the myofibrillar fraction of NRVMs and might be able to mediate acetylation of CapZ and actin capping. The translocation of HDAC3 out of the myofilaments provides a possible mechanism by which CapZ acetylation is increased. This is consistent with previous findings regarding the localization of HDAC3 and 6 in the myofilaments and the control of contractility (Samant, 2011; Demos-Davies, 2014). Aside from mediating the interaction between the myosin and actin filaments leading to altered contractility, acetylation elevated by Class I HDAC1-3 inhibitor increases CapZ and actin dynamics. This suggests that acetylation also diminishes the binding capacity of CapZ to the actin filaments (Figure 17). Therefore, HDAC3 and 6 appear to play a pivotal role in regulating the protein-protein interactions in the myofilaments. In response to elevated mechanical loading during cardiac hypertrophy, the increased acetylation would lead to both increased contractility and assembly of the myofibrils.

iv. The effects of acetylation and phosphorylation signaling on CapZ functions

The coordination of acetylation and phosphorylation of proteins has been extensively studied. The most well-known phosphorylation–acetylation cascade is p53 signaling, in which the phosphorylation of p53 stimulated by DNA damage increases the accessibility

of p53 to p300 and PCAF, leading to the acetylation of p53 with stimulation of its ability to bind DNA (Sakaguchi, 1998). In contrast, acetylation can affect protein phosphorylation as well. For example, Foxo1 structure is changed with acetylation, leading to its increased sensitivity to phosphorylation and DNA-binding ability (Matsuzaki, 2005). I found that CapZ can be phosphorylated and acetylated at S204 and K199, respectively. Both were elevated with hypertrophy (Figure 13 and 14) and blunted in the presence of dnPKCε (Figure 16). It is possible that the S204 phosphorylation results in structural changes of CapZ that decrease its interaction with HDACs. Also, PKCε / PKD signaling has been found to mediate the export of Class II HDAC4 and 5 (Vega, 2004; Monovich, 2010), so it is also possible that PKCε mediates the translocation of HDAC3 out of the sarcomere (Figure 19B). Interestingly, although PKCε appeared to induce both acetylation and phosphorylation of CapZ, increased or blunted acetylation of CapZ alone was sufficient to mediate CapZ dynamics (Figure 20). Thus, although PKCε and phosphorylation might initiate the phosphorylation-acetylation cascade, it appears that it is acetylation which dominates the reduction of the CapZ capping property during cardiac hypertrophy.

A model is proposed for the mechanism by which CapZ and actin dynamics are regulated by Class I HDACs and PKCε (Figure 21):

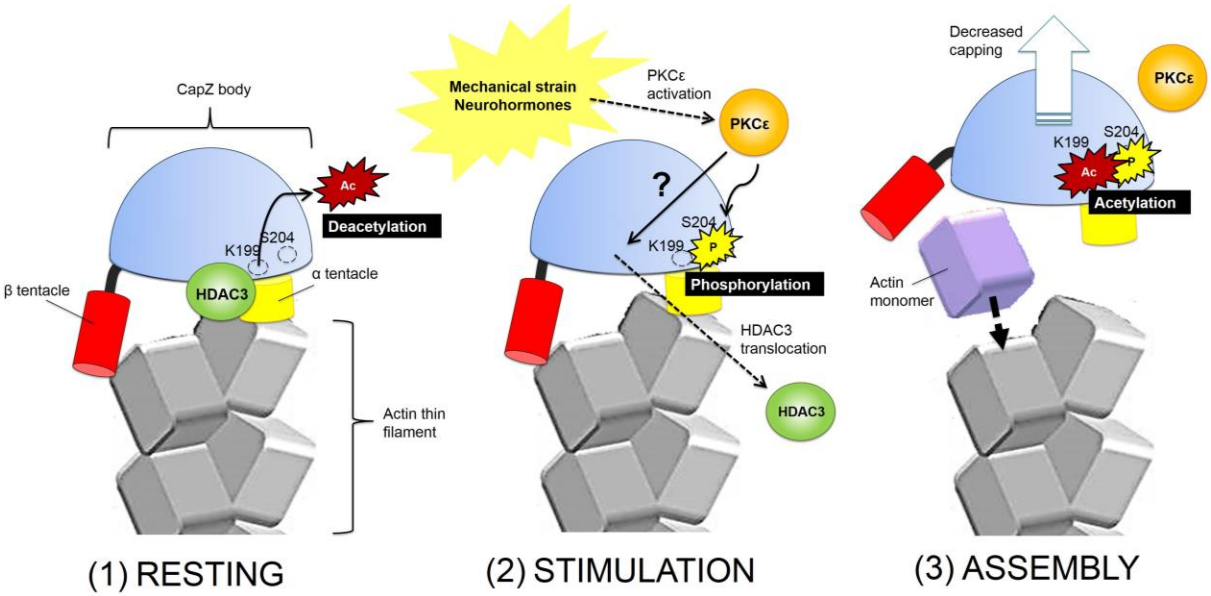

Figure 21. Model of PTMs regulate interactions between CapZ and actin to govern sarcomere assembly. (1) Resting state: The acetylation and phosphorylation levels of CapZ are low with HDAC3 consistently deacetylating in the absence of PKCε. The interaction of CapZ with the actin filament is stronger. (2) With hypertrophic stimulation, PKCε translocates to Z-disc and phosphorylates CapZ S204. Simultaneously, PKCε facilitates HDAC3 translocation out of the myofibril. (3) HDAC3 translocation allows acetylation of CapZ K199, leading to further structural changes that lower the binding affinity of CapZ to the barbed end of the actin filament. The interaction between CapZ and the actin filament is weaker. The off rate of actin is elevated and actin monomers are incorporated into the actin filament, resulting in actin assembly.

(1) Under normal conditions, the acetylation and phosphorylation levels of CapZ are low with HDAC deacetylation. Hence, CapZ tightly caps the barbed end of the actin filament. (2) With hypertrophic stimulation, PKCε activity is elevated possibly because of its translocation to the Z-disc. Thus, CapZ is phosphorylated on S204. (3) S204 phosphorylation or PKCε function leads to HDAC3 translocation out of the myofibrils with the acetylation of CapZ on K199. This step leads to further structural changes, which lower the binding affinity of CapZ to the actin filaments. With this change in the uncapping, the off rate of actin is elevated and actin monomers are incorporated into the actin filament. This results in a greater assembly of actin into the myofibril. The model suggests the regulatory role of acetylation and phosphorylation on CapZ capping by both HDACs and PKCε. This is a likely mechanism supported by proteomics, biochemistry and variations of HDACs and PKCε activities.

E. Conclusion

In conclusion, in hypertrophic myocytes, elevated acetylation and phosphorylation of CapZ result in the reduction of capping, increasing thin filament assembly with myocyte growth. A model is proposed to explain the possible process by which acetylation and phosphorylation are coordinated to reduce the actin capping function of CapZ. During myocyte growth, PKCε not only phosphorylated CapZ, but also mediated the acetylation of it. This is possibly because of the translocation of HDAC3 out of the sarcomere. Acetylation of CapZ reduces the capping of CapZ, thus initiating the remodeling of actin thin filaments by increasing actin assembly. This dual regulation through

phosphorylation and acetylation provides a novel model for the regulation of myofibril growth during cardiac hypertrophy. Since human failing heart tissue showed similar changes, they may provide potential therapeutic targets in maladaptive hypertrophic heart disease.

IV. MAJOR CONCLUSIONS

This thesis used biophysical and biochemical techniques to assess basic myocyte function with the goal of applying the results to the understanding of cardiac hypertrophy in exercise and disease. The approach was to induce hypertrophic stimulating of neonatal rat ventricular cardiomyocytes or use failing human heart tissue, and investigate how the assembly of sarcomeric actin thin filaments was regulated by the actin capping protein, CapZ. The major conclusions of this research were divided into two parts are.

Part A: CapZ and actin capping dynamics increase in myocytes after a bout of exercise and abate in hours after stimulation ends.

A. CapZβ1 dynamics increased within 0-1 hour after cyclic mechanical strain, but abated to control level in 2-3 hours.
B. Sarcomeric actin dynamics shared a similar time course of increase and recovery after cyclic mechanical strain with CapZ dynamics.
C. This time course showed that a normal bout of exercise had only short term signaling effects on actin assembly.
D. Actin dynamics were also increased after longer term neurohormonal stimulation.
E. NRVMs expressing GFP-CapZβ1ΔC had higher CapZ and actin dynamics than wild-type GFP-CapZβ1. The powerful effect of removal of the beta tentacle (CapZβ1ΔC) suggested that CapZ must undergo a structural change, which led to the release of the beta tentacle from its original binding region.

Part B: Actin assembly is regulated through phosphorylation and acetylation of the actin capping protein CapZ in cardiomyocytes.

A. PTMs of CapZβ1 were elevated in hypertrophic NRVMs and failing human heart.
B. CapZβ1 was both phosphorylated (S204) and acetylated (K199) in hypertrophic NRVM.
C. S204 and K199 were very close to the actin binding region of CapZ.
D. Increased CapZ dynamics and PTMs in NRVMs after phenylephrine treatment were regulated by PKCε.
E. CapZ capping and NRVM size were both mediated by Class I HDACs.
F. HDAC3 translocated out of the sarcomere with phenylephrine treatment.
G. Acetylation alone was sufficient to regulate CapZ dynamics.
H. During myocyte growth, S204 phosphorylation and K199 acetylation of CapZ coordinated to blunt the capping capacity of CapZ, which led to actin filament assembly.

The mechanism by which myocyte growth is generated has been investigated extensively in cardiology in the hope that maladaptive progression may be averted. The majority of the studies to date have focused on the alterations of gene expression when hypertrophy occurs and the signaling pathway leading to transcriptional changes. The differences of heart metabolism in diseased and normal heart and their potential effects on heart failure have also been addressed. However, the heart is a mechanical organ, pumping blood through the circulation continuously, and the contractile myofilaments are the primary component doing this work. Therefore, understanding the mechanism

for contractile function and thin filament assembly may provide a therapeutic target for the future treatment of hypertrophic heart diseases.

The objectives in this thesis were to determine the mechanisms for regulation of the capping property of CapZ and actin dynamics of the sarcomere in acute exercise versus chronic disease. The time course in myocyte in response to a physiologic bout of exercise mimicked by cyclic mechanical strain was studied. Chronic conditions were mimicked by sustained exposure to drugs such as phenylephrine. Furthermore, the combination of biochemical and proteomic approaches were used to identify the role of phosphorylation and acetylation of CapZ in the generation of hypertrophy.

One point worth mentioning is that studies on the regulation of actin assembly to date mostly focus on *in vitro* single molecule assays by observing the fluorescence of pyrene conjugated actin that occurs during polymerization. There are several groups trying to set up an actin polymerization assay in living cells. The Staiger lab in Purdue University has done phenomenal work on actin assembly in plant cells in response to bacterial infections, but not with animal cells (Staiger, 2010; Henty-Ridilla, 2013). The only work on actin assembly in living muscle cells was done by Takano in Chiba University in Japan (Takano, 2010). Sarcomeric α-actin-EGFP was expressed in adult mouse skeletal muscle by electroporation, and detected actin assembly by observing the incorporated fluorescent α-actin-EGFP to the Z-disc by confocal microscope. In this thesis, the commercially available actin-GFP and actin-RFP constructs were not sensitive enough to observe the incorporation of actin in the Z-disc, although I was able to show the increased dynamics of actin in hypertrophic NRVMs by FRAP. The change

in actin FRAP was linked to cell hypertrophy by measurement of cell size under all conditions.

Of note in the findings of this thesis is the rapid response of sarcomere dynamics to mechanical strain of the myocytes, compared to the slower response to neurohormonal stimulations (Lin, 2013). The transient sarcomere remodeling stimulated by a bout of mechanical strain suggests that cycles of activity and rest may be important for a healthy muscle, whereas maintained stimulation may be a factor in the maladaptation that occurs in chronic cardiac disease. Although mechanical and neurohormonal stimulations both occur during cardiac hypertrophy, they affect cell function through distinct pathways. Mechanical strain detected by the focal adhesion complex can trigger the maximum response of FAK activity in an hour (Senyo, 2007; Torsoni, 2003), and render the “slow” signals to the downstream pathways for modifying gene expression of the myocytes and probably also send the “fast” signals to the regulators of sarcomere assembly. The signaling pathways triggered by neurohormonal stimulation are initiated by small G proteins, and although they share many features with mechanical stimulation (Li, 1999), their activation of actin filament dynamics is possibly at the transcriptional level. The differences between mechanical and neurohormonal pathways still requires further investigation.

In the second part of the thesis, the significance of CapZ acetylation and phosphorylation of CapZ on actin capping was demonstrated. K199 acetylation and S204 phosphorylation were found in situations that increase CapZ and actin dynamics, suggesting decreased CapZ capping capacity. This is consistent with the CapZ capping model established by others, in which the altered dissociation rate of the basic residues

on the α tentacle and surrounding region might lead to the addition of actin monomers incorporated on the barbed end of the actin filament *in vitro* (Narita, 2006; Kim, 2010). In this thesis, both PKCε and Class I HDACs, the two signaling pathways that were found to regulate the PTMs of CapZ, have been reported to localize at the Z-disc and play important roles in the generation of cardiac hypertrophy (Disatnik, 1994; Dorn, 1999; Robia, 2001). The difference of the responding time of CapZ capping to mechanical or neurohormonal stimulation, which has not been explored in depth here, should be explored in more detail. For example, it would be interesting to observe the time course of PTM changes of CapZ to see if they respond slowly to PE as CapZ dynamics do, or respond quickly as for mechanical strain (Swanson, 2012).

This thesis has yielded new perspectives of how myocyte growth is initiated by actin assembly in cardiac hypertrophy. This is also the first study working on how post-translational modifications regulate CapZ capping while other studies focus on the CapZ regulatory proteins such as V-1 and CapZIP (Zwolak, 2010; Kotlo, 2012). Rapid response of CapZ capping indicates the ability of the myocytes to adapt to the change of local mechanical stimuli.

With significantly increased deaths (40.8%) attributed to cardiomyopathy and myocarditis in the past two decades and the projected increased prevalence of heart failure (46%) by 2030 (Mozaffarian, 2015), the finding of the involvement PKCs and HDACs in CapZ capping could provide promising therapeutic targets for regulating myocyte growth in the treatment of hypertrophy.

V. FUTURE WORK

Further work is needed in order to understand whether transient or chronic mechanical stimulation lead to different outcomes of adaptation. The rapid response of actin thin filament remodeling regulated by CapZ requires 2-3 hours of recovery time. It would be interesting to know whether there is a difference in the time course of CapZ capping and PTMs, and whether the long term maintenance of stimulation seen in chronic disease prevents this normal recovery cycle, thus leading to pathological hypertrophy. This could be done by observing the relationship between PTMs of acetylation and phosphorylation over time and compare the changes with the switching of fetal genes and myofibrillar protein isoforms (e.g., αMHC to βMHC or cTnI to ssTnI).

Furthermore, although 2DGE and MS results demonstrated the probability that acetylation and phosphorylation on S204 and K199 affect CapZ capping, it is necessary to do point mutations of S204 and K199. This would prove with direct evidence that the two PTMs are the exact two sites leading to increased dynamics. The role of S204 phosphorylation could be tested by GFP-CapZβ1 with S204A mutation (serine to alanine). K199 acetylation could be tested by GFP-CapZβ1 with K199R mutation (lysine to arginine) (Kim, 2006). Then, whether S204A and K199R mutations of CapZβ1 nullify FRAP dynamic increases can be tested in the future.

Finally, although results showed failing human heart tissue had elevated PTMs on CapZ, it is required to prove by MS that they are at the S204 phosphorylation and K199 acetylation sites. Also, the effects of PKCε and HDACs on CapZ in whole heart animal models with disease such as TAC are worth investigating. For example, it would be

important to test the PTMs of CapZ under the variations of PKCε / HDAC isoform expression. Additionally, an in depth exploration for the relationship between PKCε and HDACs activities to CapZ phosphorylation and acetylation in human heart tissue could be done. The results of these experiments may provide insight for the treatment of heart failure and cardiomyopathy.

CITED LITERATURE

1. Aikawa R, Nagai T, Kudoh S, Zou Y, Tanaka M, Tamura M, Akazawa H, Takano H, Nagai R, Komuro I. Integrins play a critical role in mechanical stress-induced p38 MAPK activation. Hypertension 39: 233–238, 2002.
2. Alberts B, Johnson A, Lewis J, Raff M, Roberts K, Walter P. The Cytoskeleton. Molecular Biology of the Cell. 5th edition. 2008;16:965-1052
3. Alcendor RR, Gao S, Zhai P, Zablocki D, Holle E, Yu X, Tian B, Wagner T, Vatner SF, Sadoshima J. Sirt1 regulates aging and resistance to oxidative stress in the heart. Circ Res. 2007 May 25;100(10):1512-21.
4. Allard MF, Schonekess BO, Henning SL, English DR, Lopaschuk GD. Contribution of oxidative metabolism and glycolysis to ATP production in hypertrophied hearts. Am J Physiol. 1994 Aug;267(2 Pt 2):H742-50.
5. Antos CL, McKinsey TA, Dreitz M, Hollingsworth LM, Zhang CL, Schreiber K, Rindt H, Gorczynski RJ, Olson EN. Dose-dependent blockade to cardiomyocyte hypertrophy by histone deacetylase inhibitors. J Biol Chem. 2003 Aug 1;278(31):28930-7.
6. Antos CL, McKinsey TA, Dreitz M, Hollingsworth LM, Zhang CL, Schreiber K, Rindt H, Gorczynski RJ, Olson EN. Dose-dependent blockade to cardiomyocyte hypertrophy by histone deacetylase inhibitors. J Biol Chem. 2003 Aug 1;278(31):28930-7.
7. Arai M, Yoguchi A, Iso T, Takahashi T, Imai S, Murata K, Suzuki T. Endothelin-1 and its binding sites are upregulated in pressure overload cardiac hypertrophy. Am J Physiol. 1995 May;268(5 Pt 2):H2084-91.

8. Atherton PJ, Szewczyk NJ, Selby A, Rankin D, Hillier K, Smith K, Rennie MJ, Loughna PT. Cyclic stretch reduces myofibrillar protein synthesis despite increases in FAK and anabolic signalling in L6 cells. J Physiol 587: 3719–3727, 2009.
9. Backs J, Song K, Bezprozvannaya S, Chang S, Olson EN. CaM kinase II selectively signals to histone deacetylase 4 during cardiomyocyte hypertrophy. J Clin Invest. 2006 Jul;116(7):1853-64.
10. Balasubramanian S, Mani SK, Kasiganesan H, Baicu CC, Kuppuswamy D. Hypertrophic stimulation increases beta-actin dynamics in adult feline cardiomyocytes. PLos One 5: e11470, 2010.
11. Barger PM, Brandt JM, Leone TC, Weinheimer CJ, Kelly DP. Deactivation of peroxisome proliferator-activated receptor-alpha during cardiac hypertrophic growth. J Clin Invest. 2000 Jun;105(12):1723-30.
12. Barron-Casella EA, Torres MA, Scherer SW, Heng HH, Tsui LC, Casella JF. Sequence analysis and chromosomal localization of human Cap Z. Conserved residues within the actin-binding domain may link Cap Z to gelsolin/severin and profilin protein families. J Biol Chem 270: 21472–21479, 1995.
13. Barron-Casella EA, Torres MA, Scherer SW, Heng HH, Tsui LC, Casella JF. Sequence analysis and chromosomal localization of human Cap Z. Conserved residues within the actin-binding domain may link Cap Z to gelsolin/severin and profilin protein families. J Biol Chem 270: 21472–21479, 1995.
14. Belin RJ, Sumandea MP, Allen EJ, Schoenfelt K, Wang H, Solaro RJ, de Tombe PP. Augmented protein kinase C-alpha-induced myofilament protein phosphorylation

contributes to myofilament dysfunction in experimental congestive heart failure. Circ Res 101: 195–204, 2007.

15. Bernardo BC, Weeks KL, Pretorius L, McMullen JR. Molecular distinction between physiological and pathological cardiac hypertrophy: experimental findings and therapeutic strategies. Pharmacol Ther. 2010 Oct;128(1):191-227.
16. Boateng SY, Belin RJ, Geenen DL, Margulies KB, Martin JL, Hoshijima M, de Tombe PP and B Russell. Cardiac dysfunction and heart failure are associated with abnormalities in the subcellular distribution and amounts of oligomeric muscle LIM protein. Am J Physiol Heart Circ Physiol. 2007 Jan; 292 (1):H259-69.
17. Boateng SY, Hartman TJ, Ahluwalia N, Vidula H, Desai TA, Russell B. Inhibition of fibroblast proliferation in cardiac myocyte cultures by surface microtopography. Am J Physiol Cell Physiol 285: C171–C182, 2003.
18. Boateng SY, Senyo SE, Qi L, Goldspink PH and B Russell. Myocyte remodelling in response to hypertrophic stimuli requires nucleocytoplasmic shuttling of muscle LIM protein. J Mol Cell Cardiol. 2009. doi: 10.1016/j.yjmcc.2009.04.006.
19. Bogomolovas J, Gasch A, Simkovic F, Rigden DJ, Labeit S, Mayans O. Titin kinase is an inactive pseudokinase scaffold that supports MuRF1 recruitment to the sarcomeric M-line. Open Biol. 2014 May;4(5):140041.
20. Bogoyevitch MA, Parker PJ, Sugden PH. Characterization of protein kinase C isotype expression in adult rat heart. Protein kinase C-epsilon is a major isotype present, and it is activated by phorbol esters, epinephrine, and endothelin. Circ Res. 1993 Apr;72(4):757-67.

21. Caldwell JE, Heiss SG, Mermall V, Cooper JA. Effects of CapZ, an actin capping protein of muscle, on the polymerization of actin. Biochemistry. 1989 28: 8506–8514.
22. Caldwell JE, Heiss SG, Mermall V, Cooper JA. Effects of CapZ, an actin capping protein of muscle, on the polymerization of actin. Biochemistry. 1989 Oct17; 28(21):8506-14.
23. Canton DA, Olsten ME, Kim K, Doherty-Kirby A, Lajoie G, Cooper JA, Litchfield DW. The pleckstrin homology domain-containing protein CKIP-1 is involved in regulation of cell morphology and the actin cytoskeleton and interaction with actin capping protein. Mol Cell Biol. 2005 May;25(9):3519-34.
24. Casella JF, Craig SW, Maack DJ, Brown AE. Cap Z(36/32), a barbed end actin-capping protein, is a component of the Z-line of skeletal muscle. J Cell Biol. 1987 Jul;105(1):371-9.
25. Catley L, Weisberg E, Kiziltepe T, Tai YT, Hideshima T, Neri P, Tassone P, Atadja P, Chauhan D, Munshi NC, Anderson KC. Aggresome induction by proteasome inhibitor bortezomib and alpha-tubulin hyperacetylation by tubulin deacetylase (TDAC) inhibitor LBH589 are synergistic in myeloma cells. Blood. 2006 Nov 15;108(10):3441-9.
26. Chang S, McKinsey TA, Zhang CL, Richardson JA, Hill JA, Olson EN. Histone deacetylases 5 and 9 govern responsiveness of the heart to a subset of stress signals and play redundant roles in heart development. Mol Cell Biol. 2004 Oct;24(19):8467-76.
27. Chen L, Hahn H, Wu G, Chen CH, Liron T, Schechtman D, Cavallaro G, Banci L, Guo Y, Bolli R, Dorn GW 2nd, Mochly-Rosen D. Opposing cardioprotective actions

and parallel hypertrophic effects of delta PKC and epsilon PKC. Proc Natl Acad Sci U S A. 2001 Sep 25;98(20):11114-9.

28. Cho YK, Eom GH, Kee HJ, Kim HS, Choi WY, Nam KI, Ma JS, Kook H. Sodium valproate, a histone deacetylase inhibitor, but not captopril, prevents right ventricular hypertrophy in rats. Circ J. 2010 Apr;74(4):760-70.
29. Choudhary C, Kumar C, Gnad F, Nielsen ML, Rehman M, Walther TC, Olsen JV, Mann M. Lysine acetylation targets protein complexes and co-regulates major cellular functions. Science. 2009 Aug 14;325(5942):834-40.
30. Christe ME, Rodgers RL. Altered glucose and fatty acid oxidation in hearts of the spontaneously hypertensive rat. J Mol Cell Cardiol. 1994 Oct;26(10):1371-5.
31. Clark KA, McElhinny AS, Beckerle MC, Gregorio CC. Striated muscle cytoarchitecture: an intricate web of form and function. Annu Rev Cell Dev Biol. 2002;18:637-706.
32. Cooper JA, Pollard TD. Effect of capping protein on the kinetics of actin polymerization. Biochemistry. 1985 Jan 29;24(3):793-9.
33. Cooper JA, Sept D. New insights into mechanism and regulation of actin capping protein. Int Rev Cell Mol Biol 267: 183–206, 2008.
34. Demos-Davies KM, Ferguson BS, Cavasin MA, Mahaffey JH, Williams SM, Spiltoir JI, Schuetze KB, Horn TR, Chen B, Ferrara C, Scellini B, Piroddi N, Tesi C, Poggesi C, Jeong MY, McKinsey TA. HDAC6 contributes to pathological responses of heart and skeletal muscle to chronic angiotensin-II signaling. Am J Physiol Heart Circ Physiol. 2014 Jul 15;307(2):H252-8.

35. Deng XF, Mulay S, Varma DR. Role of Ca(2+)-independent PKC in alpha 1-adrenoceptor-mediated inotropic responses of neonatal rat hearts. Am J Physiol. 1997 Sep;273(3 Pt 2):H1113-8.
36. Depre C, Shipley GL, Chen W, Han Q, Doenst T, Moore ML, Stepkowski S, Davies PJ, Taegtmeyer H. Unloaded heart in vivo replicates fetal gene expression of cardiac hypertrophy. Nat Med. 1998 Nov;4(11):1269-75.
37. Disatnik MH, Buraggi G, Mochly-Rosen D. Localization of protein kinase C isozymes in cardiac myocytes. Exp Cell Res. 1994 Feb;210(2):287-97.
38. Dorn GW 2nd, Mochly-Rosen D. Intracellular transport mechanisms of signal transducers. Annu Rev Physiol. 2002;64:407-29. Review.
39. Dorn GW 2nd, Souroujon MC, Liron T, Chen CH, Gray MO, Zhou HZ, Csukai M, Wu G, Lorenz JN, Mochly-Rosen D. Sustained in vivo cardiac protection by a rationally designed peptide that causes epsilon protein kinase C translocation. Proc Natl Acad Sci U S A. 1999 Oct 26;96(22):12798-803.
40. Duquesnes N, Lezoualc'h F, Crozatier B. PKC-delta and PKC-epsilon: foes of the same family or strangers? J Mol Cell Cardiol. 2011 Nov;51(5):665-73.
41. Ebashi S, Endo M. Calcium ion and muscle contraction. Prog Biophys Mol Biol. 1968;18:123-83.
42. Ebashi S, Kodama A, Ebashi F. Troponin. I. Preparation and physiological function. J Biochem. 1968 Oct;64(4):465-77.
43. Ebashi S. Third Component Participating in the Super precipitation of "Natural Actomyosin". Nature. 1963 Dec 7;200:1010.

44. Eisenberg B. Quantitative ultrastructure of mammalian skeletal muscle. Handbook of Physiology. Section 10: Skeletal Muscle. 1983;chapter 3:73-112
45. Fischer JE, Horst WD, Kopin IJ. Norepinephrine metabolism in hypertrophied rat hearts. Nature 207: 951–953, 1965.
46. Forfar JC, Muir AL, Sawers SA, Toft AD. Abnormal left ventricular function in hyperthyroidism: evidence for a possible reversible cardiomyopathy. N Engl J Med. 1982 Nov 4;307(19):1165-70.
47. Frey N, Olson EN. Cardiac hypertrophy: the good, the bad, and the ugly. Annu Rev Physiol. 2003;65:45-79.
48. Gao L, Cueto MA, Asselbergs F, Atadja P. Cloning and functional characterization of HDAC11, a novel member of the human histone deacetylase family. J Biol Chem. 2002 Jul 12;277(28):25748-55.
49. Gertz EW, Wisneski JA, Stanley WC, Neese RA. Myocardial substrate utilization during exercise in humans. Dual carbon-labeled carbohydrate isotope experiments. J Clin Invest. 1988 Dec;82(6):2017-25.
50. Glacy SD. Pattern and time course of rhodamine-actin incorporation in cardiac myocytes. J Cell Biol. 1983 Apr;96(4):1164-7.
51. Goldstein MA, Schroeter JP, Sass RL. Two structural states of the vertebrate Z band. Electron Microsc Rev. 1990;3(2):227-48.
52. Gregoretti IV, Lee YM, Goodson HV. Molecular evolution of the histone deacetylase family: functional implications of phylogenetic analysis. J Mol Biol. 2004 Apr 16;338(1):17-31.

53. Gregorio CC, Trombitas K, Centner T, Kolmerer B, Stier G, Kunke K, Suzuki K, Obermayr F, Herrmann B, Granzier H, Sorimachi H, Labeit S. The NH2 terminus of titin spans the Z-disc: its interaction with a novel 19-kD ligand (T-cap) is required for sarcomeric integrity. J Cell Biol. 1998 Nov 16;143(4):1013-27.
54. Grossman W, Jones D, McLaurin LP. Wall stress and patterns of hypertrophy in the human left ventricle. J Clin Invest. 1975 Jul;56(1):56-64.
55. Gupta A, Dey CS. PTEN and SHIP2 regulates PI3K/Akt pathway through focal adhesion kinase. Mol Cell Endocrinol 309: 55–62, 2009.
56. Han A, He J, Wu Y, Liu JO, Chen L. Mechanism of recruitment of class II histone deacetylases by myocyte enhancer factor-2. J Mol Biol. 2005 Jan 7;345(1):91-102.
57. Hanson J and Lowy J. The structure of F-actin and actin filaments isolated from muscle. J Mol Biol 1963 6:49–60.
58. Hanson J, Huxley HE. Structural basis of the cross-striations in muscle. Nature. 1953 Sep 19;172(4377):530-2.
59. Hart MC, Cooper JA. Vertebrate isoforms of actin capping protein beta have distinct functions In vivo. J Cell Biol. 1999 Dec 13;147(6):1287-98.
60. Hart MC, Korshunova YO, Cooper JA. Vertebrates have conserved capping protein alpha isoforms with specific expression patterns. Cell Motil Cytoskeleton. 1997;38(2):120-32.
61. Hartman TJ, Martin JL, Solaro RJ, Samarel AM, Russell B. CapZ dynamics are altered by endothelin-1 and phenylephrine via PIP2- and PKC-dependent mechanisms. Am J Physiol Cell Physiol. 2009 May;296(5):C1034-9.

62. Henderson JR, Pomies P, Auffray C, Beckerle MC. ALP and MLP distribution during myofibrillogenesis in cultured cardiomyocytes. Cell Motil Cytoskeleton. 2003 Mar;54(3):254-65.
63. Henty-Ridilla JL, Shimono M, Li J, Chang JH, Day B, Staiger CJ. The plant actin cytoskeleton responds to signals from microbe-associated molecular patterns. PLoS Pathog. 2013;9(4):e1003290.
64. Hernandez OM, Jones M, Guzman G, Szczesna-Cordary D. Myosin essential light chain in health and disease. Am J Physiol Heart Circ Physiol. 2007 Apr;292(4):H1643-54.
65. Hoshijima M. Mechanical stress-strain sensors embedded in cardiac cytoskeleton: Z disk, titin, and associated structures. Am J Physiol Heart Circ Physiol. 2006 Apr;290(4):H1313-25.
66. House C1, Kemp BE. Protein kinase C contains a pseudosubstrate prototope in its regulatory domain. Science. 1987 Dec 18;238(4834):1726-8.
67. Huang XP, Pi Y, Lokuta AJ, Greaser ML, Walker JW. Arachidonic acid stimulates protein kinase C-epsilon redistribution in heart cells. J Cell Sci. 1997 Jul;110 (Pt 14):1625-34.
68. Hubbert C, Guardiola A, Shao R, Kawaguchi Y, Ito A, Nixon A, Yoshida M, Wang XF, Yao TP. HDAC6 is a microtubule-associated deacetylase. Nature. 2002 May 23;417(6887):455-8.
69. Hug C, Miller TM, Torres MA, Casella JF, Cooper JA. Identification and characterization of an actin-binding site of CapZ. J Cell Biol. 1992 Feb;116(4):923-31.

70. Humphries MJ. Integrin structure. Biochem Soc Trans. 2000;28(4):311-39.
71. Hunter JJ, Chien KR. Signaling pathways for cardiac hypertrophy and failure. N Engl J Med. 1999 Oct 21;341(17):1276-83.
72. Huxley AF, Niedergerke R. Structural changes in muscle during contraction; interference microscopy of living muscle fibres. Nature. 1954 May 22;173(4412):971-3.
73. Huxley AF, Taylor RE. Function of Krause's membrane. Nature. 1955 Dec 3;176(4492):1068.
74. Huxley AF. Muscle structure and theories of contraction. Prog Biophys Biophys Chem. 1957;7:255-318.
75. Iskratsch T, Reijntjes S, Dwyer J, Toselli P, Degano IR, Dominguez I, Ehler E. Two distinct phosphorylation events govern the function of muscle FHOD3. Cell Mol Life Sci. 2013 Mar;70(5):893-908.
76. Israeli-Rosenberg S, Manso AM, Okada H, Ross RS. Integrins and integrin-associated proteins in the cardiac myocyte. Circ Res. 2014 Jan 31;114(3):572-86.
77. Iyer A, Fenning A, Lim J, Le GT, Reid RC, Halili MA, Fairlie DP, Brown L. Antifibrotic activity of an inhibitor of histone deacetylases in DOCA-salt hypertensive rats. Br J Pharmacol. 2010 Apr;159(7):1408-17.
78. Jung G, Remmert K, Wu X, Volosky JM, Hammer JA 3rd. The Dictyostelium CARMIL protein links capping protein and the Arp2/3 complex to type I myosins through their SH3 domains. J Cell Biol. 2001 Jun 25; 153(7):1479-97
79. Kamm KE, Stull JT. Signaling to myosin regulatory light chain in sarcomeres. J Biol Chem. 2011 Mar 25;286(12):9941-7.

80. Kannel WB, Gordon T, Offutt D. Left ventricular hypertrophy by electrocardiogram. Prevalence, incidence, and mortality in the Framingham study. Ann Intern Med. 1969 Jul;71(1):89-105.
81. Katz AM. Physiology of the Heart. Fifth Edition. 2010.
82. Keranen LM, Dutil EM, Newton AC. Protein kinase C is regulated in vivo by three functionally distinct phosphorylations. Curr Biol. 1995 Dec 1;5(12):1394-1403.
83. Kilimann MW, Isenberg G. Actin filament capping protein from bovine brain. EMBO J 1: 889–894, 1982.
84. Kim K, McCully ME, Bhattacharya N, Butler B, Sept D, Cooper JA. Structure/function analysis of the interaction of phosphatidylinositol 4,5-bisphosphate with actin-capping protein: implications for how capping protein binds the actin filament. J Biol Chem. 2007 Feb 23;282(8):5871-9.
85. Kim K, Yamashita A, Wear MA, Maeda Y, Cooper JA. Capping protein binding to actin in yeast: biochemical mechanism and physiological relevance. J Cell Biol 164: 567–580, 2004.
86. Kim K, Yamashita A, Wear MA, Maeda Y, Cooper JA. Capping protein binding to actin in yeast: biochemical mechanism and physiological relevance. J Cell Biol. 2004 164: 567–580.
87. Kim T, Cooper JA, Sept D. The interaction of capping protein with the barbed end of the actin filament. J Mol Biol. 2010 Dec 17;404(5):794-802.
88. Kim MY, Woo EM, Chong YT, Homenko DR, Kraus WL. Acetylation of estrogen receptor alpha by p300 at lysines 266 and 268 enhances the deoxyribonucleic acid

binding and transactivation activities of the receptor. Mol Endocrinol. 2006 Jul;20(7):1479-93.

89. Knappeis GG, Carlsen F. The ultrastructure of the Z disc in skeletal muscle. J Cell Biol. 1962 May;13:323-35.

90. Knoll R, Kostin S, Klede S, Savvatis K, Klinge L, Stehle I, Gunkel S, Kotter S, Babicz K, Sohns M, Miocic S, Didie M, Knoll G, Zimmermann WH, Thelen P, Bickeboller H, Maier LS, Schaper W, Schaper J, Kraft T, Tschope C, Linke WA, Chien KR. A common MLP (muscle LIM protein) variant is associated with cardiomyopathy. Circ Res. 2010 Mar 5;106(4):695-704.

91. Knoll R, Linke WA, Zou P, Miocic S, Kostin S, Buyandelger B, Ku CH, Neef S, Bug M, Schafer K, Knoll G, Felkin LE, Wessels J, Toischer K, Hagn F, Kessler H, Didie M, Quentin T, Maier LS, Teucher N, Unsold B, Schmidt A, Birks EJ, Gunkel S, Lang P, Granzier H, Zimmermann WH, Field LJ, Faulkner G, Dobbelstein M, Barton PJ, Sattler M, Wilmanns M, Chien KR. Telethonin deficiency is associated with maladaptation to biomechanical stress in the mammalian heart. Circ Res. 2011 Sep 16;109(7):758-69.

92. Knöll R. Myosin binding protein C: implications for signal-transduction. J Muscle Res Cell Motil. 2012 May;33(1):31-42.

93. Kojic S, Radojkovic D, Faulkner G. Muscle ankyrin repeat proteins: their role in striated muscle function in health and disease. Crit Rev Clin Lab Sci. 2011 Sep-Dec;48(5-6):269-94.

94. Kong Y, Flick MJ, Kudla AJ, Konieczny SF. Muscle LIM protein promotes myogenesis by enhancing the activity of MyoD. Mol Cell Biol. 1997 Aug;17(8):4750-60.

95. Kong Y, Tannous P, Lu G, Berenji K, Rothermel BA, Olson EN, Hill JA. Suppression of class I and II histone deacetylases blunts pressure-overload cardiac hypertrophy. Circulation. 2006 Jun 6;113(22):2579-88.

96. Kook H, Lepore JJ, Gitler AD, Lu MM, Wing-Man Yung W, Mackay J, Zhou R, Ferrari V, Gruber P, Epstein JA. Cardiac hypertrophy and histone deacetylase-dependent transcriptional repression mediated by the atypical homeodomain protein Hop. J Clin Invest. 2003 Sep;112(6):863-71.

97. Koren MJ, Devereux RB, Casale PN, Savage DD, Laragh JH. Relation of left ventricular mass and geometry to morbidity and mortality in uncomplicated essential hypertension. Ann Intern Med. 1991 Mar 1;114(5):345-52.

98. Koshman YE, Kim T, Chu M, Engman SJ, Iyengar R, Robia SL, Samarel AM. FRNK inhibition of focal adhesion kinase-dependent signaling and migration in vascular smooth muscle cells. Arterioscler Thromb Vasc Biol 30: 2226–2233, 2010.

99. Kotlo K, Johnson KR, Grillon JM, Greenen DL, Detombe P, Danzigar RS. Phosphoprotein abundance changes in hypertensive cardiac remodeling. J Proteomics. 2012;77:1–3

100. Lange S, Xiang F, Yakovenko A, Vihola A, Hackman P, Rostkova E, Kristensen J, Brandmeier B, Franzen G, Hedberg B, Gunnarsson LG, Hughes SM, Marchand S, Sejersen T, Richard I, Edstrom L, Ehler E, Udd B, Gautel M. The kinase domain of

titin controls muscle gene expression and protein turnover. Science. 2005 Jun 10;308(5728):1599-603.

101. Lee TM, Lin MS, Chang NC. Inhibition of histone deacetylase on ventricular remodeling in infarcted rats. Am J Physiol Heart Circ Physiol. 2007 Aug;293(2):H968-77.

102. Li C, Hu Y, Mayr M, Xu Q. Cyclic strain stress-induced mitogen-activated protein kinase (MAPK) phosphatase 1 expression in vascular smooth muscle cells is regulated by Ras/Rac-MAPK pathways. J Biol Chem 274: 25273–25280, 1999.

103. Li J, Russell B. Phosphatidylinositol 4,5-bisphosphate regulates CapZβ1 and actin dynamics in response to mechanical strain. Am J Physiol Heart Circ Physiol. 2013 Dec 1;305(11):H1614-23.

104. Li J, Umar S, Amjedi M, Iorga A, Sharma S, Nadadur RD, Regitz-Zagrosek V, Eghbali M. New frontiers in heart hypertrophy during pregnancy. Am J Cardiovasc Dis. 2012;2(3):192-207.

105. Lin YH, Li J, Swanson ER, Russell B. CapZ and actin capping dynamics increase in myocytes after a bout of exercise and abates in hours after stimulation ends. J Appl Physiol 114: 1603–1609, 2013.

106. Littlefield R, Almenar-Queralt A, Fowler VM. Actin dynamics at pointed ends regulates thin filament length in striated muscle. Nat Cell Biol 3: 544–551, 2001.

107. Lopez-Rodas G, Brosch G, Georgieva EI, Sendra R, Franco L, Loidl P. Histone deacetylase. A key enzyme for the binding of regulatory proteins to chromatin. FEBS Lett. 1993 Feb 15;317(3):175-80.

108. Lu J, McKinsey TA, Zhang CL, Olson EN. Regulation of skeletal myogenesis by association of the MEF2 transcription factor with class II histone deacetylases. Mol Cell. 2000 Aug;6(2):233-44.

109. Lu QW, Wu XY, Morimoto S. Inherited cardiomyopathies caused by troponin mutations. J Geriatr Cardiol. 2013 Mar;10(1):91-101.

110. Lundby A, Lage K, Weinert BT, Bekker-Jensen DB, Secher A, Skovgaard T, Kelstrup CD, Dmytriyev A, Choudhary C, Lundby C, Olsen JV. Proteomic analysis of lysine acetylation sites in rat tissues reveals organ specificity and subcellular patterns. Cell Rep. 2012 Aug 30;2(2):419-31.

111. Luo J, Su F, Chen D, Shiloh A, Gu W. Deacetylation of p53 modulates its effect on cell growth and apoptosis. Nature. 2000 Nov 16;408(6810):377-81.

112. Luther PK. Three-dimensional reconstruction of a simple Z-band in fish muscle. J Cell Biol. 1991 Jun;113(5):1043-55.

113. MacDougall JD, Tuxen D, Sale DG, Moroz JR, Sutton JR. Arterial blood pressure response to heavy resistance exercise. J Appl Physiol (1985). 1985 Mar;58(3):785-90.

114. Mackay K, Mochly-Rosen D. Localization, anchoring, and functions of protein kinase C isozymes in the heart. J Mol Cell Cardiol. 2001 Jul;33(7):1301-7.

115. Mansour H, de Tombe PP, Samarel AM, Russell B. Restoration of resting sarcomere length after uniaxial static strain is regulated by protein kinase Cepsilon and focal adhesion kinase. Circ Res. 2004 Mar 19;94(5):642-9.

116. Marks PA. Histone deacetylase inhibitors: a chemical genetics approach to understanding cellular functions. Biochim Biophys Acta. 2010 Oct-Dec;1799(10-12):717-25.

117. Maruyama K, Obinata T. Presence of beta-actinin in the soluble fraction of the muscle cells of the chick embryo. J Biochem. 1965 Apr;57:575-7.

118. Matsuzaki H, Daitoku H, Hatta M, Aoyama H, Yoshimochi K, Fukamizu A. Acetylation of Foxo1 alters its DNA-binding ability and sensitivity to phosphorylation. Proc Natl Acad Sci U S A. 2005 Aug 9;102(32):11278-83.

119. McCain ML, Parker KK. Mechanotransduction: the role of mechanical stress, myocyte shape, and cytoskeletal architecture on cardiac function. Pflugers Arch 462: 89–104, 2011.

120. McKenna N, Meigs JB, Wang YL. Identical distribution of fluorescently labeled brain and muscle actins in living cardiac fibroblasts and myocytes. J Cell Biol. 1985 100: 292–296.

121. McKinsey TA, Zhang CL, Olson EN. MEF2: a calcium-dependent regulator of cell division, differentiation and death. Trends Biochem Sci. 2002 Jan;27(1):40-7.

122. Miller MK, Bang ML, Witt CC, Labeit D, Trombitas C, Watanabe K, Granzier H, McElhinny AS, Gregorio CC, Labeit S. The muscle ankyrin repeat proteins: CARP, ankrd2/Arpp and DARP as a family of titin filament-based stress response molecules. J Mol Biol. 2003 Nov 7;333(5):951-64.

123. Mochly-Rosen D. Localization of protein kinases by anchoring proteins: a theme in signal transduction. Science. 1995 Apr 14;268(5208):247-51.

124. Monovich L, Koch KA, Burgis R, Osimboni E, Mann T, Wall D, Gao J, Feng Y, Vega RB, Turner BA, Hood DB, Law A, Papst PJ, Koditek D, Chapo JA, Reid BG, Melvin LS, Pagratis NC, McKinsey TA. Suppression of HDAC nuclear export and cardiomyocyte hypertrophy by novel irreversible inhibitors of CRM1. Biochim Biophys Acta. 2009 May;1789(5):422-31.

125. Monovich L, Vega RB, Meredith E, Miranda K, Rao C, Capparelli M, Lemon DD, Phan D, Koch KA, Chapo JA, Hood DB, McKinsey TA. A novel kinase inhibitor establishes a predominant role for protein kinase D as a cardiac class IIa histone deacetylase kinase. FEBS Lett. 2010 Feb 5;584(3):631-7.

126. Montgomery RL, Davis CA, Potthoff MJ, Haberland M, Fielitz J, Qi X, Hill JA, Richardson JA, Olson EN. Histone deacetylases 1 and 2 redundantly regulate cardiac morphogenesis, growth, and contractility. Genes Dev. 2007 Jul 15;21(14):1790-802.

127. Moscat J, Diaz-Meco MT, Wooten MW. Of the atypical PKCs, Par-4 and p62: recent understandings of the biology and pathology of a PB1-dominated complex. Cell Death Differ. 2009 Nov;16(11):1426-37.

128. Moulopoulos SD, Anthopoulos LP Reversible atrio-ventricular conduction changes during exercise. Acta Cardiol. 1968;23(4):352-66.

129. Mozaffarian D, Benjamin EJ, Go AS, Arnett DK, Blaha MJ, Cushman M, de Ferranti S, Després JP, Fullerton HJ, Howard VJ, Huffman MD, Judd SE, Kissela BM, Lackland DT, Lichtman JH, Lisabeth LD, Liu S, Mackey RH, Matchar DB, McGuire DK, Mohler ER 3rd, Moy CS, Muntner P, Mussolino ME, Nasir K, Neumar RW, Nichol G, Palaniappan L, Pandey DK, Reeves MJ, Rodriguez CJ, Sorlie PD,

Stein J, Towfighi A, Turan TN, Virani SS, Willey JZ, Woo D, Yeh RW, Turner MB; American Heart Association Statistics Committee and Stroke Statistics Subcommittee. Heart disease and stroke statistics-2015 update: a report from the american heart association. Circulation. 2015 Jan 27;131(4):e29-e322.

130. Nakagawa M, Hamaoka K, Hattori T, Sawada T. Postnatal DNA synthesis in hearts of mice: autoradiographic and cytofluorometric investigations. Cardiovasc Res. 1988 Aug;22(8):575-83.

131. Nakagawa N, Hoshijima M, Oyasu M, Saito N, Tanizawa K, Kuroda S. ENH, containing PDZ and LIM domains, heart/skeletal muscle-specific protein, associates with cytoskeletal proteins through the PDZ domain. Biochem Biophys Res Commun. 2000 Jun 7;272(2):505-12.

132. Nakao K, Minobe W, Roden R, Bristow MR, Leinwand LA. Myosin heavy chain gene expression in human heart failure. J Clin Invest. 1997 Nov 1;100(9):2362-70.

133. Neri Serneri GG, Boddi M, Modesti PA, Cecioni I, Coppo M, Padeletti L, Michelucci A, Colella A, Galanti G. Increased cardiac sympathetic activity and insulin-like growth factor-I formation are associated with physiological hypertrophy in athletes. Circ Res. 2001 Nov 23;89(11):977-82.

134. Newton AC. Protein kinase C: structure, function, and regulation. J Biol Chem. 1995 Dec 1;270(48):28495-8.

135. Newton AC. Regulation of the ABC kinases by phosphorylation: protein kinase C as a paradigm. Biochem J. 2003 Mar 1;370(Pt 2):361-71.

136. North BJ, Marshall BL, Borra MT, Denu JM, Verdin E. The human Sir2 ortholog, SIRT2, is an NAD+-dependent tubulin deacetylase. Mol Cell. 2003 Feb;11(2):437-44.

137. Ono S. Dynamic regulation of sarcomeric actin filaments in striated muscle. Cytoskeleton (Hoboken). 2010 Nov;67(11):677-92.

138. Pappas CT, Bhattacharya N, Cooper JA, Gregorio CC. Nebulin interacts with CapZ and regulates thin filament architecture within the Z-disc. Mol Biol Cell. 2008 May;19(5):1837-47.

139. Pardo JV, Siliciano JD, Craig SW. A vinculin-containing cortical lattice in skeletal muscle: transverse lattice elements ("costameres") mark sites of attachment between myofibrils and sarcolemma. Proc Natl Acad Sci U S A. 1983 Feb;80(4):1008-12.

140. Peter AK, Cheng H, Ross RS, Knowlton KU, Chen J. The costamere bridges sarcomeres to the sarcolemma in striated muscle. Prog Pediatr Cardiol. 2011 May;31(2):83-88.

141. Pi Y, Walker JW. Diacylglycerol and fatty acids synergistically increase cardiomyocyte contraction via activation of PKC. Am J Physiol Heart Circ Physiol. 2000 Jul;279(1):H26-34.

142. Ping P, Zhang J, Pierce WM Jr, Bolli R. Functional proteomic analysis of protein kinase C epsilon signaling complexes in the normal heart and during cardioprotection. Circ Res. 2001 Jan 19;88(1):59-62.

143. Pluim BM, Zwinderman AH, van der Laarse A, van der Wall EE. The athlete's heart. A meta-analysis of cardiac structure and function. Circulation. 2000 Jan 25;101(3):336-44.

144. Pollard TD, Mooseker MS. Direct measurement of actin polymerization rate constants by electron microscopy of actin filaments nucleated by isolated microvillus cores. J Cell Biol 88: 654–659, 1981.

145. Popescu LM, Gherghiceanu M, Hinescu ME, Cretoiu D, Ceafalan L, Regalia T, Popescu AC, Ardeleanu C, Mandache E. Insights into the interstitium of ventricular myocardium: interstitial Cajal-like cells (ICLC). J Cell Mol Med. 2006 Apr-Jun;10(2):429-58.

146. Pound KM, Arteaga GM, Fasano M, Wilder T, Fischer SK, Warren CM, Wende AR, Farjah M, Abel ED, Solaro RJ, Lewandowski ED. Expression of slow skeletal TnI in adult mouse hearts confers metabolic protection to ischemia. J Mol Cell Cardiol. 2011 Aug;51(2):236-43.

147. Prekeris R, Mayhew MW, Cooper JB, Terrian DM. Identification and localization of an actin-binding motif that is unique to the epsilon isoform of protein kinase C and participates in the regulation of synaptic function. J Cell Biol. 1996 Jan;132(1-2):77-90.

148. Pyle WG, Solaro RJ. At the crossroads of myocardial signaling: the role of Z-discs in intracellular signaling and cardiac function. Circ Res. 2004 Feb 20;94(3):296-305.

149. Pyle WG, La Rotta G, de Tombe PP, Sumandea MP, Solaro RJ. Control of cardiac myofilament activation and PKC-betaII signaling through the actin capping protein, CapZ. J Mol Cell Cardiol. 2006 Sep;41(3):537-43.

150. Rapacciuolo A, Esposito G, Caron K, Mao L, Thomas SA, Rockman HA. Important role of endogenous norepinephrine and epinephrine in the development of

in vivo pressure-overload cardiac hypertrophy. J Am Coll Cardiol. 2001 Sep;38(3):876-82.

151. Robia SL, Ghanta J, Robu VG, Walker JW. Localization and kinetics of protein kinase C-epsilon anchoring in cardiac myocytes. Biophys J. 2001 May;80(5):2140-51.

152. Ron D, Mochly-Rosen D. An autoregulatory region in protein kinase C: the pseudoanchoring site. Proc Natl Acad Sci U S A. 1995 Jan 17;92(2):492-6.

153. Roth SY, Denu JM, Allis CD. Histone acetyltransferases. Annu Rev Biochem. 2001;70:81-120.

154. Roy P, Rajfur Z, Pomorski P, Jacobson K. Microscope-based techniques to study cell adhesion and migration. Nat Cell Biol 4: E91–E96, 2002.

155. Sakaguchi K, Herrera JE, Saito S, Miki T, Bustin M, Vassilev A, Anderson CW, Appella E. DNA damage activates p53 through a phosphorylation-acetylation cascade. Genes Dev. 1998 Sep 15;12(18):2831-41.

156. Salazar NC1, Chen J, Rockman HA. Cardiac GPCRs: GPCR signaling in healthy and failing hearts. Biochim Biophys Acta. 2007 Apr;1768(4):1006-18.

157. Samant SA, Courson DS, Sundaresan NR, Pillai VB, Tan M, Zhao Y, Shroff SG, Rock RS, Gupta MP. HDAC3-dependent reversible lysine acetylation of cardiac myosin heavy chain isoforms modulates their enzymatic and motor activity. J Biol Chem. 2011 Feb 18;286(7):5567-77.

158. Samarel AM. Focal adhesion signaling in heart failure. Pflugers Arch. 2014 Jun;466(6):1101-11. Samarel AM. Costameres, focal adhesions, and cardiomyocyte mechanotransduction. Am J Physiol Heart Circ Physiol. 2005 Dec;289(6):H2291-301.

159. Samarel AM. Focal adhesion signaling in heart failure. Pflugers Arch. 2014 Jun;466(6):1101-11.

160. Sanger JW, Kang S, Siebrands CC, Freeman N, Du A, Wang J, Stout AL, Sanger JM. How to build a myofibril. J Muscle Res Cell Motil. 2005;26(6-8):343-54.

161. Schafer DA, Jennings PB, Cooper JA. Dynamics of capping protein and actin assembly in vitro: uncapping barbed ends by polyphosphoinositides. J Cell Biol 135: 169–179, 1996.

162. Schafer DA, Korshunova YO, Schroer TA, Cooper JA. Differential localization and sequence analysis of capping protein beta-subunit isoforms of vertebrates. J Cell Biol. 1994 Oct;127(2):453-65.

163. Scruggs SB, Hinken AC, Thawornkaiwong A, Robbins J, Walker LA, de Tombe PP, Geenen DL, Buttrick PM, Solaro RJ. Ablation of ventricular myosin regulatory light chain phosphorylation in mice causes cardiac dysfunction in situ and affects neighboring myofilament protein phosphorylation. J Biol Chem. 2009 Feb 20;284(8):5097-106.

164. Scruggs SB, Solaro RJ. The significance of regulatory light chain phosphorylation in cardiac physiology. Arch Biochem Biophys. 2011 Jun 15;510(2):129-34.

165. Senyo SE, Koshman YE, Russell B. Stimulus interval, rate and direction differentially regulate phosphorylation for mechanotransduction in neonatal cardiac myocytes. FEBS Lett 581: 4241–4247, 2007.

166. Seqqat R, Guo X, Rafiq K, Kolpakov MA, Guo J, Koch WJ, Houser SR, Dell'italia LJ, Sabri A. Beta1-adrenergic receptors promote focal adhesion signaling

downregulation and myocyte apoptosis in acute volume overload. J Mol Cell Cardiol 53: 240–249, 2012.

167. Sheikh F, Raskin A, Chu PH, Lange S, Domenighetti AA, Zheng M, Liang X, Zhang T, Yajima T, Gu Y, Dalton ND, Mahata SK, Dorn GW 2nd, Brown JH, Peterson KL, Omens JH, McCulloch AD, Chen J. An FHL1-containing complex within the cardiomyocyte sarcomere mediates hypertrophic biomechanical stress responses in mice. J Clin Invest. 2008 Dec;118(12):3870-80.

168. Sihag S, Cresci S, Li AY, Sucharov CC, Lehman JJ. PGC-1alpha and ERRalpha target gene downregulation is a signature of the failing human heart. J Mol Cell Cardiol 2009;46:201-212.

169. Simpson P. Norepinephrine-stimulated hypertrophy of cultured rat myocardial cells is an alpha 1 adrenergic response. J Clin Invest 72: 732–738, 1983.

170. Simpson P. Norepinephrine-stimulated hypertrophy of cultured rat myocardial cells is an alpha 1 adrenergic response. J Clin Invest 72: 732–738, 1983.

171. Skwarek-Maruszewska A, Hotulainen P, Mattila PK, Lappalainen P. Contractility-dependent actin dynamics in cardiomyocyte sarcomeres. J Cell Sci 122: 2119–2126, 2009.

172. Solaro RJ, Henze M, Kobayashi T. Integration of troponin I phosphorylation with cardiac regulatory networks. Circ Res. 2013 Jan 18;112(2):355-66.

173. Solaro RJ, van der Velden J. Why does troponin I have so many phosphorylation sites? Fact and fancy. J Mol Cell Cardiol. 2010 May;48(5):810-6.

174. Sonnenblick EH, Spiro D, Cottrell TS. Fine structural changes in heart muscle in relation of the lengthtension curve. Proc Natl Acad Sci U S A. 1963 Feb 15;49:193-200.

175. Soonpaa MH, Kim KK, Pajak L, Franklin M, Field LJ. Cardiomyocyte DNA synthesis and binucleation during murine development. Am J Physiol. 1996 Nov;271(5 Pt 2):H2183-9.

176. Sorokina N, O'Donnell JM, McKinney RD, Pound KM, Woldegiorgis G, LaNoue KF, et al. Recruitment of compensatory pathways to sustain oxidative flux with reduced carnitine palmitoyltransferase I activity characterizes inefficiency in energy metabolism in hypertrophied hearts. Circulation 2007;115:2033-2041.

177. Sprague BL, Pego RL, Stavreva DA, McNally JG. Analysis of binding reactions by fluorescence recovery after photobleaching. Biophys J 86: 3473–3495, 2004.

178. Staiger CJ, Poulter NS, Henty JL, Franklin-Tong VE, Blanchoin L. Regulation of actin dynamics by actin-binding proteins in pollen. J Exp Bot. 2010 Apr;61(7):1969-86.Steinberg SF. Structural basis of protein kinase C isoform function. Physiol Rev. 2008 Oct;88(4):1341-78.

179. Sucharov CC, Dockstader K, McKinsey TA. YY1 protects cardiac myocytes from pathologic hypertrophy by interacting with HDAC5. Mol Biol Cell. 2008 Oct;19(10):4141-53.

180. Suzuki A, Goll DE, Singh I, Allen RE, Robson RM, Stromer MH. Some properties of purified skeletal muscle alpha-actinin. J Biol Chem. 1976 Nov 10;251(21):6860–6870.

181. Swanson ER. Mechanical strain regulates contractile protein dynamics related to heart remodeling. Thesis for the degree of master of science. 2012.

182. Takai Y, Kishimoto A, Inoue M, Nishizuka Y. Studies on a cyclic nucleotide-independent protein kinase and its proenzyme in mammalian tissues. I. Purification and characterization of an active enzyme from bovine cerebellum. J Biol Chem. 1977 Nov 10;252(21):7603-9.

183. Takano K, Watanabe-Takano H, Suetsugu S, Kurita S, Tsujita K, Kimura S, Karatsu T, Takenawa T, Endo T. Nebulin and N-WASP cooperate to cause IGF-1-induced sarcomeric actin filament formation. Science. 2010 Dec 10;330(6010):1536-40.

184. Takeda S, Minakata S, Koike R, Kawahata I, Narita A, Kitazawa M, Ota M, Yamakuni T, Maéda Y, Nitanai Y. Two distinct mechanisms for actin capping protein regulation--steric and allosteric inhibition. PLoS Biol. 2010 Jul 6;8(7):e1000416.

185. Takeishi Y, Ping P, Bolli R, Kirkpatrick DL, Hoit BD, Walsh RA. Transgenic overexpression of constitutively active protein kinase C epsilon causes concentric cardiac hypertrophy. Circ Res. 2000 Jun 23;86(12):1218-23.

186. Taoka M, Ichimura T, Wakamiya-Tsuruta A, Kubota Y, Araki T, Obinata T, Isobe T. V-1, a protein expressed transiently during murine cerebellar development, regulates actin polymerization via interaction with capping protein. J Biol Chem. 2003 Feb 21; 278(8):5864-70.

187. Tarafdar A, Michie AM. Protein kinase C in cellular transformation: a valid target for therapy? Biochem Soc Trans. 2014 Dec;42(6):1556-62.

188. Taunton J, Hassig CA, Schreiber SL. A mammalian histone deacetylase related to the yeast transcriptional regulator Rpd3p. Science. 1996 Apr 19;272(5260):408-11.

189. Terracio L, Miller B, Borg TK. Effects of cyclic mechanical stimulation of the cellular components of the heart: in vitro. Cell Dev Biol 24: 53–58, 1988

190. Tian R, Musi N, D'Agostino J, Hirshman MF, Goodyear LJ. Increased adenosine monophosphate-activated protein kinase activity in rat hearts with pressure-overload hypertrophy. Circulation 2001;104:1664-1669.

191. Thiagalingam S, Cheng KH, Lee HJ, Mineva N, Thiagalingam A, Ponte JF. Histone deacetylases: unique players in shaping the epigenetic histone code. Ann N Y Acad Sci. 2003 Mar;983:84-100.

192. Torsoni AS, Constancio SS, Nadruz W, Jr, Hanks SK, Franchini KG. Focal adhesion kinase is activated and mediates the early hypertrophic response to stretch in cardiac myocytes. Circ Res 93: 140–147, 2003.

193. Trivedi CM, Lu MM, Wang Q, Epstein JA. Transgenic overexpression of Hdac3 in the heart produces increased postnatal cardiac myocyte proliferation but does not induce hypertrophy. J Biol Chem. 2008 Sep 26;283(39):26484-9.

194. Vakili BA, Okin PM, Devereux RB. Prognostic implications of left ventricular hypertrophy. Am Heart J. 2001 Mar;141(3):334-41.

195. van der Vusse GJ, Glatz JF, Stam HC, Reneman RS. Fatty acid homeostasis in the normoxic and ischemic heart. Physiol Rev. 1992 Oct;72(4):881-940. Review.

196. von Bülow M, Rackwitz HR, Zimbelmann R, Franke WW. CP beta3, a novel isoform of an actin-binding protein, is a component of the cytoskeletal calyx of the mammalian sperm head. Exp Cell Res. 1997 May 25;233(1):216-24.

197. Waltregny D, Glenisson W, Tran SL, North BJ, Verdin E, Colige A, Castronovo V. Histone deacetylase HDAC8 associates with smooth muscle alpha-actin and is essential for smooth muscle cell contractility. FASEB J. 2005 Jun;19(8):966-8.

198. Wear MA, Yamashita A, Kim K, Maeda Y, Cooper JA. How capping protein binds the barbed end of the actin filament. Curr Biol. 2003 13: 1531–1537.

199. Webb, MR, and Trentham, DR. Chemical mechanism of myosin-catalyzed ATP hydrolysis. In: Peachy, L.D., Adrian, R.H., and Geiger, S.R., ed. Handbook of Physiology. Bethesda, MD: American Physiological Society.1983;237-255.

200. Weber A, Murray JM. Molecular control mechanisms in muscle contraction. Physiol Rev. 1973 Jul;53(3):612-73.

201. Weeks KL, McMullen JR. The athlete's heart vs. the failing heart: can signaling explain the two distinct outcomes? Physiology (Bethesda). 2011 Apr;26(2):97-105. Review.

202. Wendt T, Guenebaut V, Leonard KR. Structure of the Lethocerus troponin-tropomyosin complex as determined by electron microscopy. J Struct Biol. 1997 Feb;118(1):1-8.

203. Williams SM, Golden-Mason L, Ferguson BS, Schuetze KB, Cavasin MA, Demos-Davies K, Yeager ME, Stenmark KR, McKinsey TA. Class I HDACs regulate angiotensin II-dependent cardiac fibrosis via fibroblasts and circulating fibrocytes. J Mol Cell Cardiol. 2014 Feb;67:112-25.

204. Witt CC, Burkart C, Labeit D, McNabb M, Wu Y, Granzier H, Labeit S. Nebulin regulates thin filament length, contractility, and Z-disk structure in vivo. EMBO J. 2006 Aug 23;25(16):3843-55.

205. Yamashita A, Maeda K, Maeda Y. Crystal structure of CapZ: structural basis for actin filament barbed end capping. EMBO J. 2003 Apr 1;22(7):1529-38.

206. Yang WM, Tsai SC, Wen YD, Fejer G, Seto E. Functional domains of histone deacetylase-3. J Biol Chem. 2002 Mar 15;277(11):9447-54.

207. Zak R, Kizu A, Bugaisky L. Cardiac hypertrophy: its characteristics as a growth process. Am J Cardiol. 1979 Oct 22;44(5):941-6.

208. Zeng L, Webster SV, Newton PM. The biology of protein kinase C. Adv Exp Med Biol. 2012;740:639-61.

209. Zhou Q, Ruiz-Lozano P, Martone ME, Chen J. Cypher, a striated muscle-restricted PDZ and LIM domain-containing protein, binds to alpha-actinin-2 and protein kinase C. J Biol Chem. 1999 Jul 9;274(28):19807-13.

210. Zou P, Pinotsis N, Lange S, Song YH, Popov A, Mavridis I, Mayans OM, Gautel M, Wilmanns M. Palindromic assembly of the giant muscle protein titin in the sarcomeric Z-disk. Nature. 2006 Jan 12;439(7073):229-33.

211. Zwolak A, Fujiwara I, Hammer JA 3rd, Tjandra N. Structural basis for capping protein sequestration by myotrophin (V-1). J Biol Chem. 2010 Aug 13;285(33):25767-81.

VITA

Ying-Hsi Lin

Education Experience

09/1998-06/2002	BS in Zoology, Department of Zoology, National Taiwan University
09/2002-06/2004	MS in Physiology, Department of Physiology, National Taiwan University
	Thesis: The Relationship between Intracellular pH and Mechanism of Apoptosis in Rat Cardiomyocytes
12/2004-02/2005	Primary Emergency Medical Training (EMT-1)
09/2009-present	PHD candidate in Physiology and Biophysics, University of Illinois at Chicago

Publications/Research Abilities:

Lin YH. The Relationship between Intracellular pH and Mechanism of Apoptosis in Rat Cardiomyocytes. *Master's Thesis,* National Taiwan University, 2004

Pang PH, Lin YH, Lee YH, Hou HH, Hsu SP, Juan SH. Molecular mechanisms of p21 and p27 induction by 3-methylcholanthrene, an aryl-hydrocarbon receptor agonist, involved in antiproliferation of human umbilical vascular endothelial cells. *Journal of Cellular Physiology*. 2008 Apr; 215 (1):161-71.

Lin YH, Li J, Swanson ER, Russell B. CapZ and actin capping dynamics increase in myocytes after a bout of exercise and abates in hours after stimulation ends. *Journal of Applied Physiology.* 2013 Jun; 114(11):1603-9.

Memberships:

01/2012 - present	American Heart Association
01/2014 - present	Biophysics Society

Work Experience:

03/2005 - 01/2006	Medical Sergeant, Army, Taipei City, Taiwan

08/2006 - 08/2008	Research Assistant, Taipei Medical University, Taipei City, Taiwan
09/2008 - 03/2009	Research Assistant, National Taiwan University Hospital, Taipei City, Taiwan
08/2009 - present	Graduate Research Assistant at UIC, Chicago, Illinois

Honors & Awards:

01/1992	Gold medal, Eugenics & Health Care Contest, Taipei County, Taiwan.
04/1993	Gold medal, Environmental Poster Contest, Taipei County, Taiwan.
05/1993	Honorable Mention, 33rd National Primary School Science Fair, Taipei City, Taiwan.
05/1996 - 05/1998	Top student in high school class, Legal Foundation of Lungshan Temple Scholarship, Taipei City, Taiwan, 3 times (1996, 1997, 1998).
06/1998	Mayor's Award, Shunshan Senior High School, Taipei City, Taiwan
07/2012 - 06/2014	Predoctoral Fellowship, American Heart Association Midwest Affiliate Chicago, Illinois.
09/2013	First place, poster prize, 2013 Center for Cardiovascular Research (CCVR) annual research forum.
04/2014 - present	Dean's Scholar Award at UIC (one of top five PhD students), Chicago, Illinois
08/2014	First place, poster prize, 2014 Center for Cardiovascular Research (CCVR) annual research forum.

Poster Presentations:

•Ying-Hsi Lin, Erik R. Swanson and Brenda Russell. Cardiac protein complex stability changes with activity and recovers within three hours of cessation of work. *2012 UIC Student Research Forum*, Chicago, IL. April 17 2012.

•Ying-Hsi Lin, Erik R. Swanson and Brenda Russell. Cardiac protein complex stability changes with activity and recovers within three hours of cessation of work. *2012 CCVR Research Forum*, Chicago, IL. Nov. 9 2012.

•Ying-Hsi Lin, Jieii Li, Erik R. Swanson and Brenda Russell. CapZ and actin capping dynamics increase in myocytes after a bout of exercise and abates in hours after stimulation ends. *2013 Chicago Cytoskeletion Conference*, Chicago, IL. March. 15 2012.

•Ying-Hsi Lin, Kathleen M. Broughton and Brenda Russell. Increased stiffness alters contractile filament assembly in myocytes by increasing the exchange dynamics of capping of actin by CapZ. *2013 UIC Student Research Forum*, Chicago, IL. April 16 2013.

•Ying-Hsi Lin, Kathleen M. Broughton and Brenda Russell. Increased stiffness alters contractile filament assembly in myocytes by increasing the exchange dynamics of capping of actin by CapZ. *2013 Midwest Biomedical Engineering Career Conference*, Chicago, IL. April 19 2013.

•Ying-Hsi Lin, Kathleen M. Broughton and Brenda Russell. ”Increased stiffness alters contractile filament assembly in myocytes by increasing the exchange dynamics of capping of actin by CapZ.” *2013 CCVR Conference,* Chicago, IL. September 10 2013.

•Ying-Hsi Lin, Kathleen M. Broughton and Brenda Russell. Increased stiffness alters contractile filament assembly in myocytes by increasing the exchange dynamics of capping of actin by CapZ. *2013 Chicago Research Network Symposium*, Chicago, IL., September 20 2013.

•Ying-Hsi Lin, Chad M. Warren and Brenda Russell. Acetylation and phosphorylation post-translational modifications of the CapZ beta1 subunit regulate actin dynamics leading to myocyte hypertrophy. *2014 Biophysics Conference*, San Francisco, CA., February 15-19 2014.

•Ying-Hsi Lin, Chad M. Warren and Brenda Russell. CapZ beta1 subunit acetylation and actin assembly are regulated by HDAC in cardiomyocytes. *2014 International Society for Heart Research Meeting*, Miami, FL., May 12-15 2014.

•Ying-Hsi Lin, Chad M. Warren and Brenda Russell. CapZ beta1 subunit acetylation and actin assembly are regulated by HDAC in cardiomyocytes. *2014 Myofilament Meeting*, Madison, WI., June 7-10 2014.

Technical Skills:

Computer: Microsoft Office, Photoshop, Dreamwave, ImageLab, ImageJ, OriginLab, Zen, PyMOL, Scaffold 3, Mascot

Lab skills: Cloning (restriction digests, ligation, transformation, plasmid preparation), retroviral vector production, viral infection, PCR, RT-PCR, RNA extraction, primer design, immunocytochemistry, luciferase assay, real-time PCR, primary cell culture, protein extraction, myofibril protein extraction, fluorescence microscopy, protein quantification, subcellular fractionation, immunoprecipitation, co-immunoprecipitation, confocal microscopy, FRAP and statistical normalization, one-dimensional western blotting, two-dimensional western blotting, 2D clean-up, OFFGEL fractionation, mass spectrometry

APPENDIX A - Animal Approval Form

UIC UNIVERSITY OF ILLINOIS AT CHICAGO

Office of Animal Care and Institutional
Biosafety Committee (OACIB) (M/C 672)
Office of the Vice Chancellor for Research
206 Administrative Office Building
1737 West Polk Street
Chicago, Illinois 60612

9/17/2014

Brenda Russell
Physiology & Biophysics
M/C 901

Dear Dr. Russell:

The protocol indicated below was reviewed in accordance with the Animal Care Policies and Procedures of the University of Illinois at Chicago and **renewed on 9/17/2014.**

Title of Application: **Isolation of Heart Cells from Neonatal Rats**
ACC NO: **13-146**
Original Protocol Approval: **9/17/2013 (3 year approval with annual continuation required).**
Current Approval Period: **9/17/2014 to 9/17/2015**

Funding: ***Portions of this protocol are supported by the funding sources indicated in the table below.***
Number of funding sources: 2

Funding Agency	**Funding Title**			**Portion of Funding Matched**
NIH	*Integrated Mechanisms Of Cardiac Maladaptation*			*Protocol is linked to form G 13-055*
Funding Number	**Current Status**	**UIC PAF NO.**	**Performance Site**	**Funding PI**
PO1HL62426 (Years 11-15)	*Funded*	*2009-06478*	*UIC*	*John Solaro (Brenda Russell, PI of project 2)*
Funding Agency	**Funding Title**			**Portion of Funding Matched**
AHA- American Heart Association	*Regulation of Actin Assembly in Cardiomyocytes with Mechanical Stimulation*			*All matched*
Funding Number	**Current Status**	**UIC PAF NO.**	**Performance Site**	**Funding PI**
12PRE12050371	*Funded*	*2012-03610*	*UIC*	*Ying-His Lin*

This institution has Animal Welfare Assurance Number A3460.01 on file with the Office of Laboratory Animal Welfare, NIH. **This letter may only be provided as proof of IACUC approval for those specific funding sources listed above in which all portions of the grant are matched to this ACC protocol.**

Thank you for complying with the Animal Care Policies and Procedures of the UIC.

Sincerely,

Bradley Merrill, PhD
Chair, Animal Care Committee

BM/*kg*
cc: BRL, ACC File, Ying Hsi Lin

Phone (312) 996-1972 • Fax (312) 996-9088

APPENDIX B - Institutional Review Board Approval Form

UNIVERSITY OF ILLINOIS
AT CHICAGO

Office for the Protection of Research Subjects (OPRS)
Office of the Vice Chancellor for Research (MC 672)
203 Administrative Office Building
1737 West Polk Street
Chicago, Illinois 60612-7227

Approval Notice
Continuing Review (Response To Modifications)

March 2, 2015

R. John Solaro, PhD
Physiology and Biophysics
835 South Wolcott Ave., E202 MSB, M/C 901
Chicago, IL 60612
Phone: (312) 996-7620 / Fax: (312) 996-1414

RE: Protocol # 2012-0061
"Mechanical Activity & Myocyte Remodeling (PPG Project 21)"

Dear Dr. Solaro:

Please note that this research did not have Institutional Review Board (IRB) approval from midnight February 22, 2015 until February 24, 2015.

Your Continuing Review (Response To Modifications) was reviewed and approved by the Expedited review process on February 24, 2015. You may now continue your research.

Please note the following information about your approved research protocol:

Protocol Approval Period: February 24, 2015 - February 24, 2016
Approved Subject Enrollment #: 0
Additional Determinations for Research Involving Minors: These determinations have not been made for this study since it has not been approved for enrollment of minors.
Performance Sites: UIC, Loyola University Medical Center
Sponsor: New England Research Institutes (Subcontractor for NHLBI)
PAF#: 2009-06478
Grant/Contract No: PO1 HL62426
Grant/Contract Title: Integrated Mechanisms Of Cardiac Maladaptation
Research Protocol(s):

a) Mechanical Activity and Myocyte Remodeling, Protocol Version Number: 1, December 22, 2011

Informed Consent(s):

a) Waiver of Informed Consent granted under [45 CFR 46.116(d)]

APPENDIX B - Institutional Review Board Approval Form (continued)

Your research continues to meet the criteria for expedited review as defined in 45 CFR 46.110(b)(1) under the following specific category):

(5) Research involving materials (data, documents, records, or specimens) that have been collected, or will be collected solely for nonresearch purposes (such as medical treatment or diagnosis).

Please note the Review History of this submission:

Receipt Date	Submission Type	Review Process	Review Date	Review Action
02/10/2015	Continuing Review	Expedited	02/12/2015	Modifications Required
02/20/2015	Response To Modifications	Expedited	02/24/2015	Approved

Please remember to:

→ Use your **research protocol number** (2012-0061) on any documents or correspondence with the IRB concerning your research protocol.

→ Review and comply with all requirements on the enclosure,
"UIC Investigator Responsibilities, Protection of Human Research Subjects"
(http://tigger.uic.edu/depts/ovcr/research/protocolreview/irb/policies/0924.pdf)

Please note that the UIC IRB has the prerogative and authority to ask further questions, seek additional information, require further modifications, or monitor the conduct of your research and the consent process.

Please be aware that if the scope of work in the grant/project changes, the protocol must be amended and approved by the UIC IRB before the initiation of the change.

We wish you the best as you conduct your research. If you have any questions or need further help, please contact OPRS at (312) 996-1711 or me at (312) 355-2939. Please send any correspondence about this protocol to OPRS at 203 AOB, M/C 672.

Sincerely,

Jewell Hamilton, MSW
IRB Coordinator, IRB # 3
Office for the Protection of Research Subjects

Enclosure(s): None

cc: John Solaro, Physiology and Biophysics, M/C 901
OVCR Administration, M/C 672

APPENDIX C – Copy Right Clearance